2007-06

# Experimental investigation of high-pressure steam induced stall of a transonic rotor

Koessler, Joseph J.

Monterey, California. Naval Postgraduate School


# NAVAL POSTGRADUATE SCHOOL

**MONTEREY, CALIFORNIA**

# THESIS

**EXPERIMENTAL INVESTIGATION OF HIGH-PRESSURE STEAM INDUCED STALL OF A TRANSONIC ROTOR**

by

Joesph J. Koessler

June 2007

| | |
|---|---|
| Thesis Advisor: | Garth V. Hobson |
| Second Reader: | Anthony J. Gannon |

THIS PAGE INTENTIONALLY LEFT BLANK

| REPORT DOCUMENTATION PAGE | | | Form Approved OMB No. 0704-0188 |
|---|---|---|---|
| Public reporting burden for this collection of information is estimated to average 1 hour per response, including the time for reviewing instruction, searching existing data sources, gathering and maintaining the data needed, and completing and reviewing the collection of information. Send comments regarding this burden estimate or any other aspect of this collection of information, including suggestions for reducing this burden, to Washington headquarters Services, Directorate for Information Operations and Reports, 1215 Jefferson Davis Highway, Suite 1204, Arlington, VA 22202-4302, and to the Office of Management and Budget, Paperwork Reduction Project (0704-0188) Washington DC 20503. | | | |
| **1. AGENCY USE ONLY** *(Leave blank)* | **2. REPORT DATE** June 2007 | **3. REPORT TYPE AND DATES COVERED** Master's Thesis | |
| **4. TITLE AND SUBTITLE** Experimental Investigation of High-Pressure Steam Induced Stall of a Transonic Rotor | | **5. FUNDING NUMBERS** | |
| **6. AUTHOR(S)** Joseph J. Koessler | | | |
| **7. PERFORMING ORGANIZATION NAME(S) AND ADDRESS(ES)** Naval Postgraduate School Monterey, CA 93943-5000 | | **8. PERFORMING ORGANIZATION REPORT NUMBER** | |
| **9. SPONSORING /MONITORING AGENCY NAME(S) AND ADDRESS(ES)** N/A | | **10. SPONSORING/MONITORING AGENCY REPORT NUMBER** | |
| **11. SUPPLEMENTARY NOTES** The views expressed in this thesis are those of the author and do not reflect the official policy or position of the Department of Defense or the U.S. Government. | | | |
| **12a. DISTRIBUTION / AVAILABILITY STATEMENT** Approved for public release; distribution is unlimited | | **12b. DISTRIBUTION CODE** | |

**13. ABSTRACT (maximum 200 words)**

Steam leakage from the catapult system of U.S. Navy aircraft carriers can stall the compressors of modern jet aircraft if ingested during takeoff. This phenomenon, known as "pop stall", is of particular concern to the U.S. Navy as their current fleet of F404 engines age, the newer F414 engine comes online, and the F-35C variant of the Joint Strike Fighter begins service. The age of the F404 engine, the untested steam performance of the two stage fan in the F414 engine, and the low, serpentine intake of the F-35C make these engines and aircraft susceptible to steam-induced stall during takeoff. This study examines the high pressure steam-induced stall of a transonic rotor at both subsonic and transonic speeds. Steam stall was induced at 70%, 90% and 95% rated rotor speed and the performance map of the rotor was re-established for 70%, 90%, 95%, and 100% rated speeds. The stall margin of the rotor and the presence of a stall precursor during both normal and steam ingested operation was investigated. In addition, the inlet nozzle mass flow measurements of the rig were tested against measurements in the inlet bellmouth to determine the feasibility of a shorter intake to introduce more inlet distortion into the flow.

| **14. SUBJECT TERMS** Compressor, Steam induced stall, pop stall, transonic rotor, stall margin, stall precursor, modal oscillation | | | **15. NUMBER OF PAGES** 115 |
|---|---|---|---|
| | | | **16. PRICE CODE** |
| **17. SECURITY CLASSIFICATION OF REPORT** Unclassified | **18. SECURITY CLASSIFICATION OF THIS PAGE** Unclassified | **19. SECURITY CLASSIFICATION OF ABSTRACT** Unclassified | **20. LIMITATION OF ABSTRACT** UL |

NSN 7540-01-280-5500 Standard Form 298 (Rev. 2-89)
Prescribed by ANSI Std. 239-18

THIS PAGE INTENTIONALLY LEFT BLANK

**Approved for public release; distribution is unlimited**

# EXPERIMENTAL INVESTIGATION OF HIGH-PRESSURE STEAM INDUCED STALL OF A TRANSONIC ROTOR

Joseph J. Koessler
Ensign, United States Navy
B.S., United States Naval Academy, 2006

Submitted in partial fulfillment of the
requirements for the degree of

**MASTER OF SCIENCE IN MECHANICAL ENGINEERING**

from the

**NAVAL POSTGRADUATE SCHOOL**
**June 2007**

Author: Joseph J. Koessler

Approved by: Garth V. Hobson
Thesis Advisor

Anthony J. Gannon
Second Reader

Anthony J. Healey
Chairman, Department of Mechanical and Astronautical Engineering

THIS PAGE INTENTIONALLY LEFT BLANK

# ABSTRACT

Steam leakage from the catapult system of U.S. Navy aircraft carriers can stall the compressors of modern jet aircraft if ingested during takeoff. This phenomenon, known as “pop stall”, is of particular concern to the U.S. Navy as their current fleet of F404 engines age, the newer F414 engine comes online, and the F-35C variant of the Joint Strike Fighter begins service. The age of the F404 engine, the untested steam performance of the two stage fan in the F414 engine, and the low, serpentine intake of the F-35C make these engines and aircraft susceptible to steam-induced stall during takeoff. This study examines the high pressure steam-induced stall of a transonic rotor at both subsonic and transonic speeds. Steam stall was induced at 70%, 90% and 95% of rated rotor speed and the performance map of the rotor was re-established for 70%, 90%, 95%, and 100% of rated speed. The stall margin of the rotor and the presence of a stall precursor during both normal and steam ingested operation was investigated. In addition, the inlet nozzle mass flow measurements of the rig were tested against measurements in the inlet bellmouth to determine the feasibility of a shorter intake to introduce more inlet distortion into the flow.

THIS PAGE INTENTIONALLY LEFT BLANK

# TABLE OF CONTENTS

# LIST OF FIGURES

THIS PAGE INTENTIONALLY LEFT BLANK

# LIST OF TABLES

THIS PAGE INTENTIONALLY LEFT BLANK

# ACKNOWLEDGMENTS

The completion of this work would not have been possible without the assistance of several key people. First, Prof. Garth Hobson acted as a great mentor, teacher, and motivator as my primary advisor. Asst. Prof. Anthony Gannon went to great lengths to provide technical support and was always available to answer questions and give advice. John, Rick, and Doug keep the lab up and running, an integral role when the experimental rig is so complex. Finally, my wife, Michaela, put up with many long nights of studying and entertained me by looking at my “pretty pictures”.

THIS PAGE INTENTIONALLY LEFT BLANK

# I. INTRODUCTION

The concepts of compressor stall and surge are two highly studied phenomena of turbomachinery. The conditions that create stall and surge in compressors are varied, and a compressor can be stalled as a result of inlet distortion, throttle setting, hot gas ingestion, and several other flow field effects. In particular, the U. S. Navy is interested in the performance characteristic of a compressor during steam-induced stall. Steam is commonly encountered on the flight deck of aircraft carriers as it is the actuating fluid in the Navy's steam catapult system. Aging ships, systems, and specifically steam seals result in excess steam leaking onto the flight deck during operation. The ingestion of this steam has been shown to cause 'pop stall', or steam-induced stall, in the jet engines of current platforms.


Figure 1. F-18 experiencing "pop stall"

The Navy has a threefold interest in this problem. The F404 engine is currently employed in Navy F-18A and B jet aircraft, and this engine's age results in a reduced stall margin on its operational curve. Secondly, the Navy is currently updating the F-18E and F aircraft by replacing the F414 engine with a more modern two stage fan engine.

The stall margin and the effect of steam on this two stage fan are not as established as the characteristics of the F414. Finally, the Navy will soon be phasing in the F-35 Joint Strike Fighter, a single engine stealth fighter. This aircraft will only have one engine, so the steam-induced stall characteristic of its compressor must be well understood to help prevent any catastrophic failures of the aircraft during take-off. Additionally, the intake of the F-35C is serpentine to reduce its infrared and radar signature. This adds inlet distortion to the flow, which could potentially increase the effect of steam ingestion.

The focus of research conducted at the Turbopropulsion Laboratory (TPL) at the Naval Postgraduate School (NPS) involves the steam-induced stall of a transonic compressor rotor (TCR). This rotor, studied in the rotor-only configuration, was specifically designed for the TPL by Sanger (1996) at the NASA Glenn Research Center (Ref. 8). The performance of this rotor in the speed range of 70% to 100% is well established in previous work by Payne, Zarro, and Gannon et al. In addition, these works investigated the low-pressure steam-induced stall of the rotor at several speeds (Refs. 4, 7, and 9). With a compressor map having been well established for the TCR, the current study focused on the high pressure steam-induced stall of the rotor and attempted to better identify the presence of a stall precursor oscillation. Additionally evaluation of the mass flow rate of the current rig was investigated for the incorporation of a shorter inlet in future studies. The rotor was run at both subsonic (70% rated speed) and transonic speeds (90%, 95%, and 100% rated speed), utilizing Kulite pressure transducers and hot-film probes to obtain real-time measurements of the flow. Steam-induced stall, using steam at 9 atm. pressure, was studied at 70%, 90% and 95% speed.

# II. BACKGROUND INFORMATION

## A. STALL THEORY

Stall is a phenomenon occurring in turbomachinery during which the angle of incidence on a rotor or stator blade increases to the point of causing the flow to separate from that blade. This type of flow disturbance can occur anywhere in a turbomachine and may be present during typical operation in small areas. When localized disturbances expand, stall becomes a problem for engine systems, causing reductions in thrust, mechanical engine damage, and possibly total engine failure. Stall can be categorized into three main categories: progressive stall, abrupt stall, and surge (Ref. 2).

### 1. Progressive Stall

Progressive stall begins as localized flow separation in the tip region of a rotor or stator. Localized regions of stalled flow are often referred to as "cells" and are found in circumferentially non-uniform patterns on stalled rotors or stators (Ref. 2). During progressive stall, flow separation in the tip region causes a deflection of the inlet flow surrounding the stall cell. As a result, separated flow on the suction side of a blade increases the angle of incidence on the next blade. When the angle of incidence on the next blade causes separation, the flow field surrounding the previously stalled blade, due to deflection of air around the newly separated flow, unstalls as the angle of incidence on the previous blade is reduced. In this manner, rotating stall occurs in localized regions near the tips of blades rows. While this succession of stalled and unstalled blades physically moves opposite to the rotational direction of the rotor, the process occurs at a speed such that the stall cells propagate circumferentially at 50% – 70% of the blade speed (Ref. 6). While progressive stall may not cause catastrophic engine failure, reducing the throttle and thereby reducing the inlet mass flow to an engine further may cause progressive stall to develop into abrupt stall (Ref. 2).

### 2. Abrupt Stall

Abrupt stall is a total, asymmetric breakdown of the inlet flow over a rotor or stator. Abrupt stall is a much more catastrophic occurrence than progressive stall and is characterized by a full blade span breakdown of flow. This breakdown appears as a large blockage of through flow in a machine as inlet flow stagnates in the stall region (Ref. 2). In a manner similar to progressive stall but occurring over a large number of blades, abrupt stall also rotates at approximately 10%-20% of rotor speed. In this manner, the stage can share the reduced mass flow that both causes and occurs during abrupt stall. In the stalled region, little or no flow exists, while outside this region the blades may have full or almost full flow over them (Ref. 2).

Abrupt stall is a term used to describe the flow breakdown over a particular stage of a turbomachine. Stall, however, often leads to a more damaging phenomenon known as surge.

### 3. Surge

The cyclic stalling of a stage in a turbomachine is referred to as surge. Surge occurs when both the rotor and stator in a certain stage stall in succession of each other. The stalling of a rotor can distort the inlet flow to its accompanying stator such that the stator then stalls. In turn, the stalling of the stator can result in the flow field surrounding the rotor to recover and resume normal operation. As the stator recovers from stall, the original inlet conditions that caused the rotor to stall reoccur, pushing the rotor back into stall. In this manner, both the rotor and stator alternately stall and unstall, resulting in high transverse loading on the rotor, casing, and machine, potential blade rubbing on the casewall due to overspeed, and reversal of flow through the engine. During surge, the rotor or stator may be transiently experiencing either form of rotating stall described above. Deep surge is the term used when the surge of a compressor is so severe that previously compressed gases emerge from the engine inlet (Ref. 2).

### 4. Hysteresis

A compressor that enters stall will remain in that state unless the throttle position of the engine is changed. Hysteresis in a compressor is the amount that the throttle must be changed in order to recover from a stall event. Hysteresis is a function of the flow coefficient through a compressor and is thus highly dependent on overall compressor design (Ref. 2). Higher flow coefficients result in higher pressure ratios per stage in a compressor, which leads to more efficient operation of the engine. However, high flow coefficients increase the hysteresis of the compressor (Ref. 2). Operating at high pressure ratios is common in modern compressors, so understanding how much throttle is needed to recover from a stall event is necessary to restart stalled aircraft in flight. The operation of Navy aircraft, however, in a steam rich environment that may cause stall occurs during take-off. Understanding the stall characteristic of modern engines in such an environment could prevent aircraft and pilots from being lost if a stall occurred during take-off.

## B. STALL PRECURSORS

The dangerous nature of compressor stall has resulted in increased study of stall margin and how to prevent stall from occurring. Recently, research in the field of stall precursors, or conditions in the inlet flow field prior to stall that identify an imminent stall of the engine, has shown that there are two main precursors to a stall event: spike and modal oscillations (Ref. 1).

### 1. Spike

Spike is the localized stalling of a blade row. Spike rotates at approximately 60%-80% of rotor speed and rotates more quickly if the stalling occurs over fewer blades. An increase in the local angle of incidence on a blade row causes spike, which often expands and slows. Spike is exceedingly difficult to classify because it occurs so quickly during rotor operation. In order to classify spike, arrays of circumferential probes have been used. The classification of spike in the inlet of a compressor usually requires that an instrument measure the phenomenon as it happens. Since this stall precursor happens so

quickly and then slows as it expands, spike can be easily misclassified as a second type of stall precursor: the modal oscillation (Ref. 1).

### 2. Modal Oscillation

A modal oscillation is an axisymmetric flow instability in the inlet of a compressor. This oscillation, or instability, of the flow often occurs as the operating point of a particular compressor nears the peak of its operating characteristic. Modal oscillations typically result in separation of several blade rows, which in turn gives rise to a larger, slower rotating stall cell. However, the presence of a modal oscillation can result in local flow conditions that cause spike (Ref. 1). The interdependence of these phenomenon results in difficult experimental classification, however the modal oscillation tends to be easier to detect than spike because of its speed of rotation and duration.

## C. PREVIOUS THESIS WORK

Two previous theses have been conducted at the Turbopropulsion Laboratory (TPL) and the Naval Postgraduate School (NPS). These theses were both initial investigations of the low pressure steam-induced stall performance of the transonic rotor in use at TPL. The stall margin of the transonic rotor used at TPL was established, as well as a full performance map for the rotor (Ref. 9). Steam-induced stall was studied at 70% speed (Ref. 7) and 90% and 95% speed (Ref. 9). The presence of a stall precursor was identified for this particular rotor.

# III. EXPERIMENTAL FACILITY AND EQUIPMENT

## A. TRANSONIC COMPRESSOR ROTOR

For this study, as for other recent studies by Payne, Zarro, and Gannon et al. (Ref. 4, 7, and 9), the TCR was investigated in the rotor-only configuration. This configuration simplified the investigation of steam-induced stall and reduced the possibility of damage to the experimental rig due to catastrophic failure of the transonic rotor. The rotor, in the configuration as it was studied, is shown in Figure 2.

Figure 2. Transonic rotor

The rotor has 22 blades, a design pressure ratio of 1.61, and a design speed of 27,085 RPM. The design mass flow rate is 7.75 kg/s. The tip speed of the rotor is 396.2 m/s at full design speed giving a tip inlet relative mach number of 1.28. Finally, the rotor has an outer diameter of 11 inches (Ref. 4).

Payne and Zarro outlined the TCR and its operation in detail (Refs. 7 and 9). The TCR at the TPL was driven by two opposed rotor turbine stages. The compressed air for

this turbine was supplied by a 12 stage Allis-Chalmers axial compressor, which in turn was driven by an electric motor. The intake for the TCR was a 5 meter, 46 cm diameter pipe running from the intake settling chamber to the rotor. A bellmouth reduced the flow area to the dimensions of the rotor and was also used to measure the mass flow rate of air into the rotor for comparison with the traditional mass rate measurement utilizing a flow nozzle.

## B. STEAM INGESTION SYSTEM

Steam pressurized to 9 atm. was used in this study for steam-induced stall. This pressure level was higher than that previously studied by Payne and Zarro. Both Payne and Zarro outline the operation of the steam system in detail and offer technical specifications for the boiler used, piping system, and steam dumping solenoid activation (Refs. 7 and 9). Figure 3 is a photograph of the settling chamber with the steam dump pipe and solenoid visible.

Figure 3. Inlet plenum with steam dump piping, fast acting solenoid, and steam boiler

The following schematic, Figure 4, outlines the flow of steam from the boiler to the inlet plenum as well as where various sensors were installed in the experimental rig.

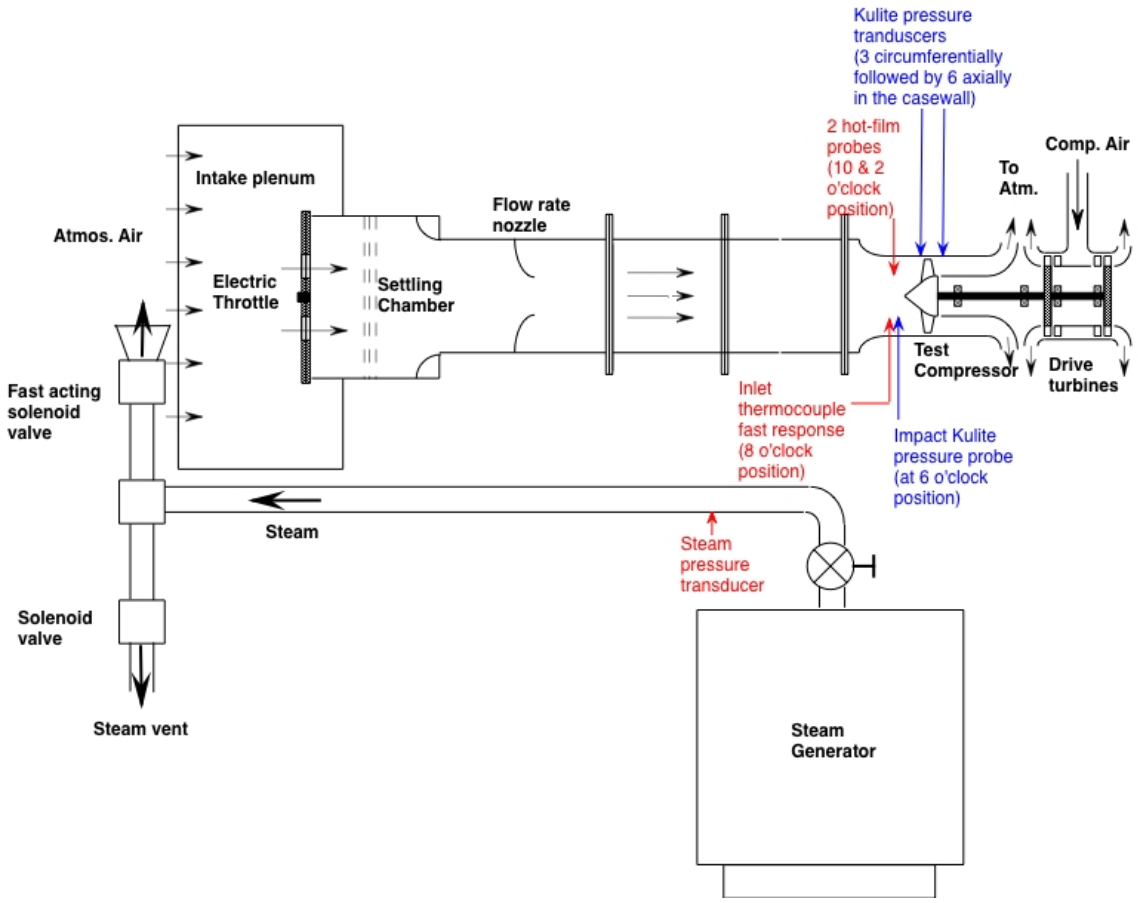


Figure 4. Experimental rig schematic

During experimental operation, air flowed to the rotor through the intake plenum. An electric throttle was used to attain various operating points by changing the mass flow into the rotor. The setting chamber and long intake pipe reduced the amount of inlet distortion in the flow by the time the inlet air reached the rotor. For a steam dump experiment, the steam generator produced steam to the necessary pressure before the opening of the valve to charge the steam line. The steam pressure transducer measured the steam pressure in the line to ensure that the pipe carrying the steam attained the same pressure as the boiler before dumping steam into the inlet plenum. Finally, the activation of the solenoid valve just outside the inlet plenum would dump steam into the intake.

This thesis examined the effect of 9 atmosphere steam because more steam was dumped into the inlet at this pressure. In addition, 9 atmosphere steam is the limit of current boiler capacity.

## C. DATA ACQUISITION SYSTEM

Figure 4 also shows the various instruments used in this study. A low-speed and high-speed data acquisition system make up the two linked systems that provide real time data during experimentation.

### 1. Low-Speed Data Acquisition

Low-speed data acquisition consisted of four sensors. In Figure 4, these sensors are the steam pressure transducer, the inlet fast response thermocouple, the flow rate nozzle, and the once per revolution indicator (not shown). During experimental operation, the low-speed instruments constantly measured steam pressure, inlet temperature, and rotor RPM. The once-per-rev signal passed through the breakout box before being recorded on the VXI mainframe, which is part of the high-speed data acquisition system. This signal provided a real time link between the low-speed and high-speed data acquisition systems during operation.

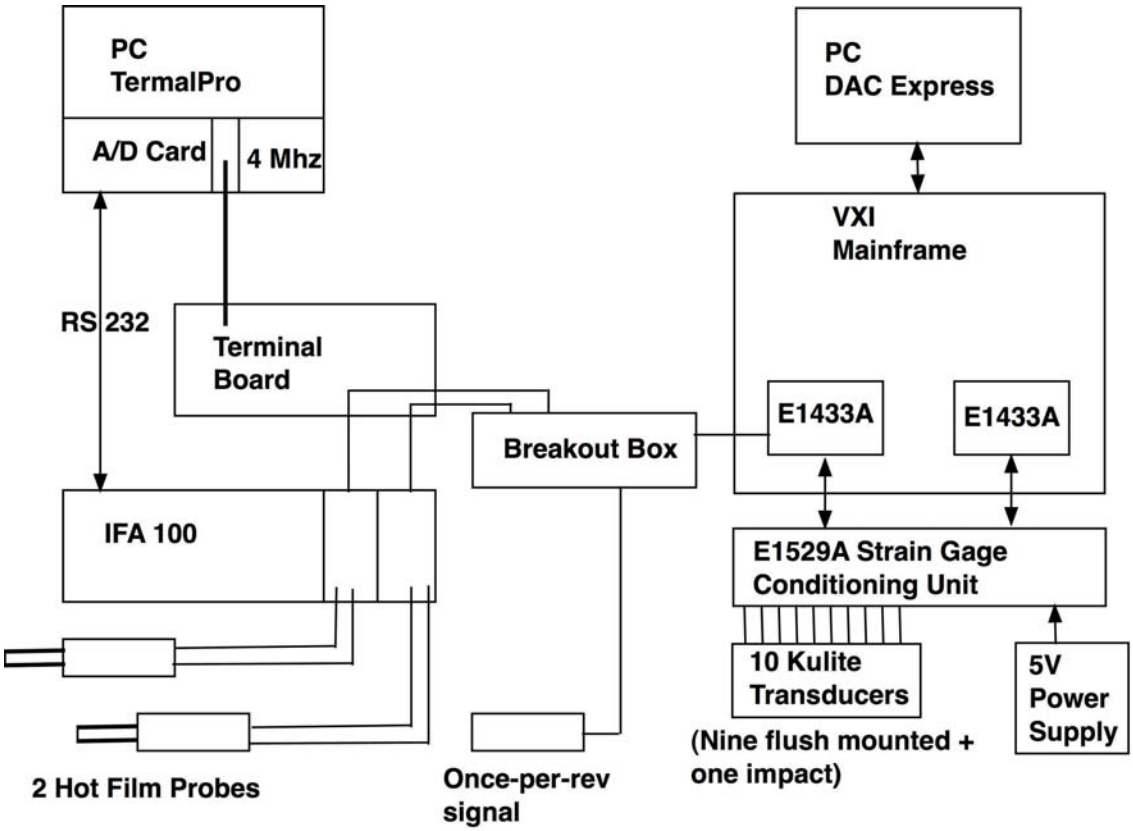


Figure 5. High speed data acquisition system

## 2. High Speed Data Acquisition

High-speed sensors used in this experiment consisted of the two hot-film probes and ten Kulite pressure transducers shown in Figures 4 and 5. The arrangement of the Kulite transducers in the case wall is shown in Figure 6.

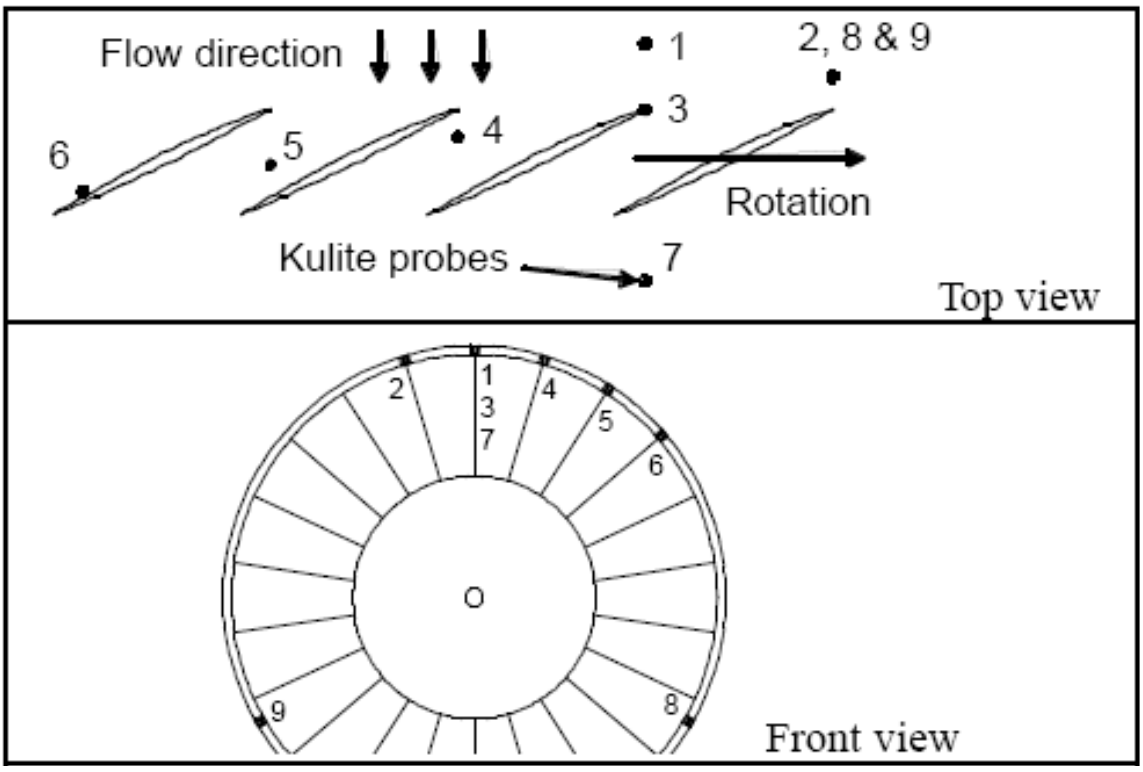


Figure 6. Kulite pressure transducer location

During steam dump operation, the low-speed data acquisition system would monitor steam pressure and steady state RPM while the flow rate nozzle measurement would verify the operating point of the throttle. Once the steam line was fully charged with steam, the operator starts the high-speed data acquisition system. This system takes readings from the 10 Kulite pressure transducers and two hot-film probes. The activation of the fast acting solenoid dumped steam into the inlet plenum while both data acquisition systems recorded data. Once the steam passed through the full stage and the audible response of the rotor was monitored for the development of stall, the high-speed data acquisition system would be stopped, and all data collected during the run would be compiled into a single spreadsheet using the once-per-rev signal as the real-time link between the Kulite pressure measurements and the hot-film velocity measurements. Further detailed explanation of the data acquisition system can be found in Payne (Ref. 7) and Zarro (Ref. 9).

# IV. EXPERIMENTAL PROCEDURE

## A. STEADY STATE OPERATION

Steady state operation of the transonic compressor provided the basis for the experimental data. Payne (Ref. 7) and Zarro (Ref. 9) established a full compressor map. Initial speed runs and data sets were taken at known operating points. For 70%, 90%, 95%, and 100% speeds, steady state data were collected from an open throttle through peak efficiency operating point of the rotor to a point nearest to but not causing stall. The low-speed data acquisition system provided RPM, pressure, temperature, and inlet mass flow data to verify the throttle position selected by the operator. The high-speed data acquisition system would record data from the Kulites and hot-film probes for a small number of revolutions.

Once satisfactory data had been taken at an operating point, the throttle position was changed to a new operating point closer to stall. Following this iterative process moved the throttle setting of the compressor as close to stall as possible without actually stalling the rotor. Once the steady state operating point closest to stall was achieved, the throttle was moved back down the compressor operating curve for a steam dump experiment. This procedure was followed for 70%, 90% and 95% speed with only steady state data being collected at 100% speed. The following table gives the four speed settings examined in this study.

| Percent Speed | RPM |
|---|---|
| 70% | 18,960 |
| 90% | 24,375 |
| 95% | 25,730 |
| 100% | 27,085 |

Table 1. Steady state speed settings

## B. DATA ACQUISITION

### 1. Kulite Data

During both steady state and steam dump operation, Kulite pressure transducer data were sampled. These data were compiled in a spreadsheet as outlined in Zarro (Ref. 9). The Kulite data was reduced using several Matlab programs. These programs, Generic_FFT_contourplot.m, Process_data.m, mov_avg.m, Find_loc.m, plot_data.m, and plot_rpm.m, are included in Appendix A.

### 2. Hot-Film Data

Just as Kulite pressure data were taken during both steady state and steam operation, hot-film data were acquired through the high-speed data acquisition system. Payne (Ref. 7) outlines the procedure for hot-film data acquisition. These data were also reduced with a Matlab program. This program, fft_auto, is included in Appendix B.

### 3. Low-Speed Data Acquisition

In addition to verifying throttle position of the rotor during operation, the low-speed data acquisition system measured amongst other parameters the inlet temperature, RPM, steam pressure, and mass flow. These data were linked to the high-speed data as a time reference for the high-speed data to the RPM of the rotor. The procedure for reducing this data and linking it to the high-speed data is outline by Gannon et al. (Ref. 4).

## C. STEAM DUMP OPERATION

Once the steady state operation of the rotor was established, steam was dumped into the inlet of the rotor at various throttle settings until stall was achieved. The steady state performance of the rotor was a reference for the expected stall point of the rotor during steam dump. Once the steady measurements of the rotor were complete, the throttle was opened slightly and the boiler was activated. When 9 atmospheres steam was fully charged through the system, the steam was dumped into the inlet plenum. The

high-speed data acquisition system was started just prior to the steam dump event, and the RPM and audible performance of the rotor was monitored to determine the existence of stall in the rotor. The throttle setting of the rotor was closed slightly for each speed setting until stall was achieved using 9 atmosphere steam.

THIS PAGE INTENTIONALLY LEFT BLANK

# V. RESULTS

## A. MASS FLOW VERIFICATION

The throttle setting of the rotor was established during each experimental run by checking the flow rate nozzle measurement against the compressor map of the rotor. In order to ensure that these measurements were accurate, the flow rate nozzle measurement was compared to that calculated from the total temperature, total pressure, and static temperature measurements in the inlet bellmouth. These experimental measurements of the flow were used, along with the known inlet area to the rotor, to calculate a mass flow rate for each run. The equations used in the calculation of this mass flow rate are included in Appendix C. Figure 7 shows the results of the measured mass flow rate from the flow rate nozzle plotted against the mass flow rate calculation from measurements in the inlet bellmouth.

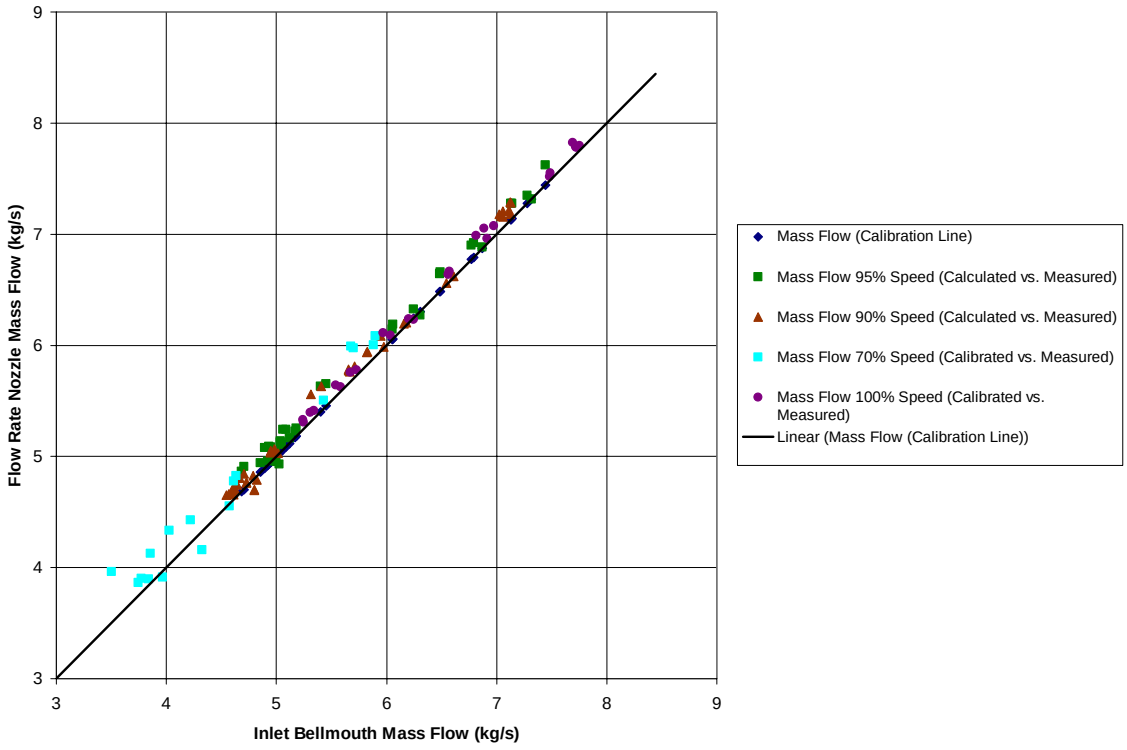


Figure 7. Mass flow rate, Measured vs. Calculated

In Figure 7, the 45° straight line represents the measured mass flow rate plotted against measured mass flow rate. In order for the measured mass flow rate to be correct, the calculated values should be plotted near this line.

## B. COMPRESSOR MAP

An updated compressor map with the new stall data for 9 atmosphere steam was plotted at the conclusion of testing. Figure 8 and 9 contain the most recent compressor maps with steam-induced stall indicated in each. Figure 8 is a plot of pressure ratio vs. mass flow rate while Figure 9 is a plot of efficiency versus mass flow rate.

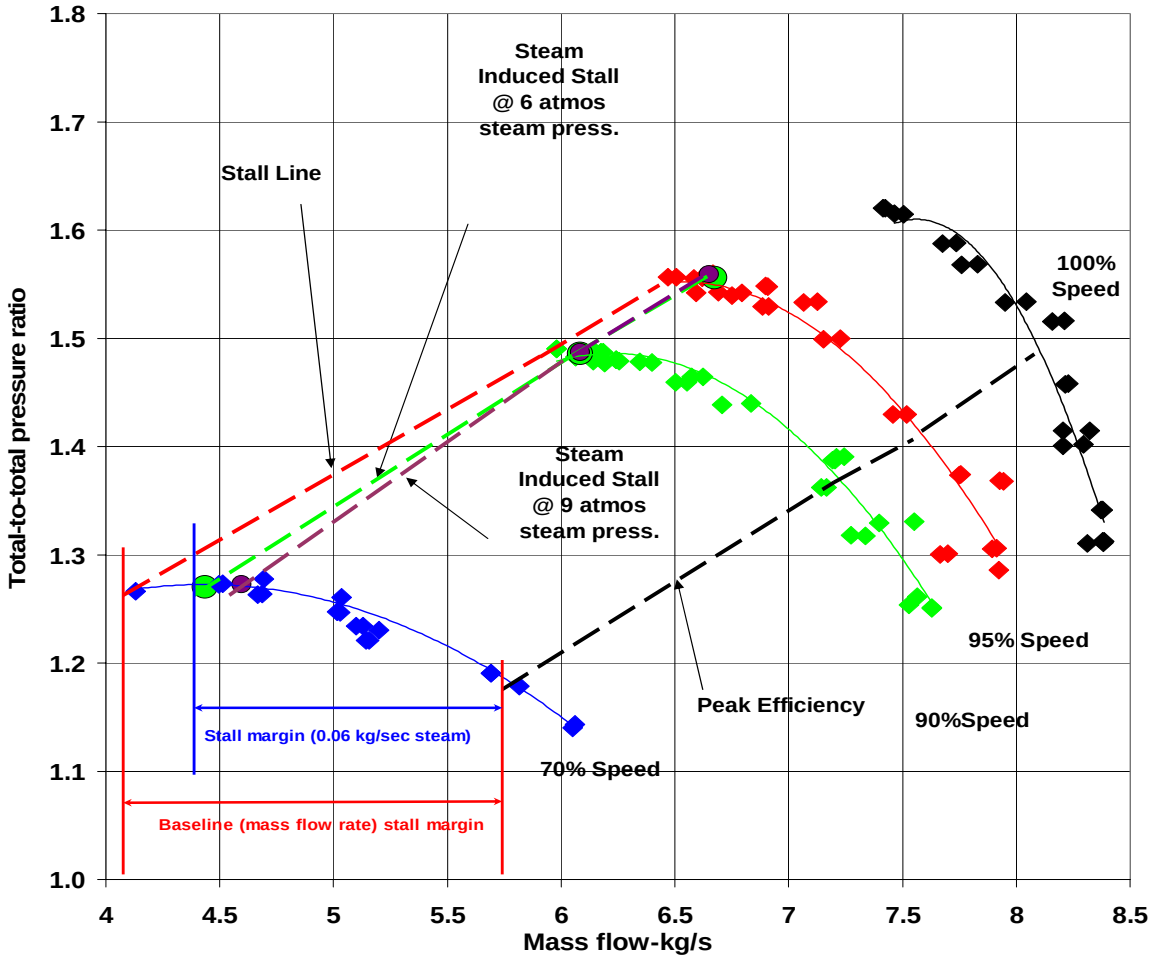


Figure 8. Updated pressure ratio map showing steam stall for 9 atmosphere steam

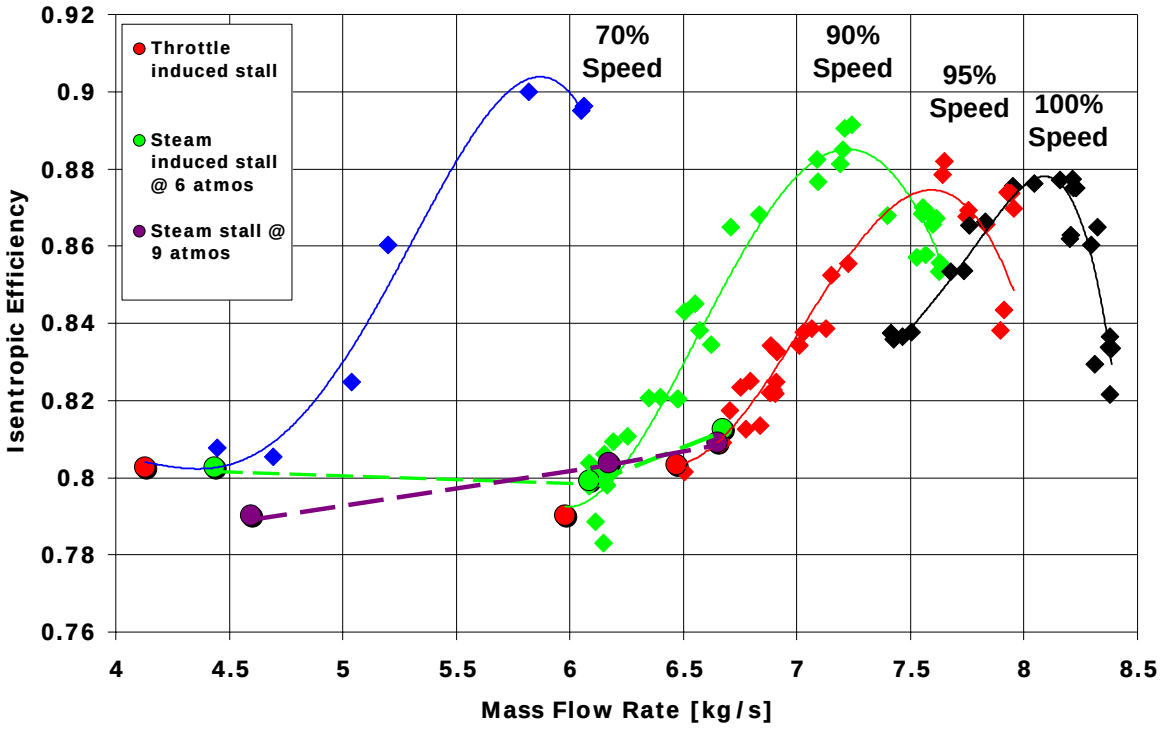


Figure 9. Updated efficiency map showing steam stall for 9 atmosphere steam

These plots show a reduced steam-induced stall margin at 70% speed for 9 atmosphere steam. The stall margin at 90% and 95% speed remained the same for both 9 atmosphere and 6 atmosphere steam.

## C. LOW-SPEED DATA ACQUISITION SYSTEM

The low-speed data acquisition system recorded the RPM, inlet temperature, and steam pipe pressure during steam operation. These plots give a real time measurement of these three instruments. Figure 10 is a typical steam strip plot.

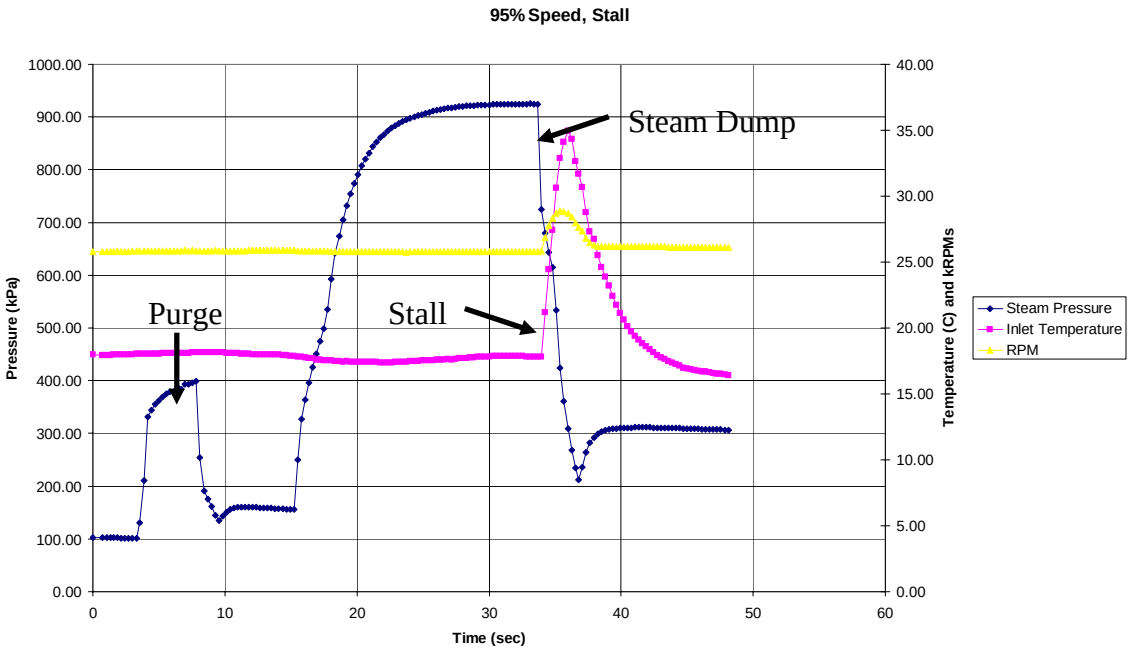


Figure 10. Steam strip plot

These plots show that as the steam is dumped into the inlet plenum, the inlet flow temperature spikes as the rotor overspeeds. Appendix G contains the steam strip plots for the various steam dump and steam stall runs.

## D. CONTOUR PLOTS – STEADY STATE OPERATION

### 1. Cut-Off Plots

Using the Matlab programs from Appendix A, a Fast Fourier Transform (FFT) was performed on the Kuilite data to look for different frequencies in the pressure data. The reduction of the Kulite data was to investigate the location of a once-per revolution frequency and a stall precursor frequency at approximately 50% of rotor speed. Initially, as shown in Figure 11, the contour plots produced with the FFT displayed high and low frequencies found in the pressure data.

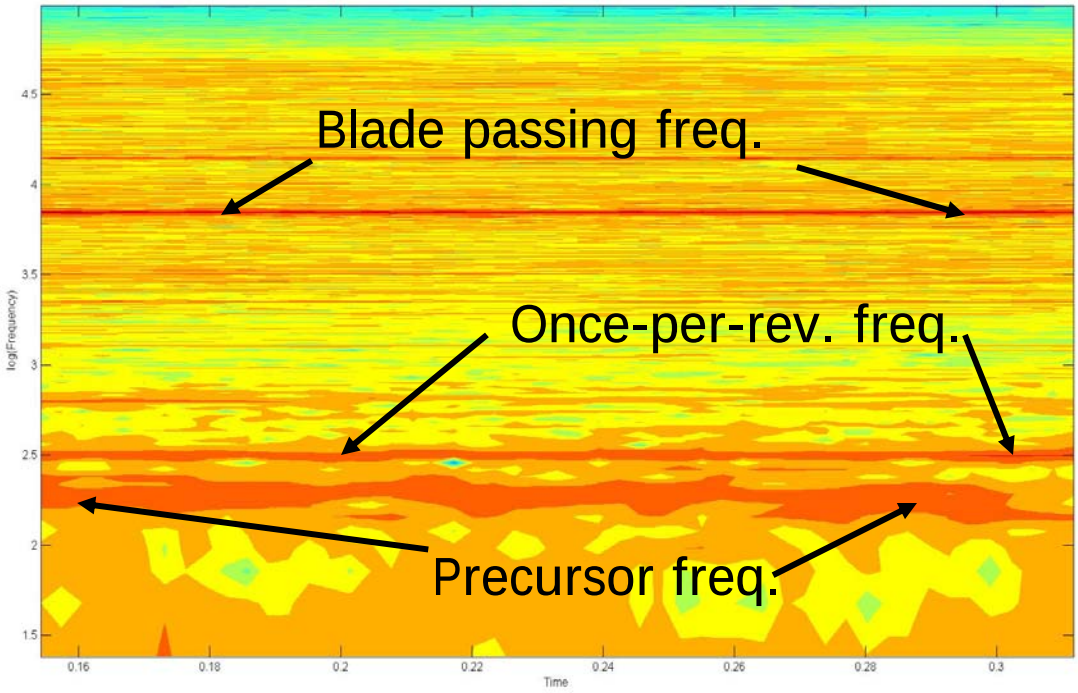


Figure 11. Full frequency spectrum contour plot, 70% speed

Figure 11 shows three frequencies: the blade passing frequency, the once-per-revolution frequency, and a precursor frequency. In this study, the blade passing frequency and any high frequency noise did not provide important information about the inlet flow field. In order to focus the FFT and contour plot on the once per revolution and precursor frequencies, the frequency data was cut off above ½ of the blade passing frequency. Figure 12 shows the same plot with the high frequency data removed.

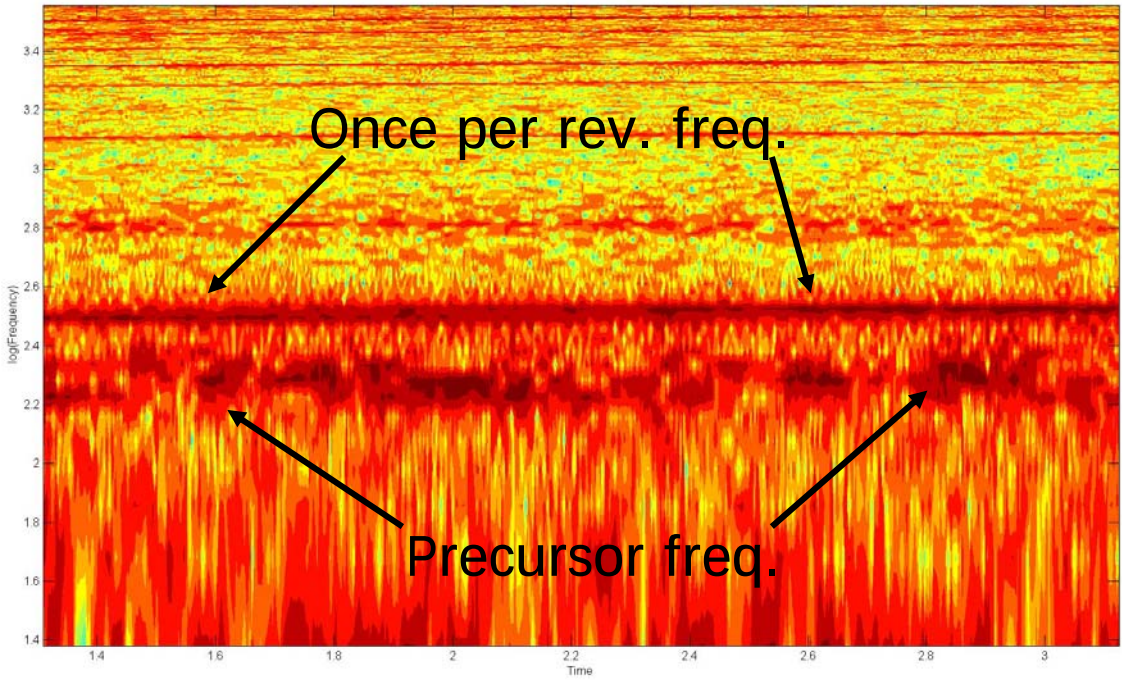


Figure 12. Cut off frequency spectrum contour plot, 70% speed

The same raw data, Figure 13, was plotted in both Figures 11 and 12. Cutting off the high frequencies in the contour plot provided better resolution around the once per revolution and precursor frequencies.

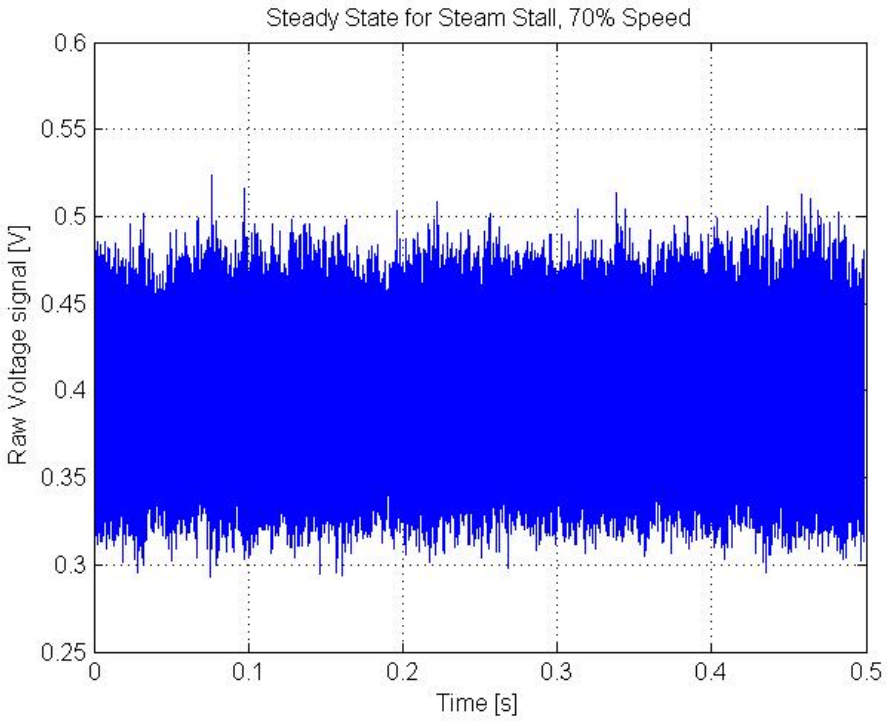


Figure 13. Raw data reduced with Generic_contour_plot.m

## 2. Contour Plots on the Compressor Map

Contour plots were produced for each Kulite and each throttle setting at all speeds studied. These contour plots were referenced to the compressor map to show the development of a stall precursor as the throttle setting moved closer to stall. This progression is significant in that it shows precursor frequencies are present during steady state operation beyond a certain throttle setting. Figure 14 shows a progression of contour plots for Kulite 9 at 70% speed. Figure 15 and Figure 16 show the same Kulite data for 90% and 95% speed. Appendix D contains these same progressions for Kulites 1, 2, 7, 8, and 9 at 70%, 90%, and 95% speed.

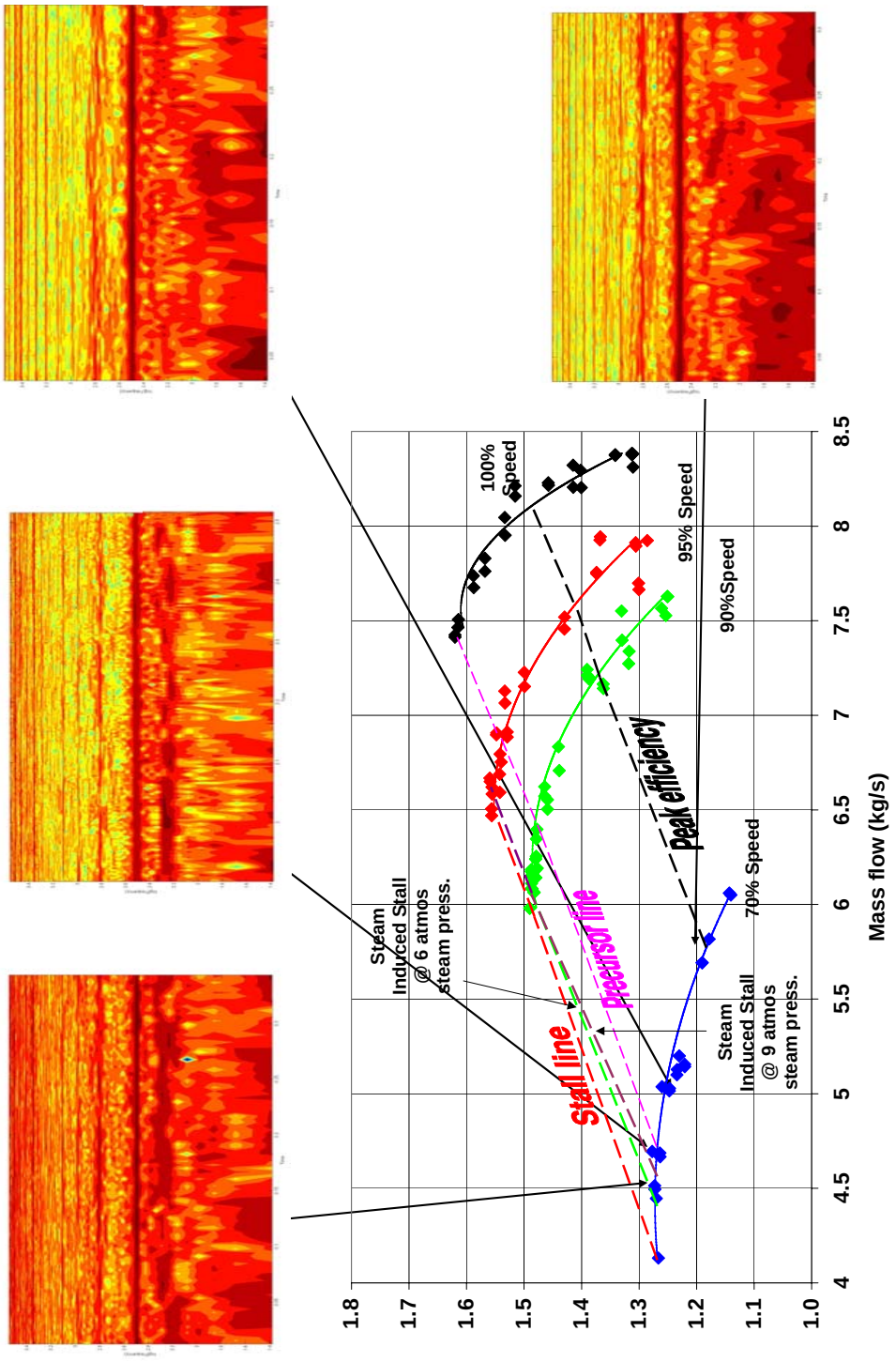


Figure 14. Compressor map progression, Kulite 9 at 70% speed

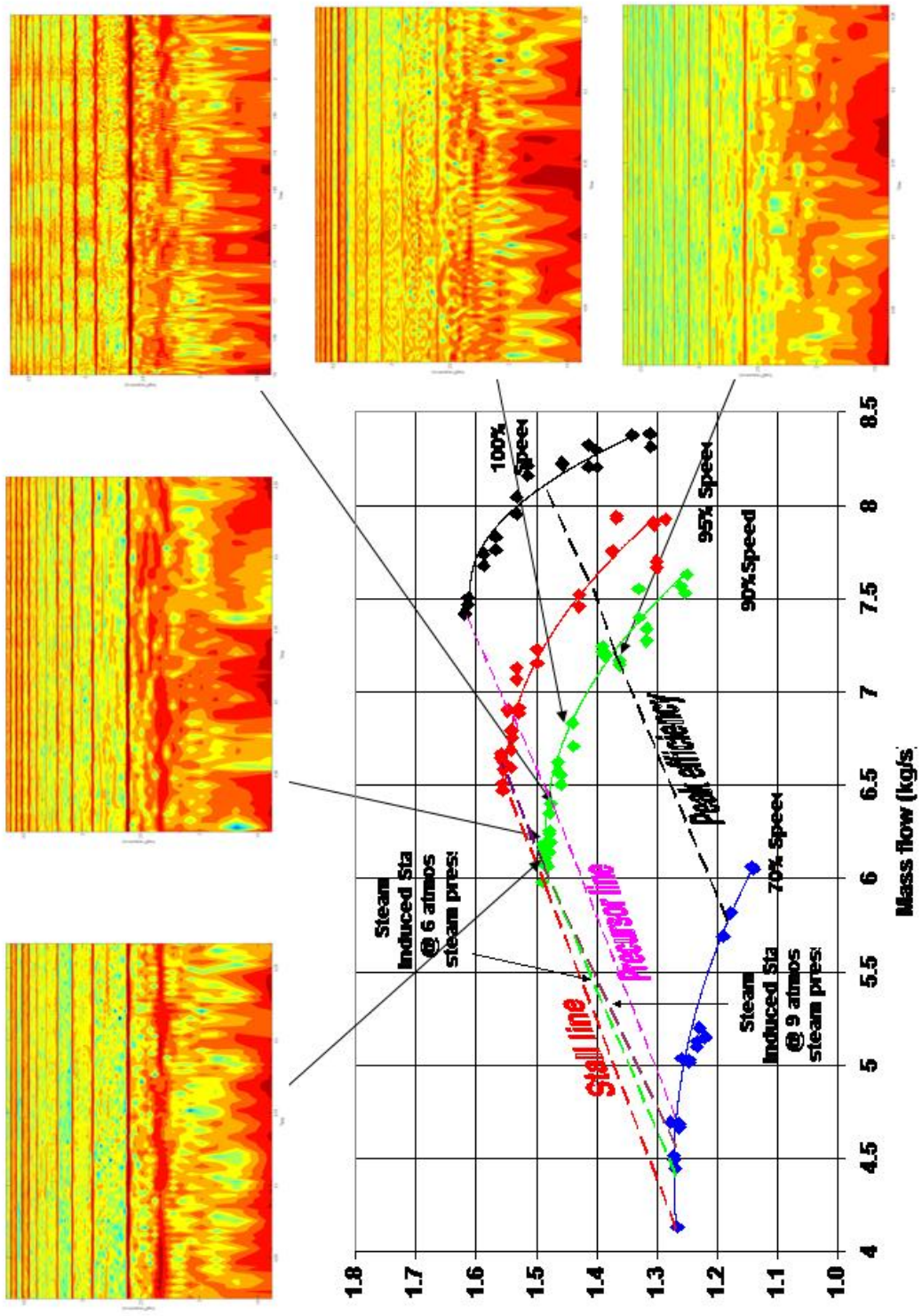


Figure 15. Compressor map progression, Kulite 9 at 90% speed

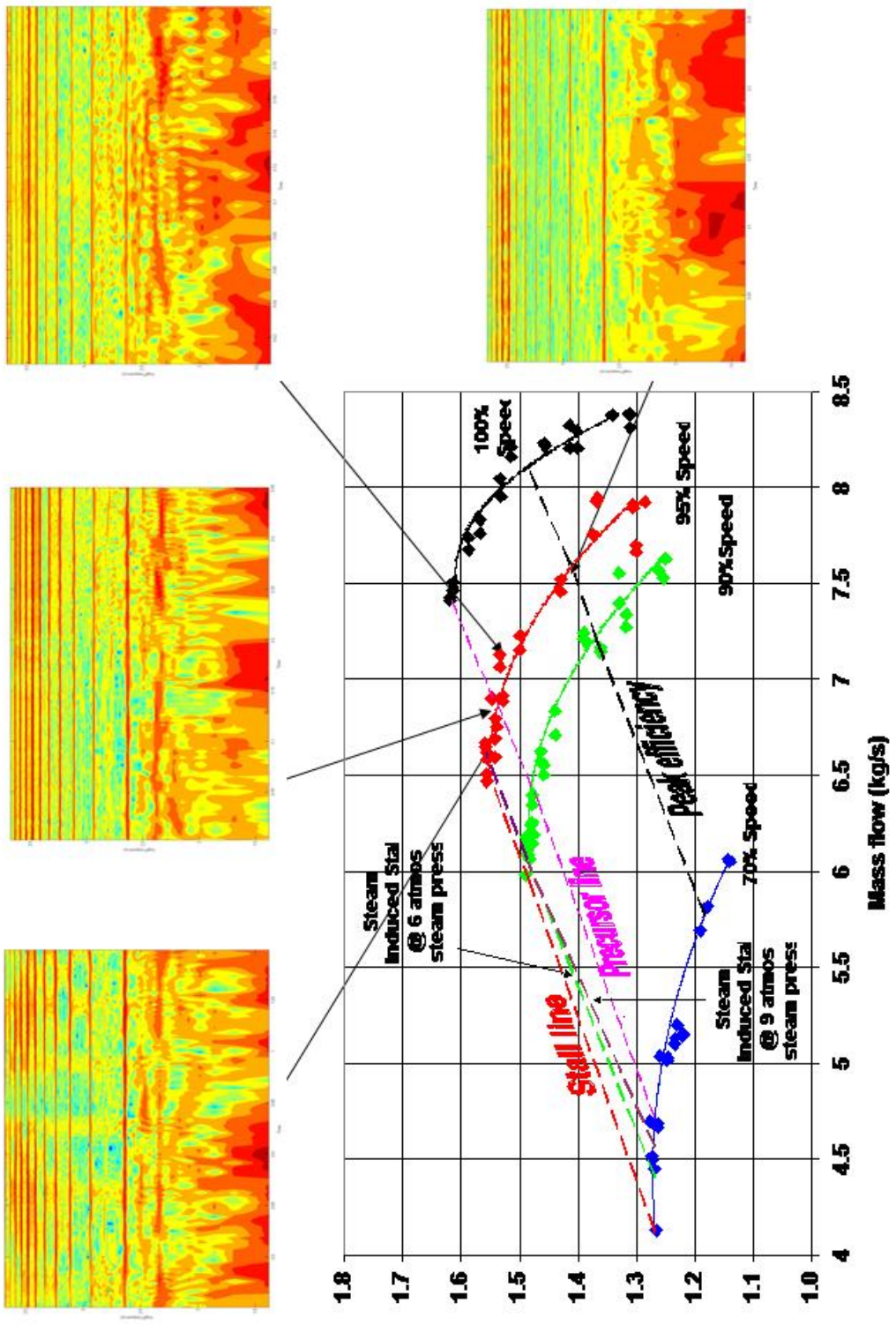


Figure 16. Compressor map progression, Kulite 9 at 95% speed

The development of the stall precursor is clearly seen in the contour plots as the throttle setting moves closer to stall. Also, at 90% speed, the once-per-revolution frequency disappears then reappears as the throttle moves from the peak efficiency point to the near stall points.

### 3. Contour Plots for Steam-Induced Stall

Kulite pressure data were also taken during steam-induced stall. Contour plots were again produced for the stall events. The RPM trace from the low-speed data acquisition system was used to find the revolution where the stall event occurred. Figure 17 shows a typical RPM trace during a stall event.

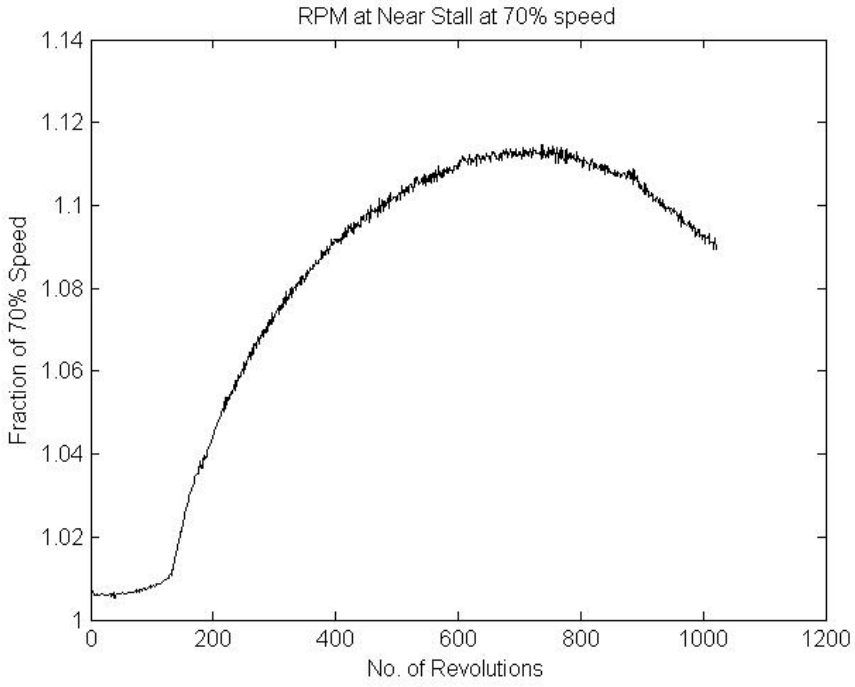


Figure 17. RPM trace for stall at 70% speed

Figure 17 shows that the stall event and corresponding rotor overspeed occurred between 125 and 175 revolutions. This information provided a time to start and stop the FFT. Figure 18 shows a Kulite pressure trace of a steam-induced stall.

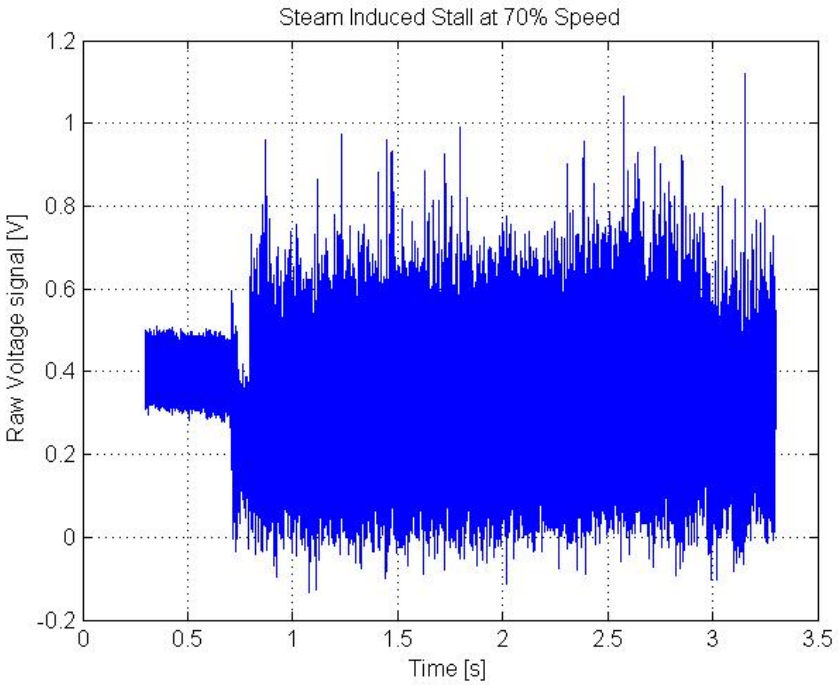


Figure 18. Raw Kulite data trace of steam stall at 70% speed

Figure 19 shows the contour plot corresponding to the raw data presented in Figure 18. The contour plot shows the presence of a stall precursor, once per revolution frequency, and a rotating stall cell with a harmonic.

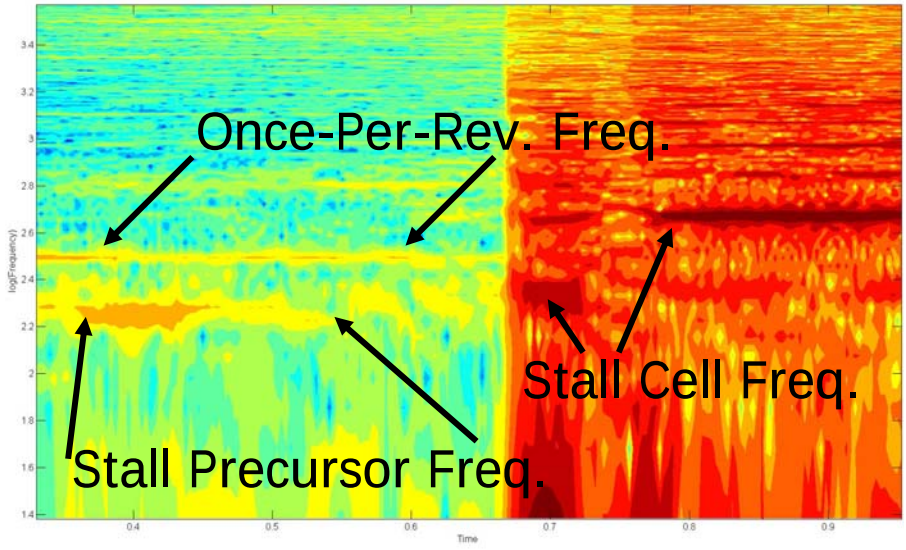


Figure 19. Contour plot of steam induced stall at 70% speed

Appendix E contains the steam stall plots for 70%, 90% and 95% speed, the RPM plots, and raw data traces corresponding to each stall event.

## E. HOT-FILM TRACES

The hot-film velocity data for each stall run were reduced using the Matlab code found in Appendix B. The presence of a stall precursor in the velocity field could be shown through the cross correlation of the hot film data. Figure 20 shows a typical hot-film trace for a near stall event.

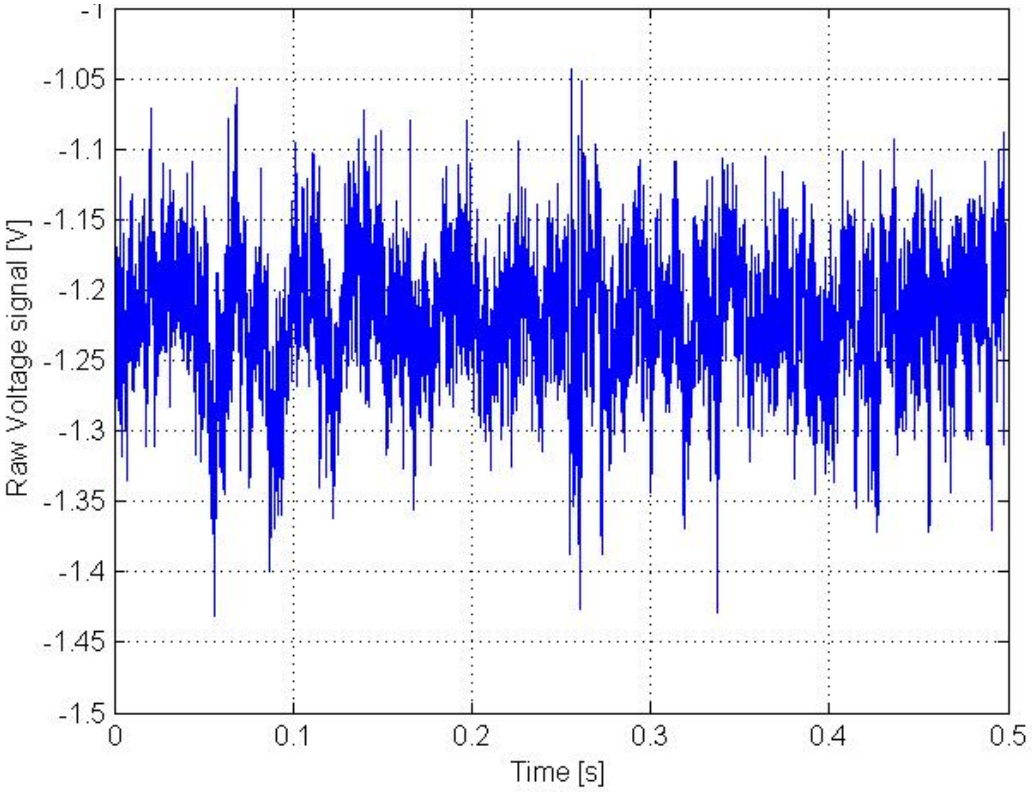


Figure 20. Hot-film raw data for a steam run at 70% speed, near stall

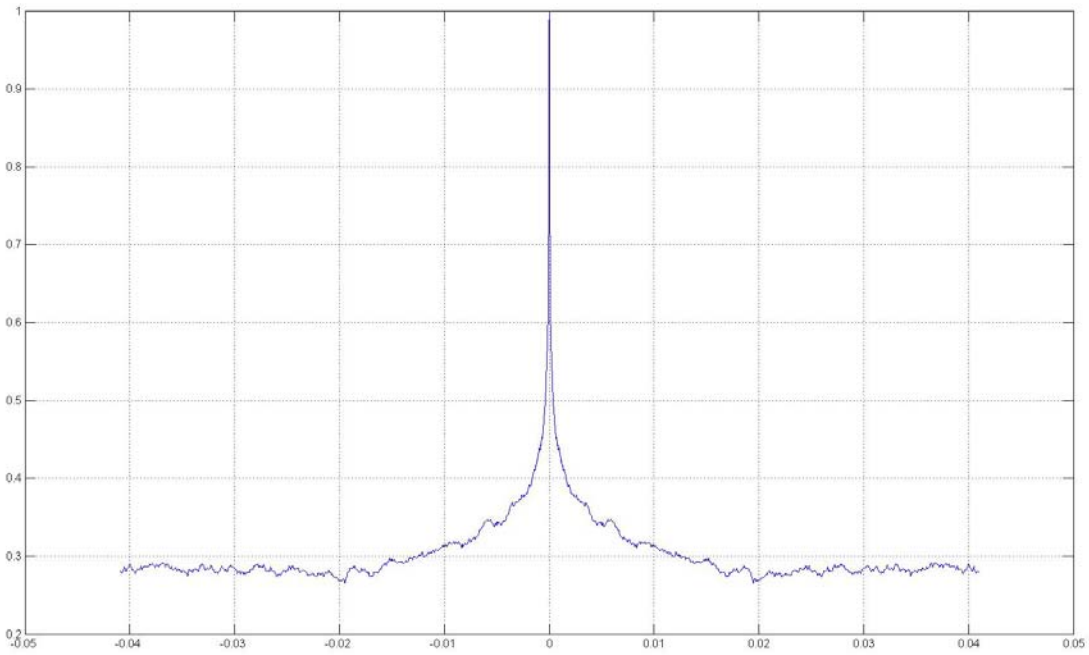


Figure 21. Auto-correlation of hot-film data

Figure 21 shows the auto-correlation of the hot-film data for a steam run at 70% speed. The auto-correlation of the data would show a velocity oscillation indicating the presence of a stall precursor. Previous research by Payne suggested that the stall precursor was evident in the auto-correlation of the hot-film data (Ref. 4). Figure 21 does not show a significant measurement of a stall precursor using the hot-film data. A periodogram of the same data, or a waterfall plot of the FFT, is shown in Figure 22.

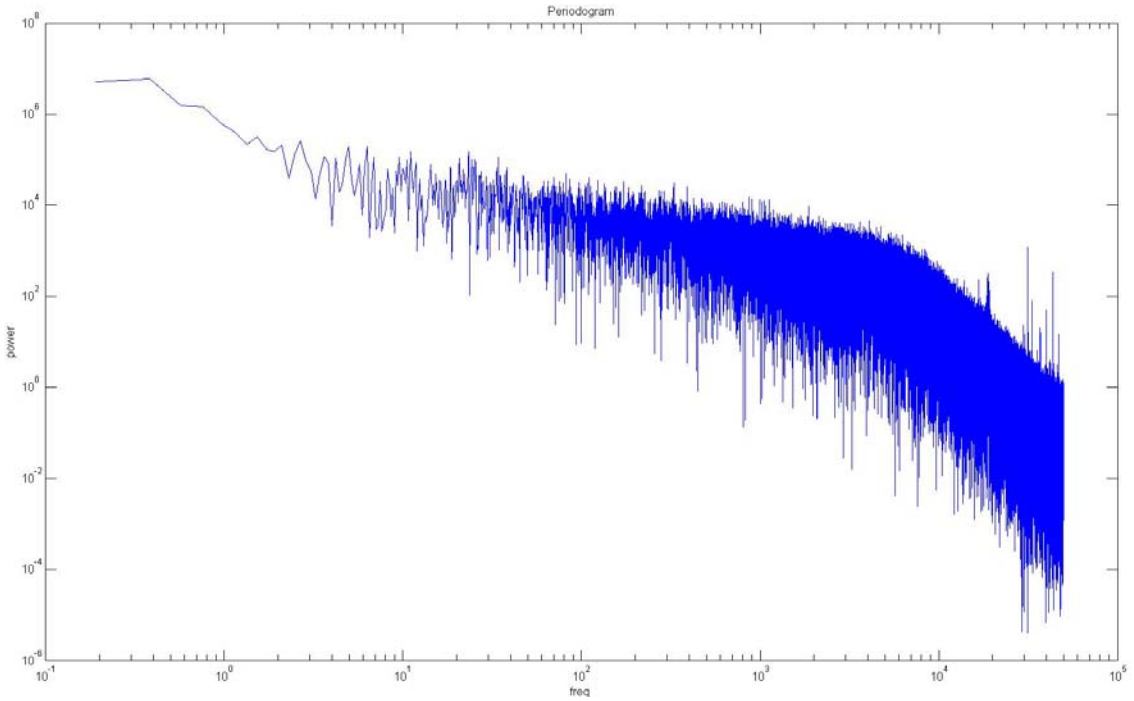


Figure 22. Periodogram of hot-film data

Figure 22 shows a spike in frequency response at the blade passing frequency, but does not show a once-per revolution or precursor frequency. Figure 23 shows an auto-correlation of a stall event at 70% speed.

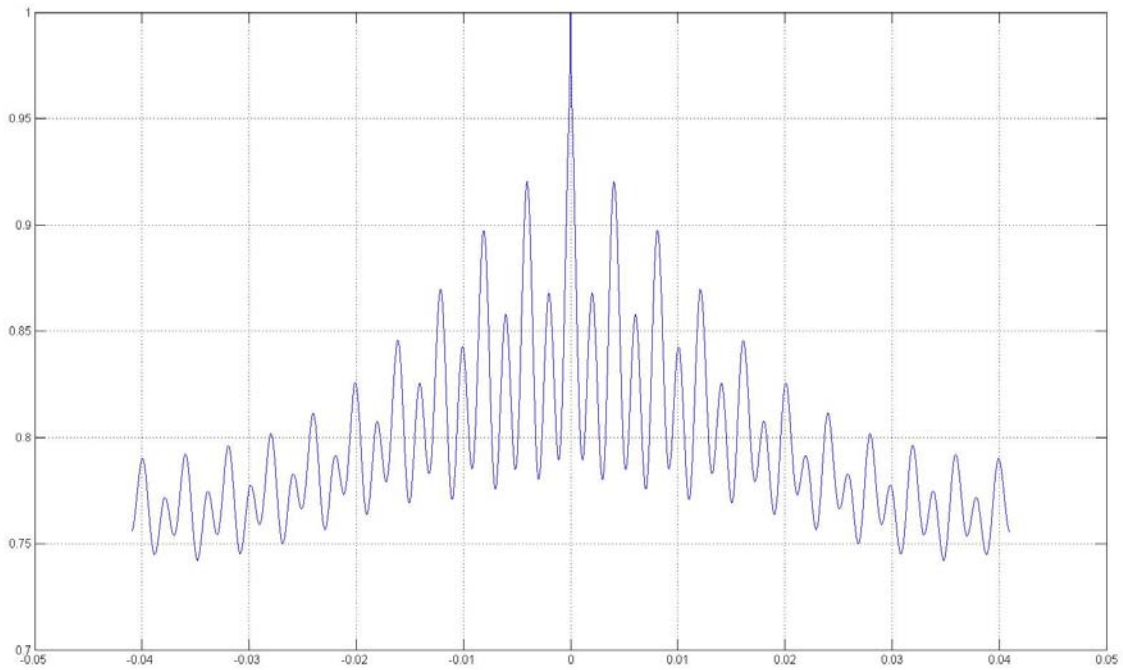


Figure 23. Auto-correlation of hot-film data during steam stall

In Figure 23, the stall cell dominates the auto-correlation of the hot-film data. Figure 24 shows the periodogram for the same data.

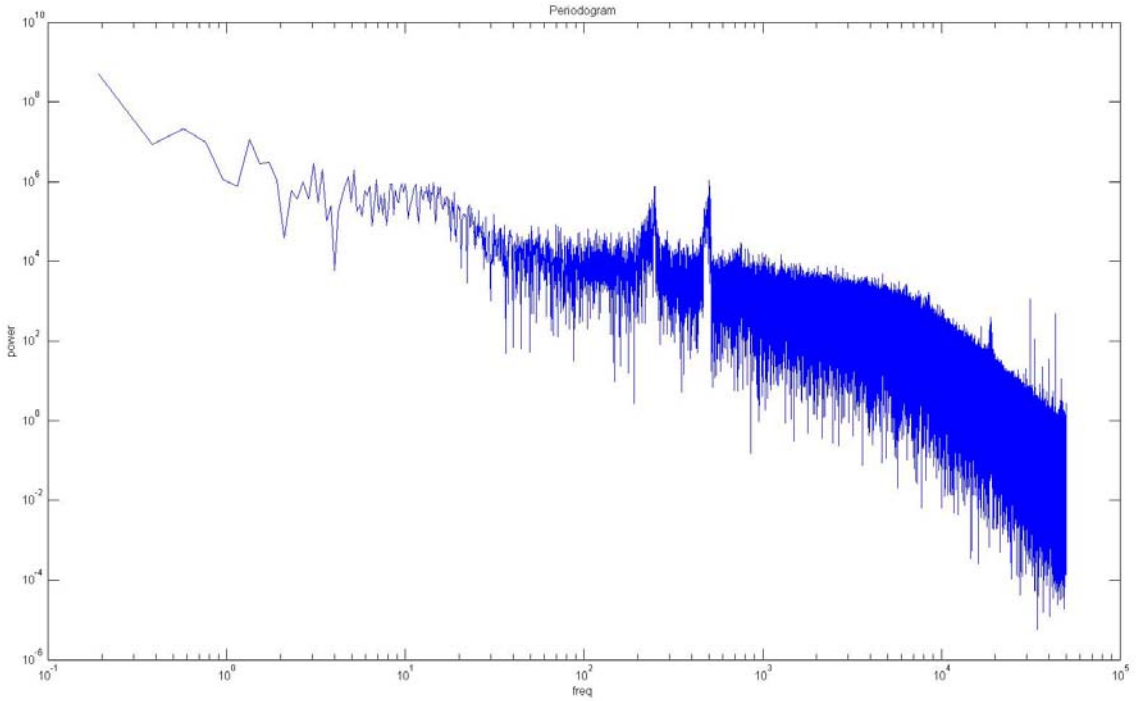


Figure 24. Periodogram of steam stall hot-film data

Figure 24 shows a frequency spike in the hot-film data at the stall cell frequency and its first harmonic. The plot also shows the blade passing frequency. A stall precursor frequency and once-per-revolution frequency are not present as the rotation of the stall cell dominates the data. The autocorrelations and periodograms for the other steam dump and steam stall runs are included in Appendix F.

## F. COMPRESSOR MAP WITH PRECURSOR LINE

The compressor map progression of Kulite plots showed a very obvious development of a stall precursor as the throttle setting moved towards stall. Figure 25 shows an updated compressor map with a precursor line subjectively drawn at the throttle settings where it first appeared. This subjective precursor map is supported by the contour plot progressions shown in Appendix D.

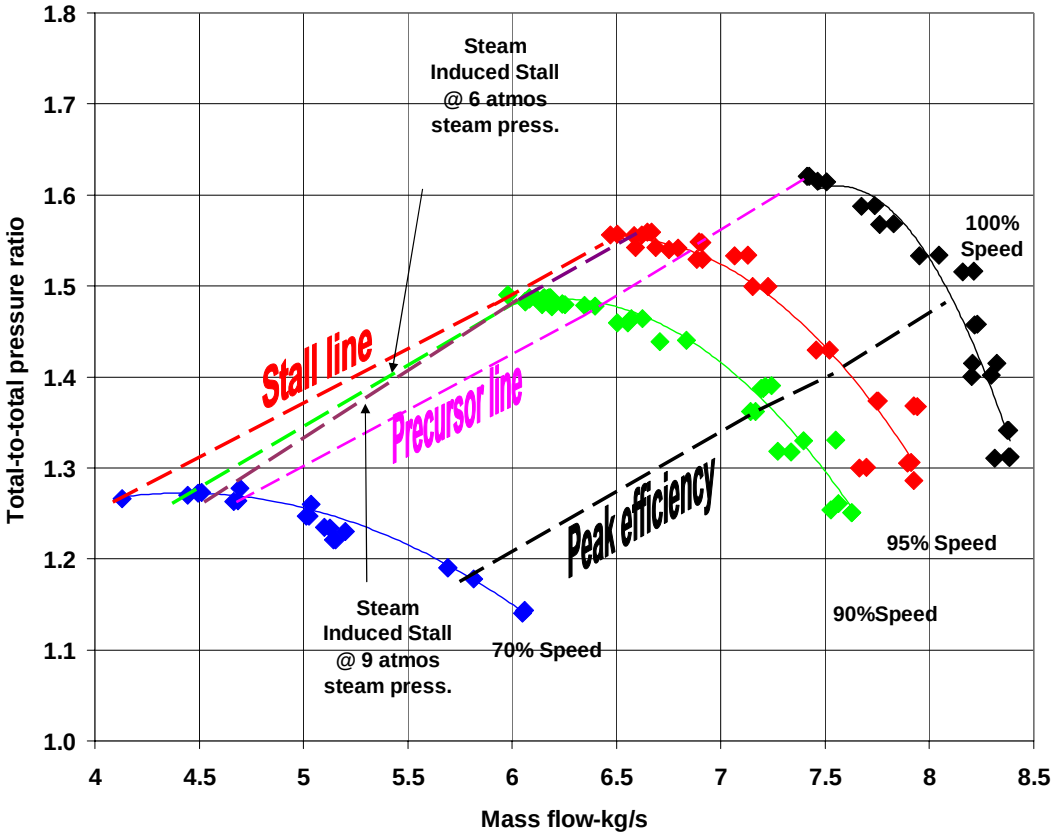


Figure 25. Compressor map with precursor line

THIS PAGE INTENTIONALLY LEFT BLANK

# VI. CONCLUSIONS

Several results are drawn from the various data collected and analyzed in this experiment. First, the verification of the inlet mass flow measurement showed that the data recorded at the inlet bellmouth matched the mass flow measured by the flow measurement nozzle. Since these measurements agree, the rotor inlet mass flow measurements can be used in the case of a shortened inlet. This verifies the throttle settings used in the experiment and validates the location of steam-induced stall on the compressor map. In future testing, the inlet flow pipe may be shortened, which allows for more distortion of the inlet flow. Distorted inlet flow is closer to the environment experienced during typical aircraft operation.

The compressor map shows a reduction in steam stall margin for 70% speed, but the steam-induced stall margin at 90% and 95% speed remain unchanged compared to data taken at 6 atmosphere steam. Table 2 shows the overall reduction in stall margin for both 6 atmosphere and 9 atmosphere steam.

| Speed | Steam @ 6 atmos. | Steam @ 9 atmos. |
|---|---|---|
| 70% | 21% | 31% |
| 90% | 12% | 12% |
| 95% | 8% | 8% |

Table 2. Steam stall margin

The presence of a stall precursor in both the steady state and steam-induced stall data suggest that active control of stall could be explored. Several methods are currently being studied to improve the stall margin of a compressor through active control (Ref. 3).

The steam-induced stall data also showed a similar precursor. The precursor is present between approximately 50% and 65% rotor speed at and above the precursor line. The speed, duration, and throttle location of the precursor all support the presence of a modal oscillation as suggested by Camp and Day (Ref. 1). Furthermore, the hot-film data did not indicate the presence of a stall precursor as strongly as in previous research.

THIS PAGE INTENTIONALLY LEFT BLANK

# VII. RECOMMENDATIONS

Several improvements can be made to this study to both recreate real world operating conditions as well as better measure the stall precursor. First, the validation of the mass flow rate data suggests that the inlet flow pipe can be shortened. This would introduce more inlet distortion to the flow during a steam dump, a flow condition that would more closely resemble the inlet flow of F-35C aircraft.

In this study, a rotor-only configuration was studied. Moving to a full stage would give a more realistic operating condition and also increase the possibility of surge. Further study could be conducted on the stall margin of the full stage and the presence of the stator could affect the precursor oscillation.

Several Kulite pressure probes in this study were located axially within the rotor. These Kulite transducers did not give evidence of a stall precursor or even, in some cases, the presence of a once per revolution frequency. The Kulite probes 1, 2, 7, 8, and 9 were most effective at measuring the stall precursor oscillation. More probes should be added in front of the rotor and behind the stator to better measure the stall precursor.

The cross correlation of the hot-film data did not show the presence of a stall precursor. Only two hot-film probes are used during typical operation, limiting the effectiveness of a cross correlation. The addition of more hot-film probes could better measure the presence of the stall precursor. However, the Kulite pressure data very successfully identified the stall precursor, so the hot-film data may not even be needed in future studies of the stall precursor in this machine.

Better identification and quantification of the stall precursor could lead to the potential active control of a compressor's throttle to increase stall margin. Cross-correlation of the Kulite data or an improved data reduction technique could help achieve faster stall precursor identification.

THIS PAGE INTENTIONALLY LEFT BLANK

# LIST OF REFERENCES


1. Camp, T. R. and Day, I. J. "A Study of Spike and Modal Stall Phenomena in a Low Speed Axial Compressor." ASME 97-GT-526. International Gas Turbine & Aeroengine Congress & Exhibition. Orlando, Florida, June 1997.

2. Cumpsty, N. A. Compressor Aerodynamics. Longman Scientific & Technical. New York, 1989.

3. Freeman, C., Day, I. J., Wilson, A. G., and Swinbanks, M. A. "Experiments in Active Control of Stall on an Aerorengine Gas Turbine." ASME 97-GT-280. International Gas Turbine & Aeroengine Congress & Exhibition. Orlando, Florida, June 1997.

4. Gannon, A. J., Hobson, G. V., Shreeve, R. P., and Villescas, I. J. "Experimental Investigation During Stall and Surge in a Transonic Fan Stage & Rotor-Only Configuration." ASME GT2006-90925. Proceedings of TURBO EXPO. Barcelona, Spain, May 2006.

5. Garnier, V. H., Epstein, A. H., and Greitzer, E. M. "Rotating Waves as a Stall Inception Indication in Axial Compressors." Journal of Turbomachinery. Transactions of the ASME. Vol. 113. 290-302. April 1991.

6. Lakshminarayana, Budugur. Fluid Dynamics and Heat Transfer of Turbomachinery. John Wiley & Sons, Inc. New York, 1996.

7. Payne, T., Inlet Flow-Field Measurements of a Transonic Compressor Rotor Prior to and During Steam-Induced Rotating Stall. Master's Thesis. Naval Postgraduate School. Monterey, California, September 2005.

8. Sanger, N. I. "Design of a Low Aspect Ratio Transonic Compressor Stage Using CFD Techniques." ASME Journal of Turbomachinery. Vol. 118. 479-491. July 1996.

9. Zarro, S. E., Steady – State and Transient Measurements Within a Compressor Rotor During Steam-Induced Stall at Transonic Operational Speeds. Master's Thesis. Naval Postgraduate School. Monterey, California, September 2006.

# APPENDIX A: KULITE DATA REDUCTION PROGRAMS

**Generic_contour_plot.m:**

```
%M-file to pull in data and plot it out


close all;
clear all;


%Raw data
tic
Raw_data=dlmread(input('Type the name of the data file in single quotes (with the .csv):'),',',input('Type the starting column and row, then .., then the finishing column and row in single quotes (For example, A6..N56000):'));
toc
%tach=Raw_data(:,8);
%time=Raw_data(:,1);
data=Raw_data(:,2:13);


% Constants
s=input('What speed was this data set collected at? (.7, .9, .95, or 1):');
RPM_design = s.*27085;          % Design RPM in RPM
RPM_Hz     = RPM_design/60; % Design RPM in Hz


[time,volts,tach,Loc,RPM] = Process_data(Raw_data);
[RPM(:,2)]                = mov_avg(RPM(:,1),RPM(:,2),1,1);
K=input('Enter the number of the kulite that you wish to plot:');
%Input value for number of revs
B=input('Enter a binary minus one (such as 511 for one rev) to select the number of revs:');


timeshort1=time(1:B,1);
deltat1=(timeshort1(end,1)-timeshort1(1,1))/(length(timeshort1));
```

```
[Loc] = Find_loc(time,tach);
kulite1=data(:,K);

%Figure 1;
%_A particular column of the data is plotted
plot_data(1,Raw_data);
title('Near Stall Setting at 90% Raw Data');

%Figure 2;
%_The RPM is plotted
plot_rpm(2,RPM/RPM_design);

%Figure 3;
count=1;
A1=input('Type the number of the revolution at which you want to start the FFT:');
A2=input('Type the number of the revolution at which you want to finish the FFT:');
for A=A1:A2;

   %_Locates triggers
   LocA=(Loc(A):(Loc(A)+B));

   yfftA=kulite1(LocA,1);
   Ya=fft(yfftA);
   Ya(1)=[];
   power1=abs(Ya(1:(length(yfftA)/2))).^2;
   N1=length(yfftA);
   n1=(1:(N1)/2)';
   freq1=(n1)/((N1)*deltat1);

   time1=(time(Loc(A)))*(ones(size(freq1)));

   if 0
```

```
        hold on;
        figure(A);5
        semilogy(freq1,power1,'r');

    end

    freq_fall(count,:)=freq1';
    power_fall(count,:)=power1';
    time_fall(count,:)=time1';

    count=count+1;

end
harmonic=.5;
Blade_no=22;
temp=mean(1./diff(time(Loc)));  %RPS
temp_2=harmonic*Blade_no*temp;   %Blade passing frequency
temp_3=min(find(freq_fall(1,:)>temp_2));  %Cut-off frequency
freq_fall=freq_fall(:,1:temp_3);
time_fall=time_fall(:,1:temp_3);
power_fall=power_fall(:,1:temp_3);
freq_fall=log10(freq_fall);
power_fall=log10(power_fall);

%Figure 4
figure(4);
%count=1;
%for A=A1:A2;

    contourf(time_fall,freq_fall,power_fall,15);
    shading flat
```

```
%_Graph settings
xlabel('Time');
ylabel('log(Frequency)');
```

**Process_data.m:**

```
% m function file to organize the data of the Raw data file

function [time,volts,tach,Loc,RPM] = Process_data(Raw_data)

% Data is sorted into simpler to use groups
time    = Raw_data(:,1);    % Kulite time data
volts   = Raw_data(:,2:12); % Kulite raw voltage data
tach    = Raw_data(:,13);   % Kulite trigger voltage
samples = length(time);     % Number of samples

% Trigger level is calculated
Trig = mean([min(tach) max(tach)]);

% Location of trigger points and correction to exact trigger timing point
Loc = find( tach(2:samples)<Trig & tach(1:samples-1)>Trig ); %location of time of start of rev
Hz = (length(Loc)-1)/(time(Loc(end))-time(Loc(1))); % Frequency of rotor revolution over the sample period

% If Loc (location) if at the beggining of the sample it is discarded
if Loc(1) < 3
   Loc = Loc(2:end);
end

% Last trigger is discarded to ensure trailing zeros resulting from probe lining up do not effect the calculations.
Loc = Loc(1:(end-1));

% Timing correction to ensure that each sample begins at the correct time
d_time_Loc(:,1) = time(Loc+1)-time(Loc);  % Time interval between trigger and next time interval
d_tach_Loc(:,1) = tach(Loc+1)-tach(Loc);  % Ramp slope between trigger and next time interval
m             = d_tach_Loc./d_time_Loc; % Slope
c             = tach(Loc);              % Intercept
time_err      = (Trig - c)./m;          % Error in trigger timing

% Error in trigger timing is converted to be directly subtracted from the period
```

```
% time_err = (time_err(2:end)-time_err(1:end-1));

% The RPM based on each trigger is calculated
RPM = time(Loc(2:end)) - time(Loc(1:end-1));
RPM = RPM + (time_err(2:end)-time_err(1:end-1));
RPM = 60./RPM;

%Hz_old = Hz;
RPM    = [time(Loc(2:end)) RPM]; % First column is time signal and the second is the
RPM
```

**mov_avg.m:**

```
% m-function file to calculate the moving averages at a particular point
% x,y data
% points ahead and behind central one ie 0 return same data, 1 = 3 points, 2 = 5 points
% n, polynomial to fit, 0 = average, 1 = linear, 2 = parabolic etc

function [y_avg] = mov_avg(x,y,points,N)

y_avg = y;

x_poly = zeros(1,(2*points+1));
y_poly = zeros(1,(2*points+1));

for i = (points+1):((length(x)-points)-1)
   for j = -points:points
      x_poly(j+points+1) = x(i+j);
      y_poly(j+points+1) = y(i+j);
   end
   y_avg(i) = mean([max(y_poly) min(y_poly)]); % Most effective method, just take the
mean of the max and min
end

% Leading points
if points > 0
   % Leading few points
   for j = 1:(2*points+1)
      y_poly(j) = y(j);
   end

   % Leading moving average
   for i = 1:points
      y_avg(i)  = mean([max(y_poly) min(y_poly)]);
```

```
    end % for i = 1:points

    % Trailing few points
    for j = (2*points+1):-1:1
       y_poly(j) = y(length(x)-j+1);
    end

    % Trailing moving average
    for i = (length(x)-points):length(x)
       y_avg(i)  = mean([max(y_poly) min(y_poly)]);
    end % for i = 1:points
end % if points > 0
```

**Find_loc.m:**

```
% Find_loc
% m-function file to find the position of the trigger for each once per rev

function [Loc] = Find_loc(time,tach);

% Number of samples
samples = length(time);

% Trigger level is calculated
Trig = mean([min(tach) max(tach)]);

% Location of trigger points and correction to exact trigger timing point
Loc = find( tach(2:samples)<Trig & tach(1:samples-1)>Trig ); % Location of time of start of rev
```

**Plot_rpm.m:**

```
% Find_loc
% m-function file to find the position of the trigger for each once per rev

function [Loc] = Find_loc(time,tach);

% Number of samples
samples = length(time);

% Trigger level is calculated
Trig = mean([min(tach) max(tach)]);
```

```
% Location of trigger points and correction to exact trigger timing point
Loc = find( tach(2:samples)<Trig & tach(1:samples-1)>Trig ); % Location of time of start of rev
```

**Plot_data.m:**

```
% m-file to plot a certain time part of the stall data file

function [fred] = Plot_data(fig_no,Raw_data)

% Time period is defined
time_start = Raw_data(1,1);   % Start time of sample
time_end   = Raw_data(end,1); % End time of sample
%time_start = 16.3           % User defined start time
%time_end   = 17             % User defined end time

% Time period entry points are found
temp = find(Raw_data(:,1)>time_start & Raw_data(:,1)<time_end);

% figure is plotted and trimmed
%if bool_new_fig
   %figure(fig_no); close; figure(fig_no);
   %else
   %figure(fig_no);
   %end

%if subplot_no ~= 0
%    subplot(subplot_tot,1,subplot_no)
%end % if subplot_no ~= 0

P=input('Enter the number of the column of data that you want to plot (This is the kulite number plus 1):');
plot(Raw_data(temp,1),Raw_data(temp,P),'b')
%hold on
xlabel('Time [s]'); ylabel('Raw Voltage signal [V]')
grid on

temp = axis;
%h                          =                          line([time(Loc(1:end),Data_column) time(Loc(1:end),Data_column)]',(ones(size(Loc(1:end)))*([temp(3) temp(4)]))');
%set(h,'Color',[0 0 0]);  % Makes colour of line black
%h   =   line([time(Loc(2:end),Data_column)-time_err   time(Loc(2:end),Data_column)-time_err]',(ones(size(Loc(2:end)))*([temp(3) temp(4)]))');
%set(h,'Color',[0 0 0]);  % Makes colour of line black
```

THIS PAGE INTENTIONALLY LEFT BLANK

# APPENDIX B: HOT-FILM CROSS CORRELATION PROGRAM

**fft_auto.m:**

```
%   Script to plot the FFT and Autocorrelation of a hotwire signal

close all
clear all

a=dlmread('95_PE_NS3_STEAM.E0001');
%time=a(1:1024,1);
%voltage=a(1:1024,2);

time=a(:,1);
voltage=a(:,2);

figure(1)
plot(time,voltage)
xlabel('time')
ylabel('voltage')
title('Raw Signal')

N=length(voltage)-1;
deltat=.00001;

Y = fft(voltage);
Y(1)=[];
n=length(Y);
power = abs(Y(1:n/2)).^2;
nyquist = .5;
%freq = (1:n/2)/(n/2)*nyquist;
freq = (1:N/2)/(N*deltat);
```

```
figure(2)
loglog(freq,power)
%plot(freq,power)
%semilogy(freq,power)
xlabel('freq')
ylabel('power')
title('Periodogram')

figure(3)
ave_volt=mean(voltage);
volt=voltage-ave_volt;
%Plot the fluctuating voltage
plot(time,volt)
figure(4)
%No. of points to take the autocorrelation over
m=4096;
[C,lags]=xcorr(volt,m,'coeff');
%plot(time,C)

plot(lags,C)

figure(5)
auto_time=deltat*lags;
plot(auto_time,C)
grid on
```

# APPENDIX C: COMPRESSIBLE FLOW MASS FLOW RATE CALCULATION

Total temperature, Total pressure, and Static pressure are measured quantities.

1 = inlet

$T_{t1}$ = total or stagnation temperature

$P_{t1}$ = total or stagnation pressure

$P_1$ = static pressure

$V_t = \sqrt{2C_p T_{t1}}$ (Definition of stagnation velocity)

$$X_1 = \frac{V_1}{\sqrt{2C_p T_{t1}}} = \frac{V_1}{V_t}$$ (Definition of X formulation)

$$T_{t1} = T_1 + \frac{V_1^{\,2}}{2C_p}$$

$$\frac{P_1}{P_{t1}} = \left(\frac{T_1}{T_{t1}}\right)^{\frac{\gamma-1}{\gamma}} = \left(1 - X_1^{\,2}\right)^{\frac{\gamma}{\gamma-1}} = PR$$

$$X_1 = \sqrt{1 - PR^{\frac{\gamma-1}{\gamma}}} \Rightarrow A$$

$$\dot{m} = \rho_1 A V_1 = \left(\frac{\rho_1}{\rho_{t1}}\right)\left(\frac{V_1}{V_{t1}}\right) A\rho_{t1} V_{t1} = \left(\frac{P_1}{P_{t1}}\right)\left(\frac{T_{t1}}{T_1}\right) X_1 A \frac{P_{t1}}{RT_{t1}} \sqrt{2C_p T_{t1}} =$$

$$\left(1 - X_1^{\,2}\right)^{\frac{\gamma}{\gamma-1}} X_1 A \frac{P_{t1}}{RT_{t1}} \sqrt{2C_p T_{t1}} \Rightarrow D$$

Use Equation A with the measured static pressure ($P_1$) and stagnation pressure ($P_{t1}$) to get $X_1$.

Subsitute that result with Equation A to get $\dot{m}$.

THIS PAGE INTENTIONALLY LEFT BLANK

# APPENDIX D: CONTOUR PLOT PROGRESSIONS

70% Speed Progressions

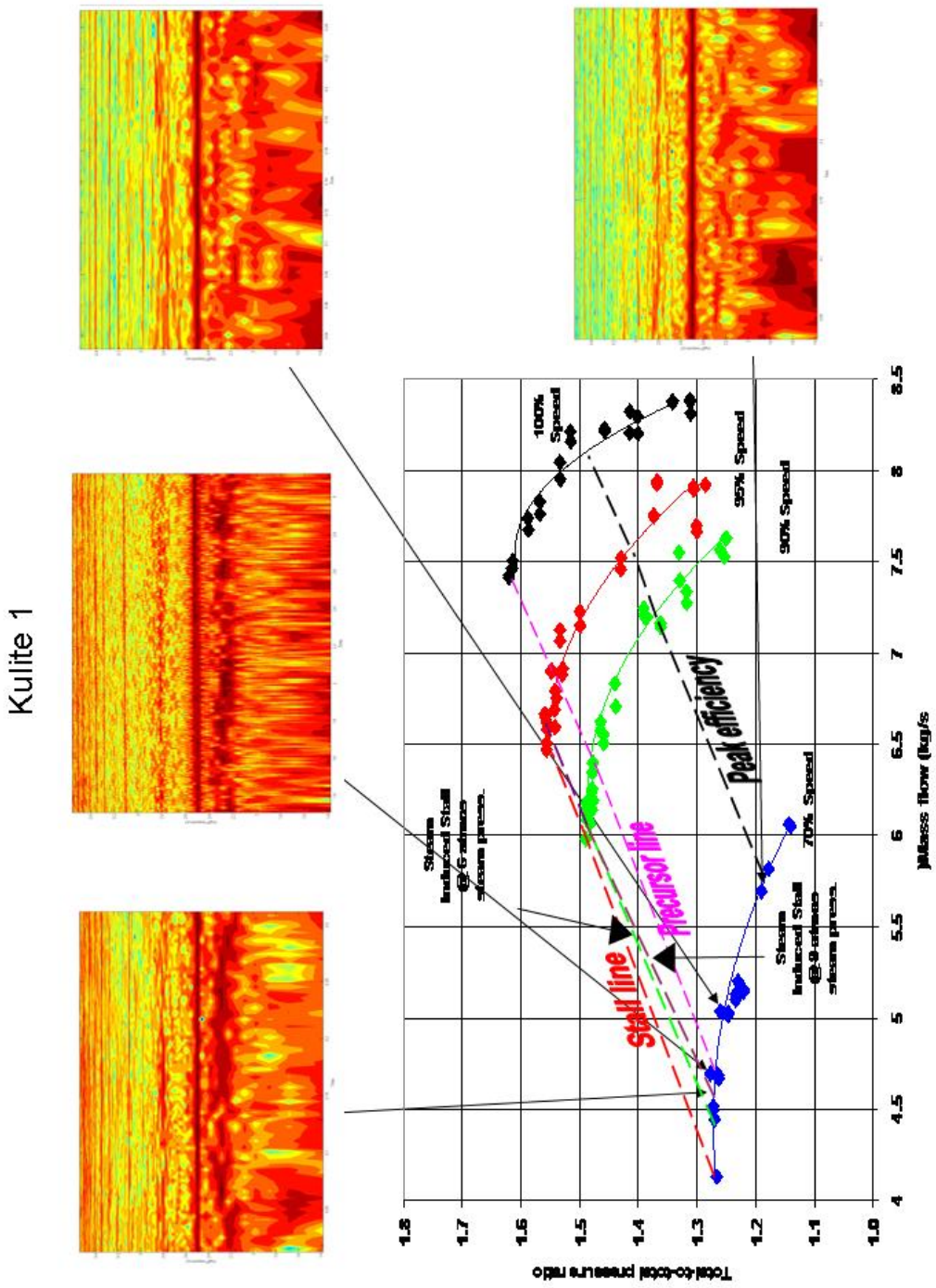

Kulite 2

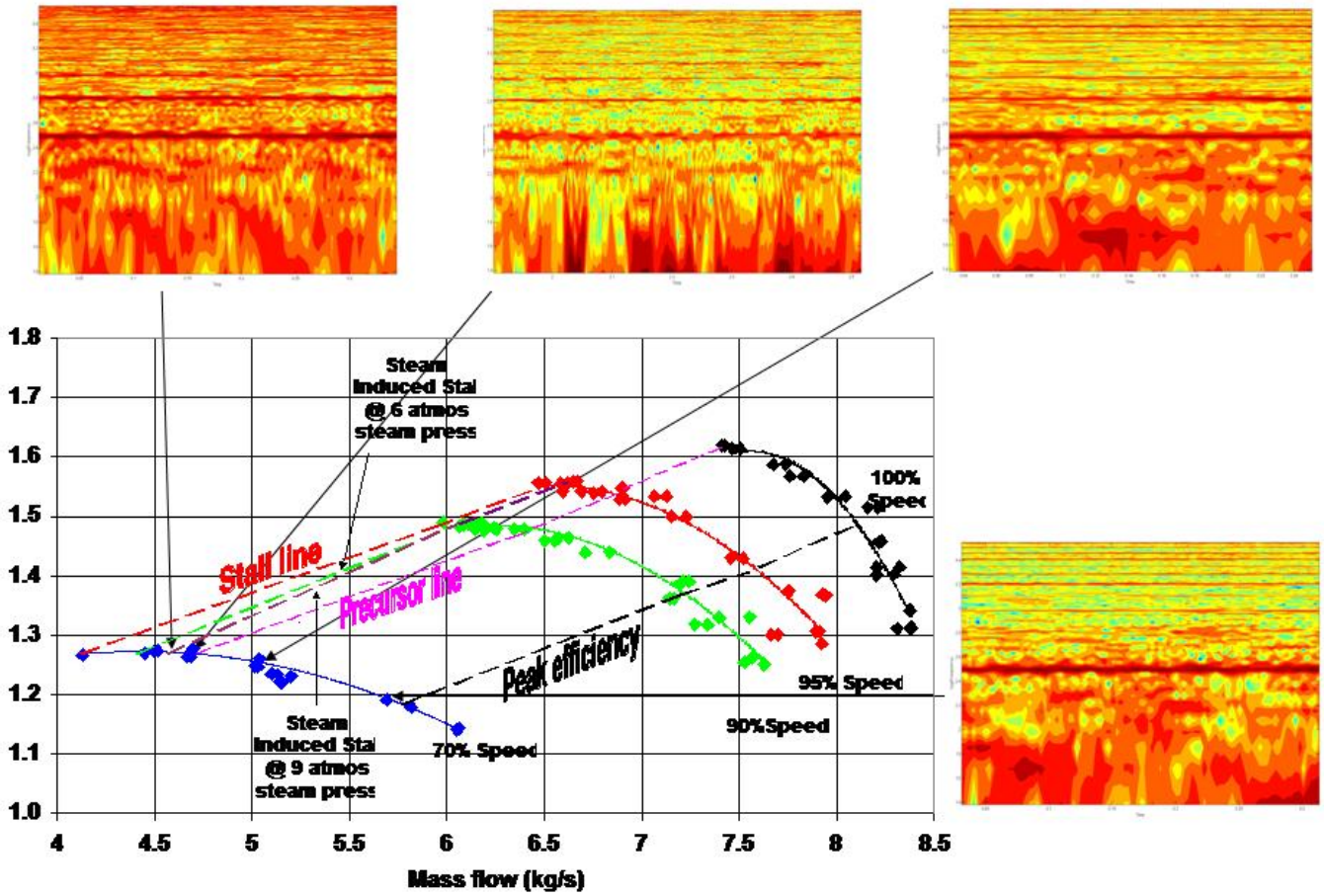
1.8
1.7
1.6
1.5
1.4
1.3
1.2
1.1
1.0
4
4.5
5
5.5
6
6.5
7
7.5
8
8.5
Mass flow (kg/s)
Steam
Induced Stal
@ 6 atmos
steam press
Stall line
Precursor line
Peak efficiency
100%
Speed
95% Speed
90%Speed
70% Speed
Steam
Induced Stal
@ 9 atmos
steam press

# Kulite 7

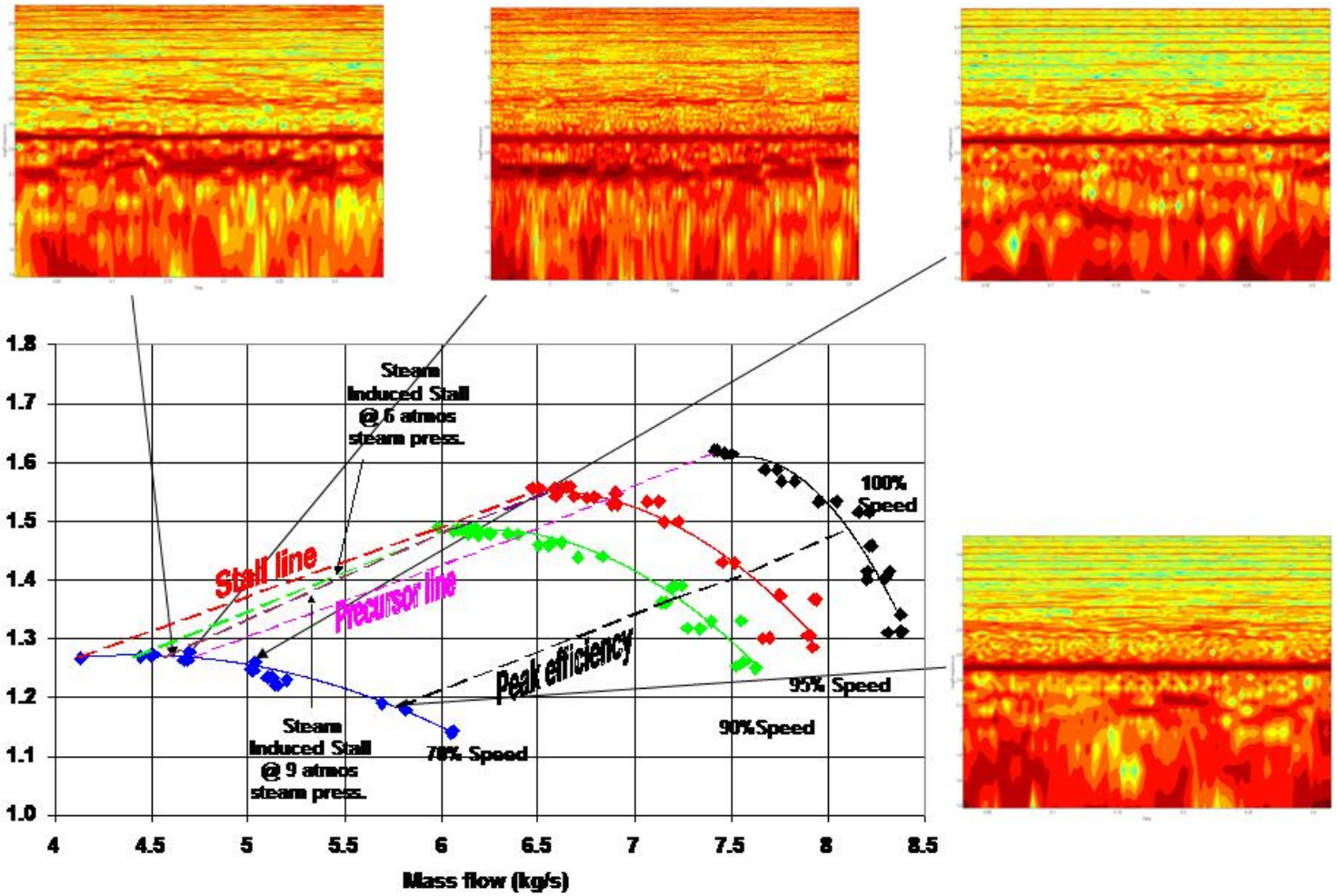
Steam
Induced Stall
@ 6 atmos
steam press.
Stall line
Precursor line
Peak efficiency
100%
Speed
95% Speed
90%Speed
70% Speed
Steam
Induced Stall
@ 9 atmos
steam press.
1.8
1.7
1.6
1.5
1.4
1.3
1.2
1.1
1.0
4
4.5
5
5.5
6
6.5
7
7.5
8
8.5
Mass flow (kg/s)

# Kulite 8

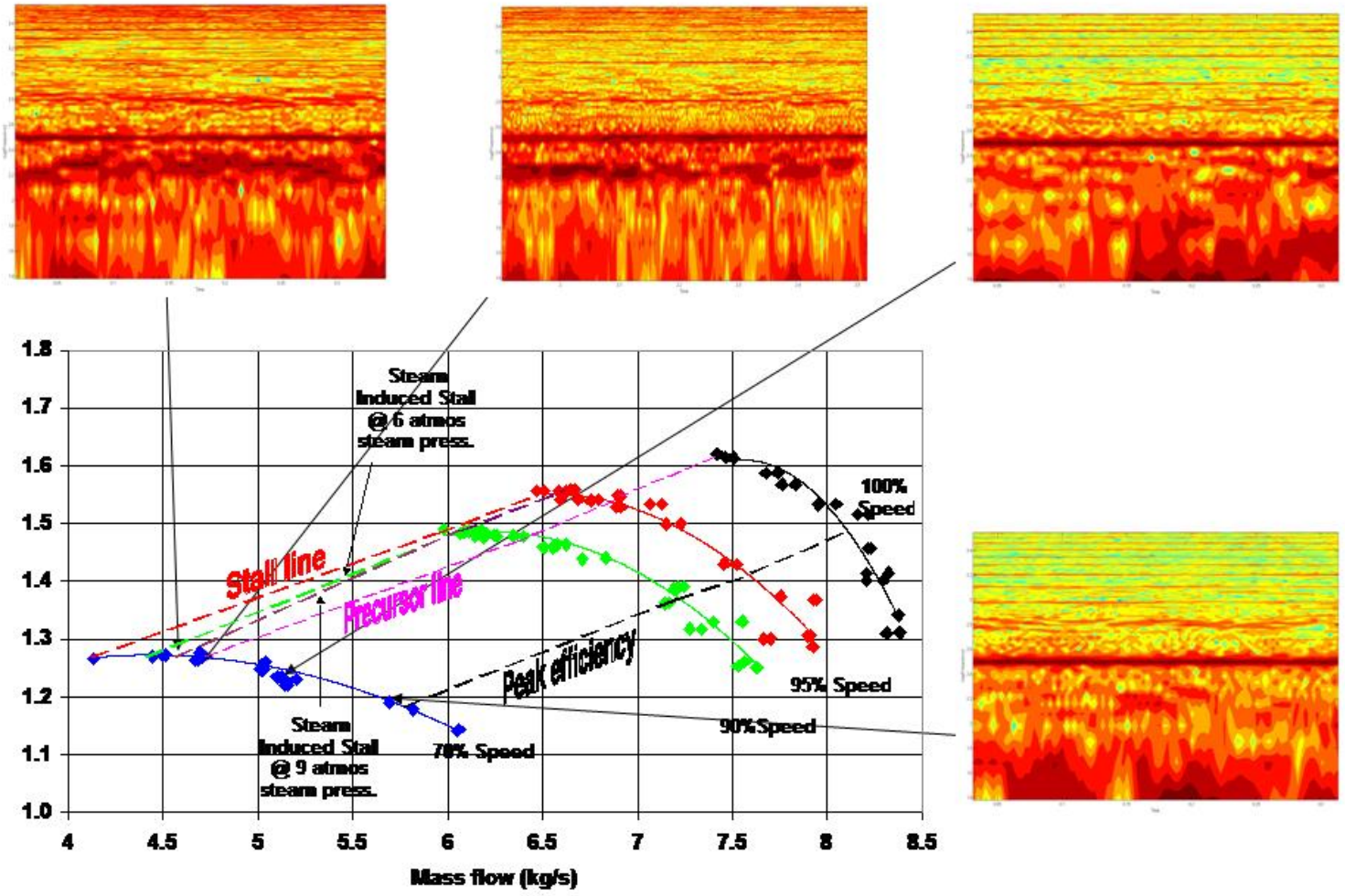
Steam
Induced Stall
@ 6 atmos
steam press.
Stall line
Precursor line
Peak efficiency
100%
Speed
95% Speed
90% Speed
70% Speed
Steam
Induced Stall
@ 9 atmos
steam press.
1.8
1.7
1.6
1.5
1.4
1.3
1.2
1.1
1.0
4
4.5
5
5.5
6
6.5
7
7.5
8
8.5
Mass flow (kg/s)

# Kulite 9

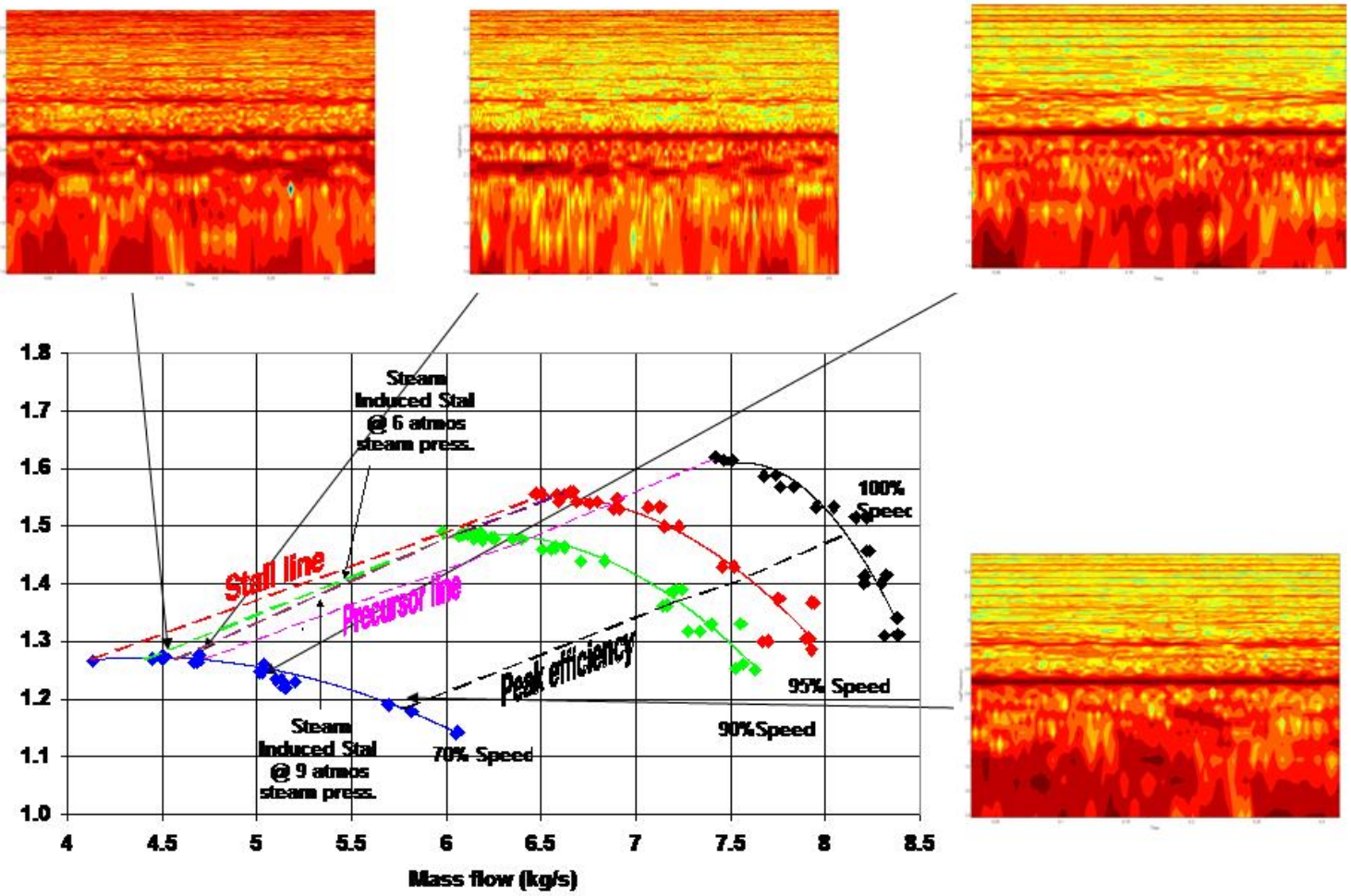
1.8
1.7
1.6
1.5
1.4
1.3
1.2
1.1
1.0
4
4.5
5
5.5
6
6.5
7
7.5
8
8.5
Mass flow (kg/s)
Steam Induced Stal @ 6 atmos steam press.
Steam Induced Stal @ 9 atmos steam press.
Stall line
Precursor line
Peak efficiency
100% Speed
95% Speed
90% Speed
70% Speed

90% Speed Progressions:

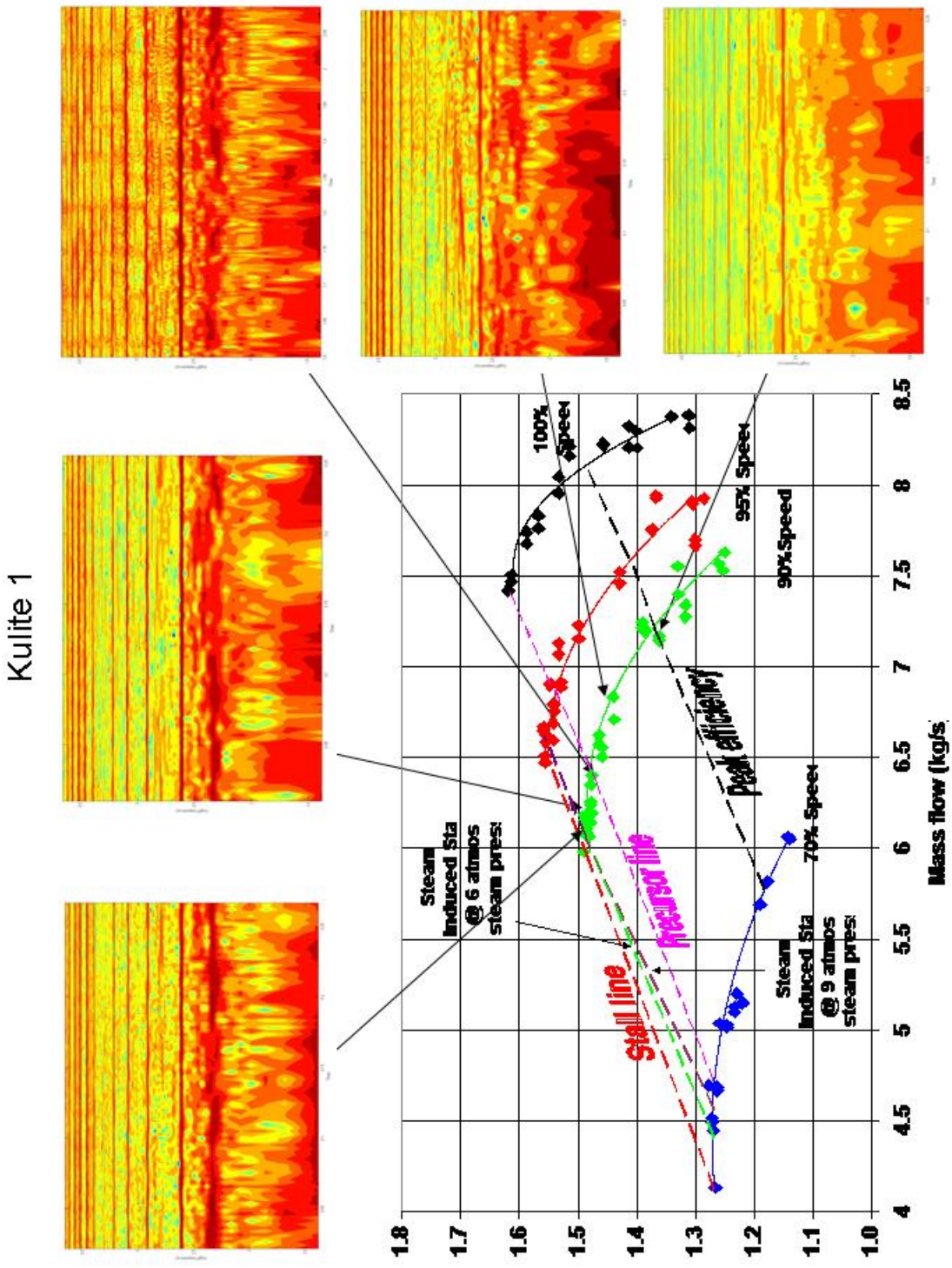

Kulite 2

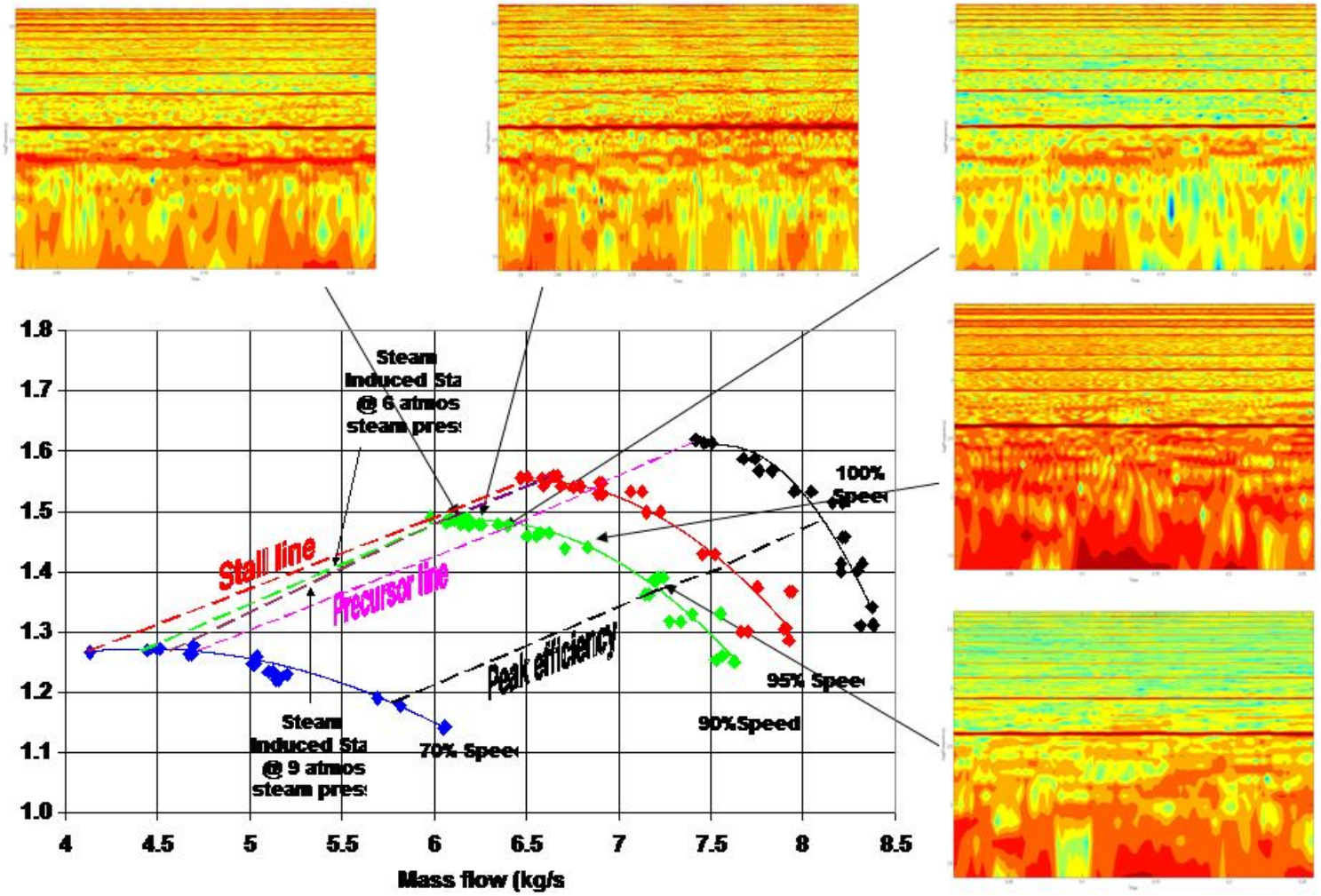
Steam
Induced Sta
@ 6 atmos
steam pres
Stall line
Precursor line
Peak efficiency
100%
Speed
95% Speed
90%Speed
70% Speed
Steam
Induced Sta
@ 9 atmos
steam pres
1.8
1.7
1.6
1.5
1.4
1.3
1.2
1.1
1.0
4
4.5
5
5.5
6
6.5
7
7.5
8
8.5
Mass flow (kg/s

Kulite 7

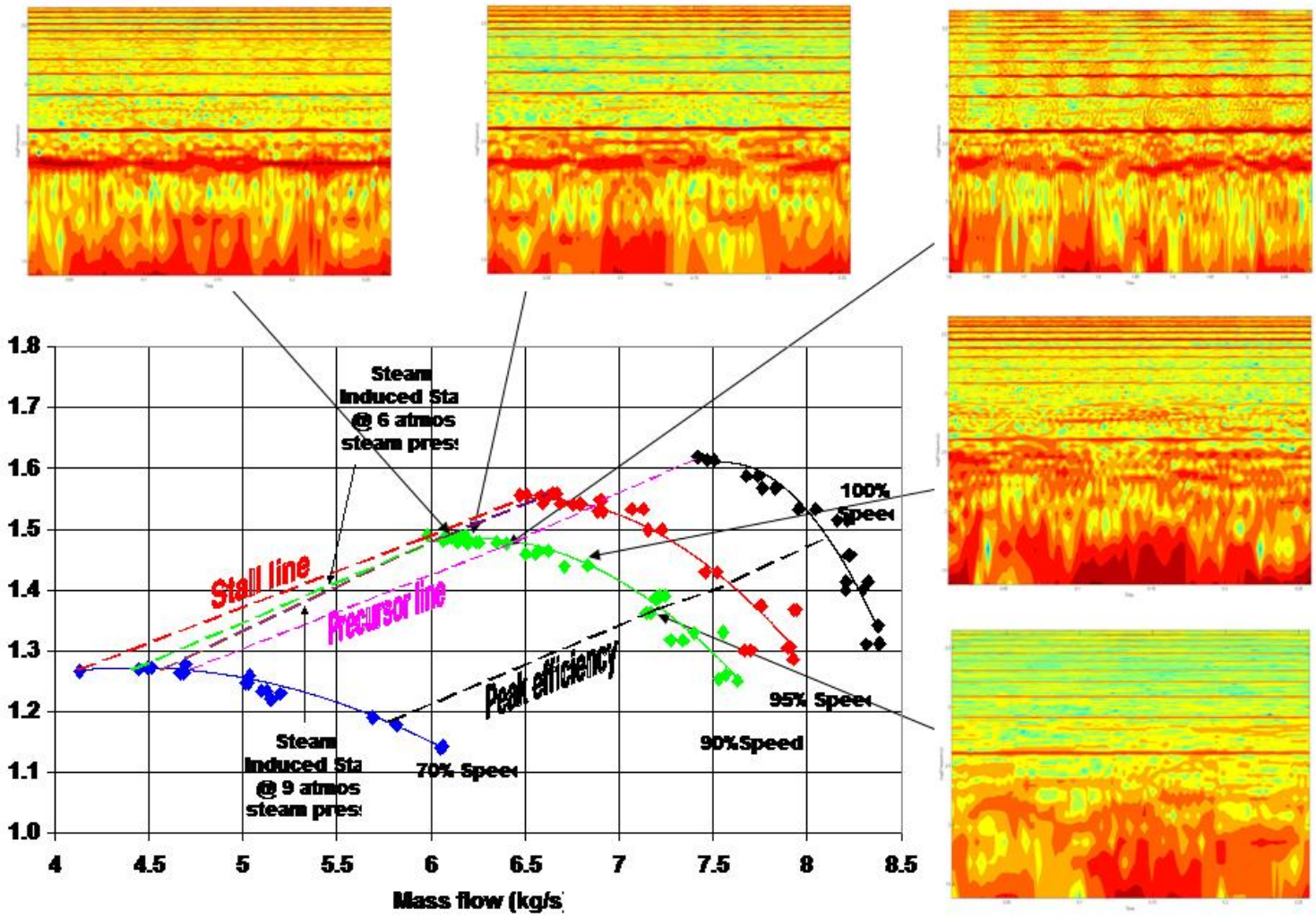
1.8
1.7
1.6
1.5
1.4
1.3
1.2
1.1
1.0
4
4.5
5
5.5
6
6.5
7
7.5
8
8.5
Mass flow (kg/s
Steam
Induced Sta
@ 6 atmos
steam pres
Stall line
Precursor line
Peak efficiency
100%
Speed
95% Speed
90%Speed
70% Speed
Steam
Induced Sta
@ 9 atmos
steam pres

Kulite 8

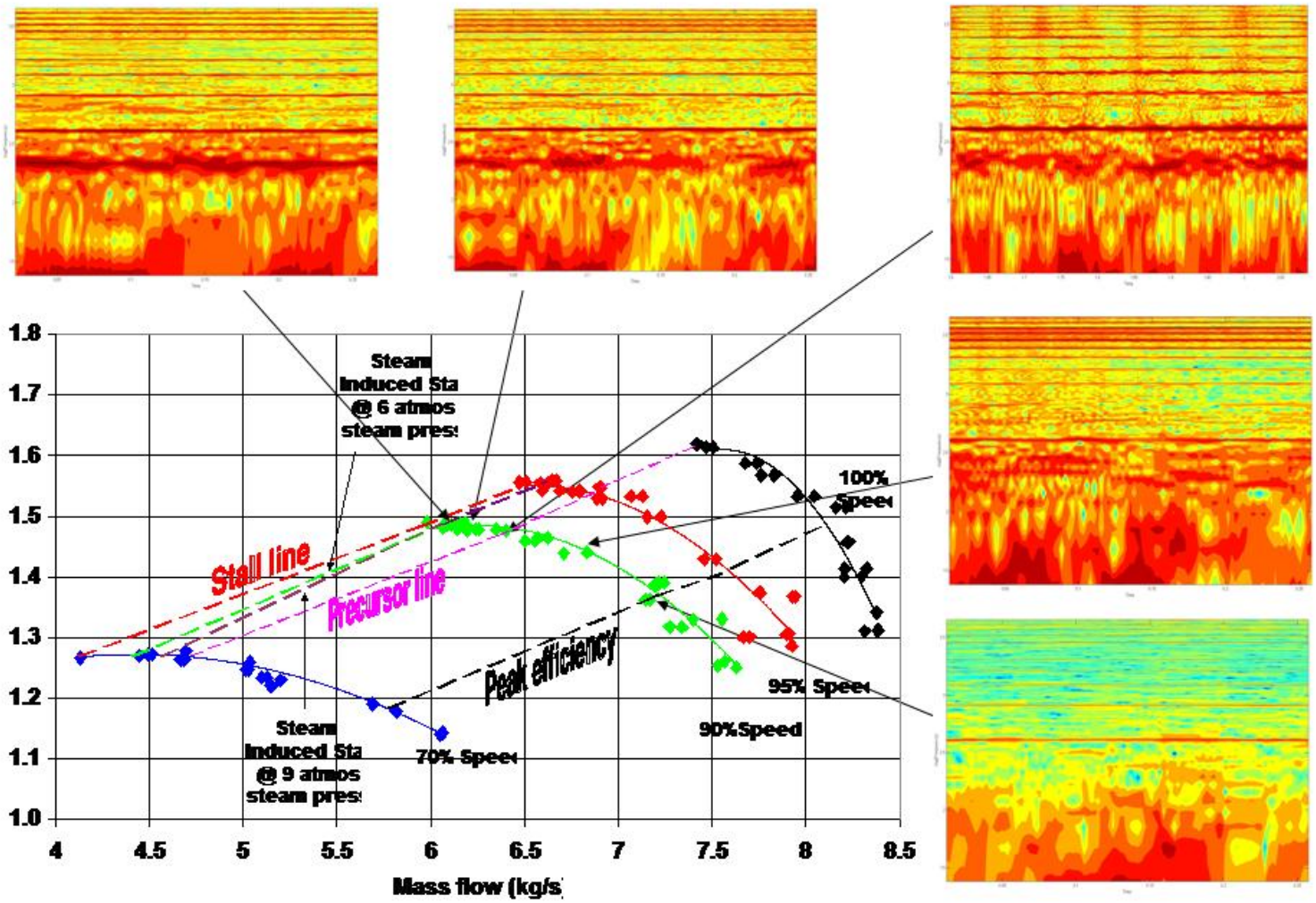
1.8
1.7
1.6
1.5
1.4
1.3
1.2
1.1
1.0
4
4.5
5
5.5
6
6.5
7
7.5
8
8.5
Mass flow (kg/s
Steam
Induced Sta
@ 6 atmos
steam pres
Stall line
Precursor line
Peak efficiency
100%
Speed
95% Speed
90%Speed
70% Speed
Steam
Induced Sta
@ 9 atmos
steam pres

Kulite 9

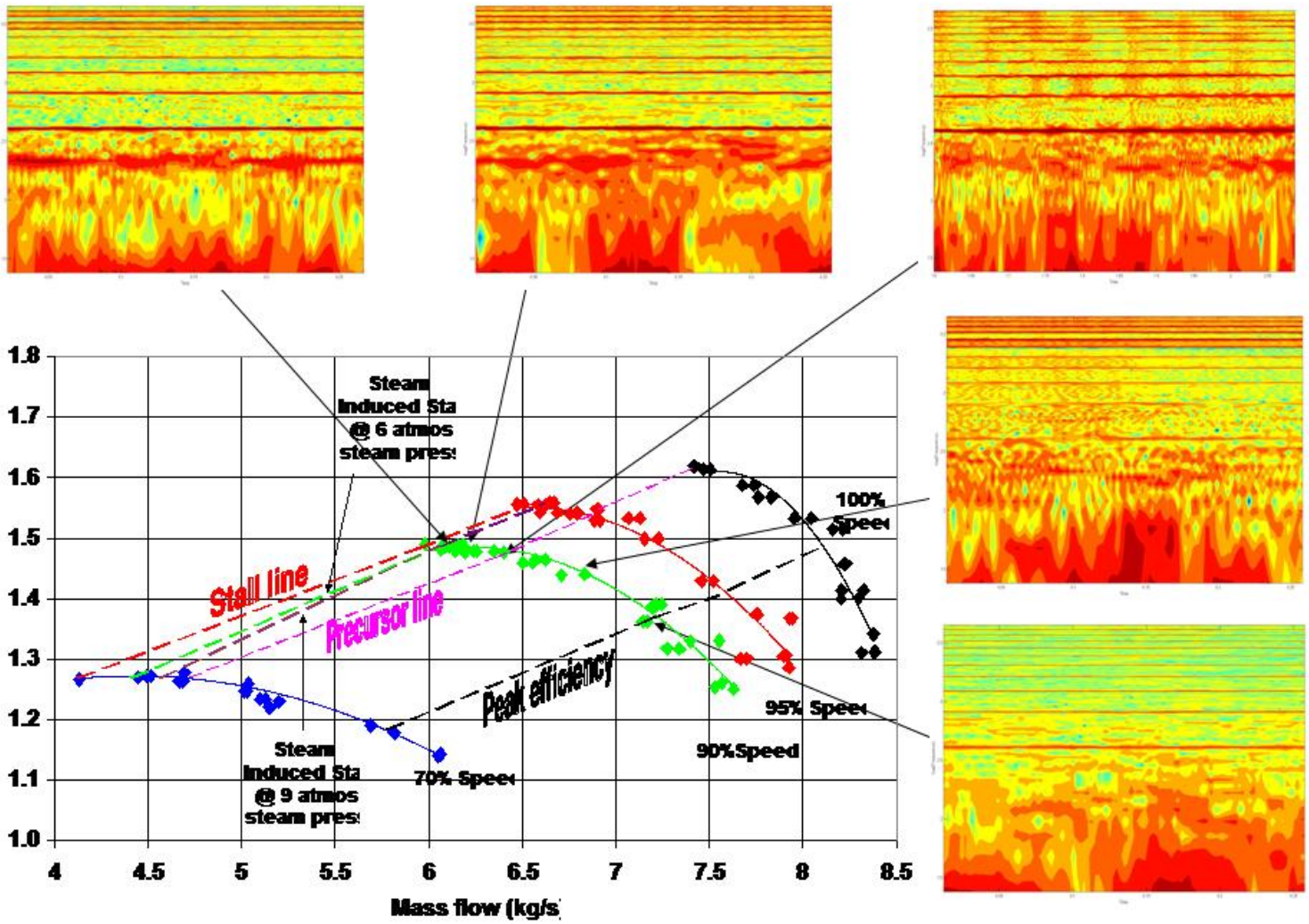
Steam
Induced Sta
@ 6 atmos
steam pres
Stall line
Precursor line
Peak efficiency
100%
Speed
95% Speed
90%Speed
70% Speed
Steam
Induced Sta
@ 9 atmos
steam pres
1.8
1.7
1.6
1.5
1.4
1.3
1.2
1.1
1.0
4
4.5
5
5.5
6
6.5
7
7.5
8
8.5
Mass flow (kg/s

95% Speed Progressions:

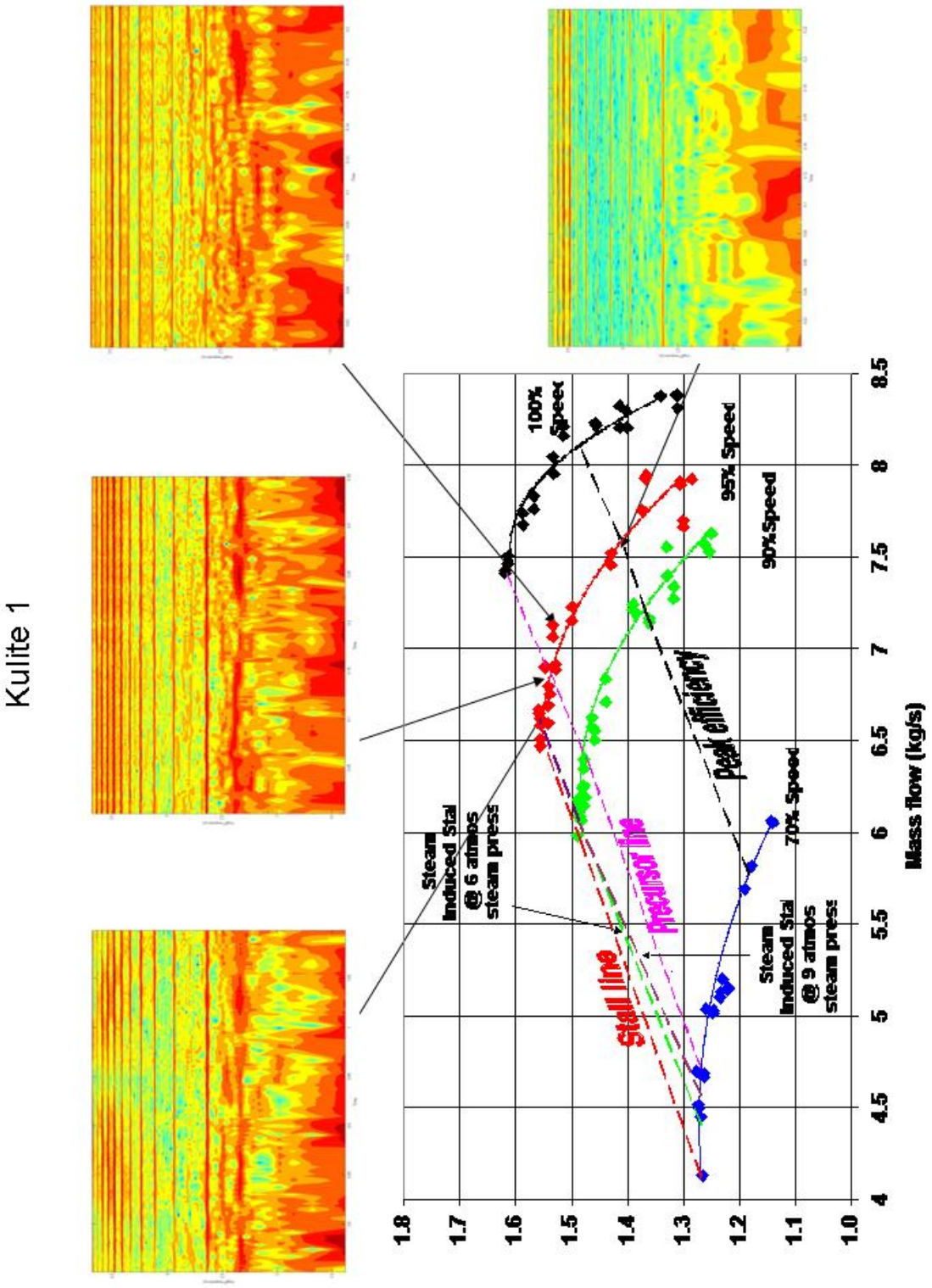

# Kulite 2

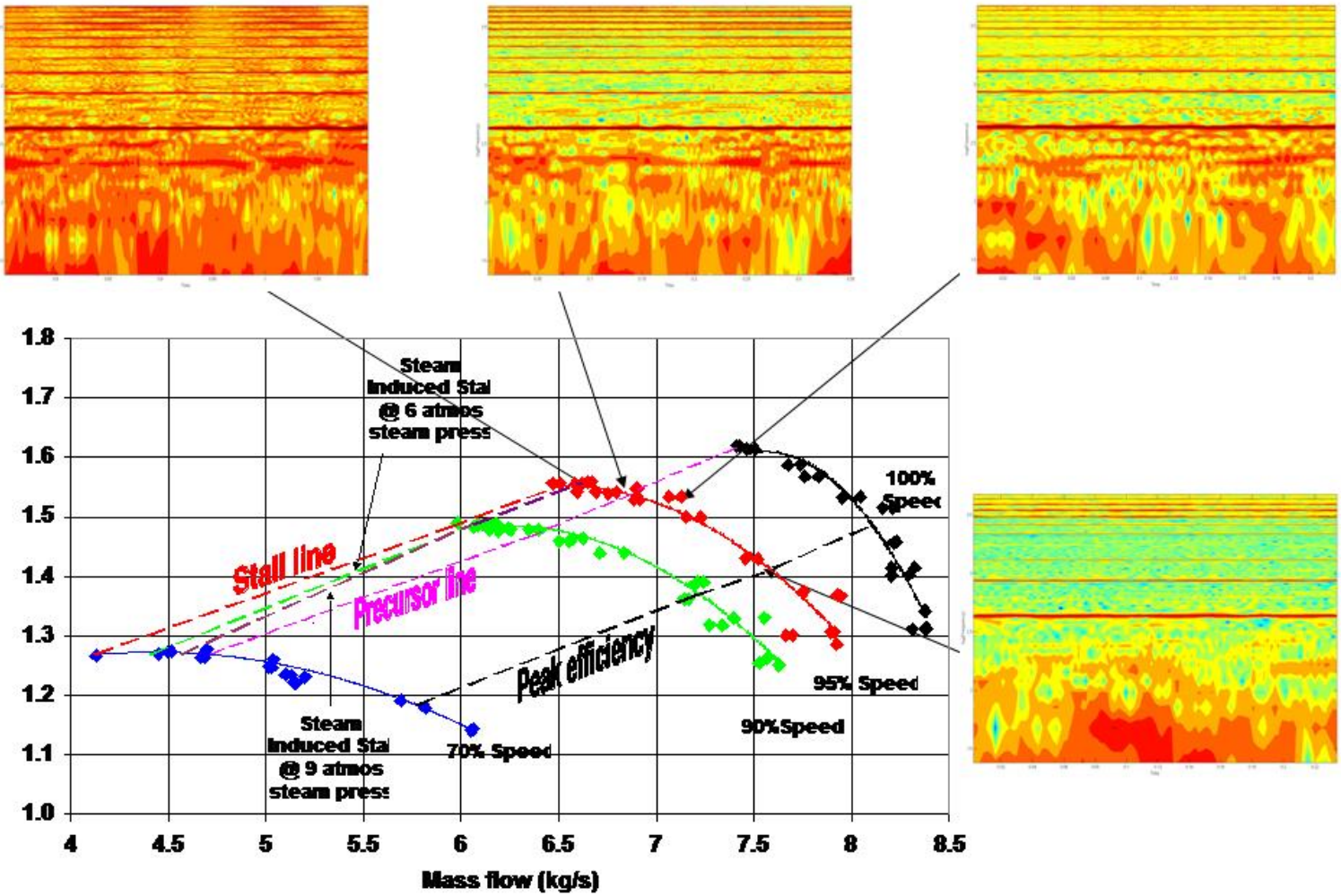
Steam
Induced Stal
@ 6 atmos
steam press
Stall line
Precursor line
Peak efficiency
100%
Speed
95% Speed
90%Speed
70% Speed
Steam
Induced Stal
@ 9 atmos
steam press
1.8
1.7
1.6
1.5
1.4
1.3
1.2
1.1
1.0
4
4.5
5
5.5
6
6.5
7
7.5
8
8.5
Mass flow (kg/s)

Kulite 7

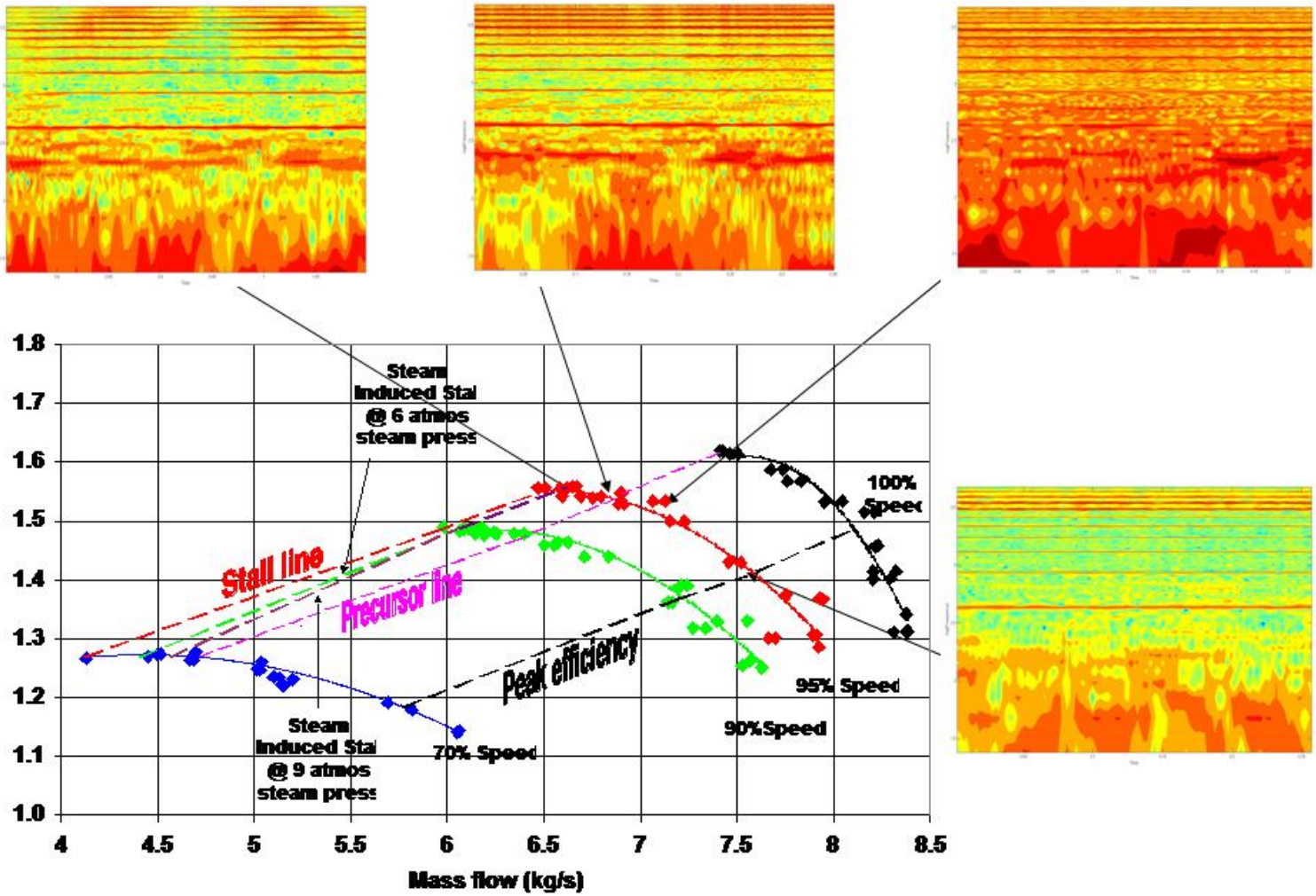
Steam
Induced Stal
@ 6 atmos
steam press
Stall line
Precursor line
Peak efficiency
100%
Speed
95% Speed
90%Speed
70% Speed
Steam
Induced Stal
@ 9 atmos
steam press
1.8
1.7
1.6
1.5
1.4
1.3
1.2
1.1
1.0
4
4.5
5
5.5
6
6.5
7
7.5
8
8.5
Mass flow (kg/s)

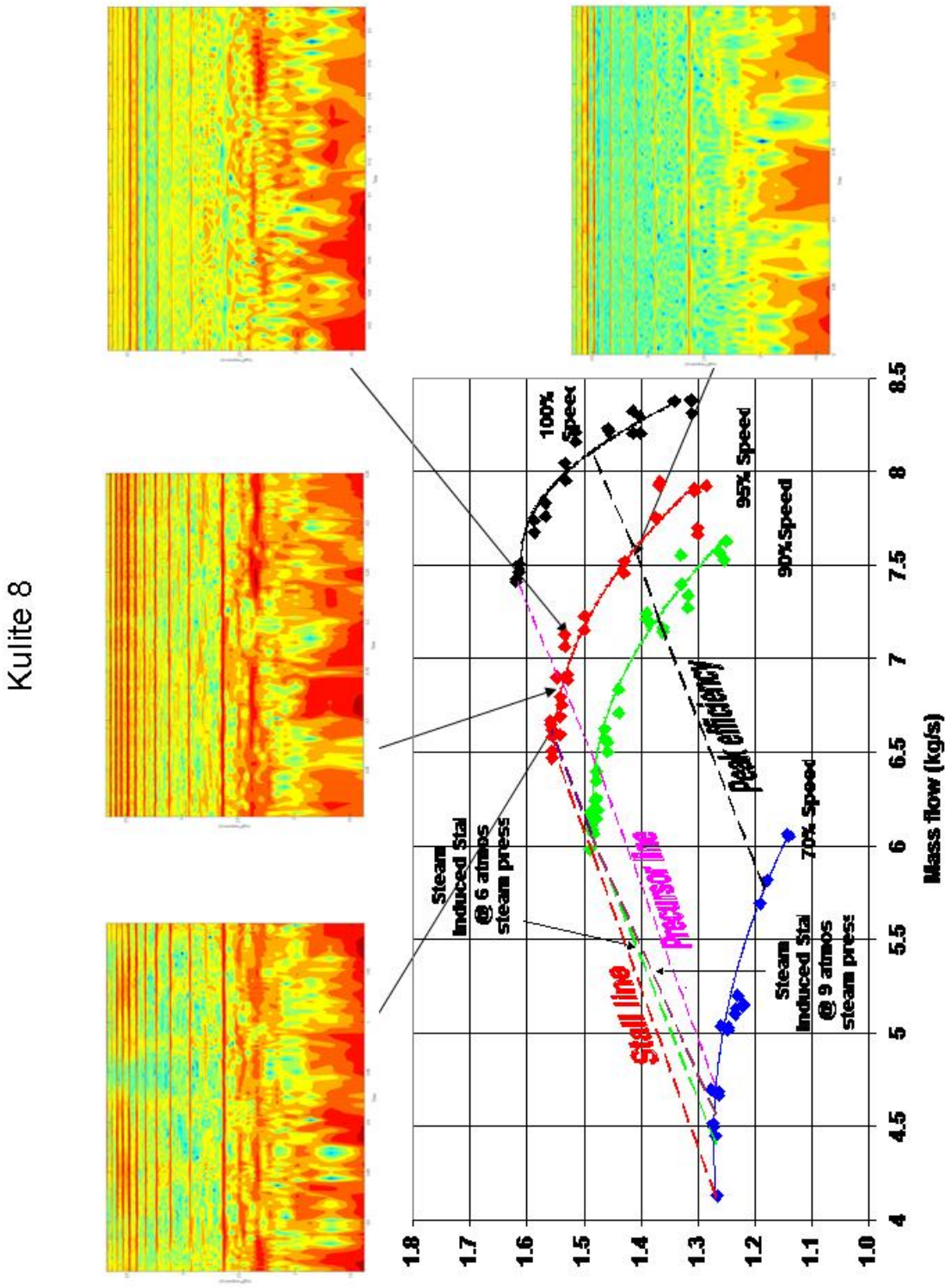
Kulite 8
Steam Induced Stal @ 6 atmos steam press
Steam Induced Stal @ 9 atmos steam press
Stall line
Precursor line
Peak efficiency
100% Speed
95% Speed
90%Speed
70% Speed
Mass flow (kg/s)
1.8
1.7
1.6
1.5
1.4
1.3
1.2
1.1
1.0
4
4.5
5
5.5
6
6.5
7
7.5
8
8.5

Kulite 9

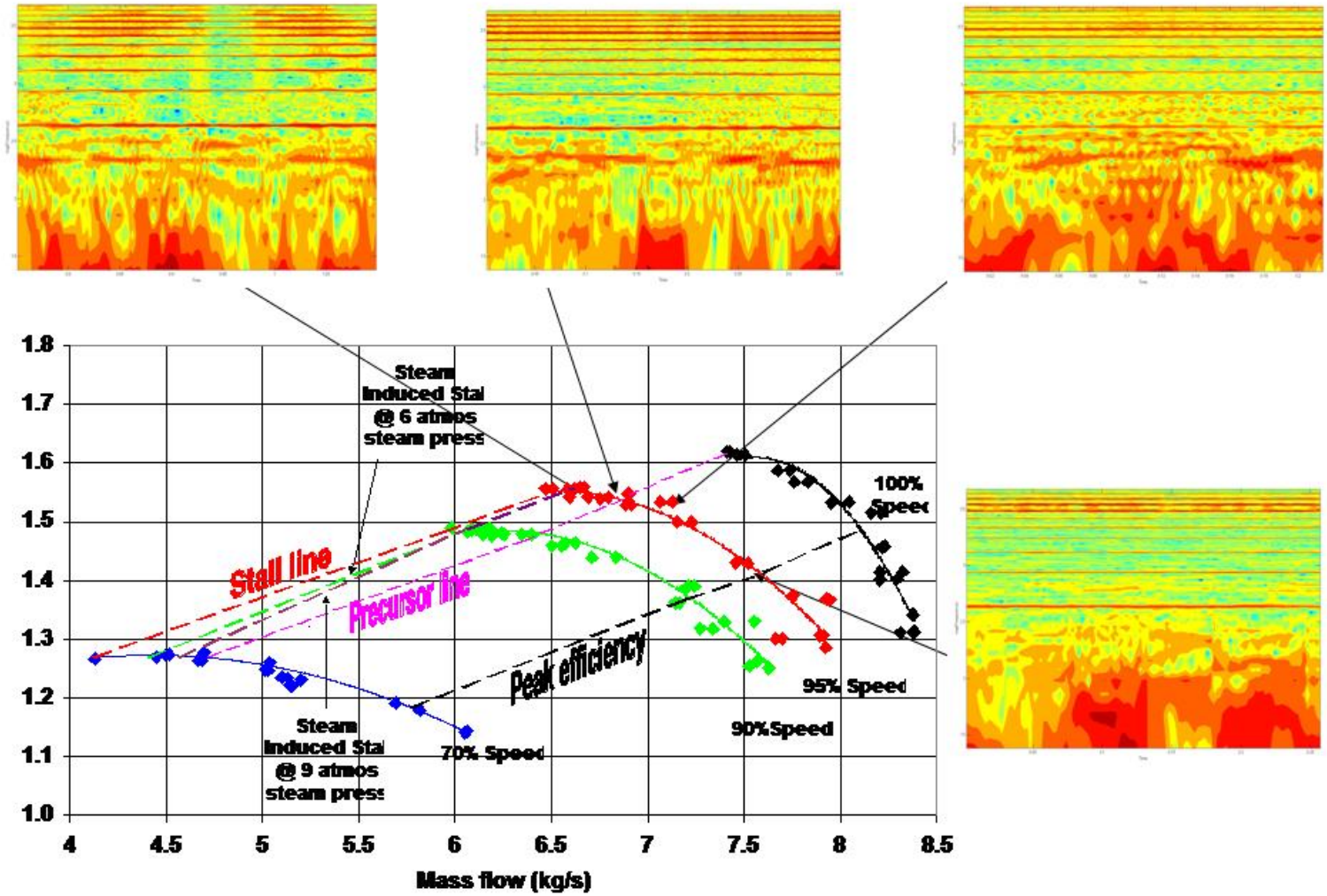
Steam
Induced Stal
@ 6 atmos
steam press
Stall line
Precursor line
Peak efficiency
100%
Speed
95% Speed
90%Speed
70% Speed
Steam
Induced Stal
@ 9 atmos
steam press
1.8
1.7
1.6
1.5
1.4
1.3
1.2
1.1
1.0
4
4.5
5
5.5
6
6.5
7
7.5
8
8.5
Mass flow (kg/s)

THIS PAGE INTENTIONALLY LEFT BLANK

# APPENDIX E: STEAM STALL DATA

70% Speed, steam stall

Kulite 1

Contour plot:

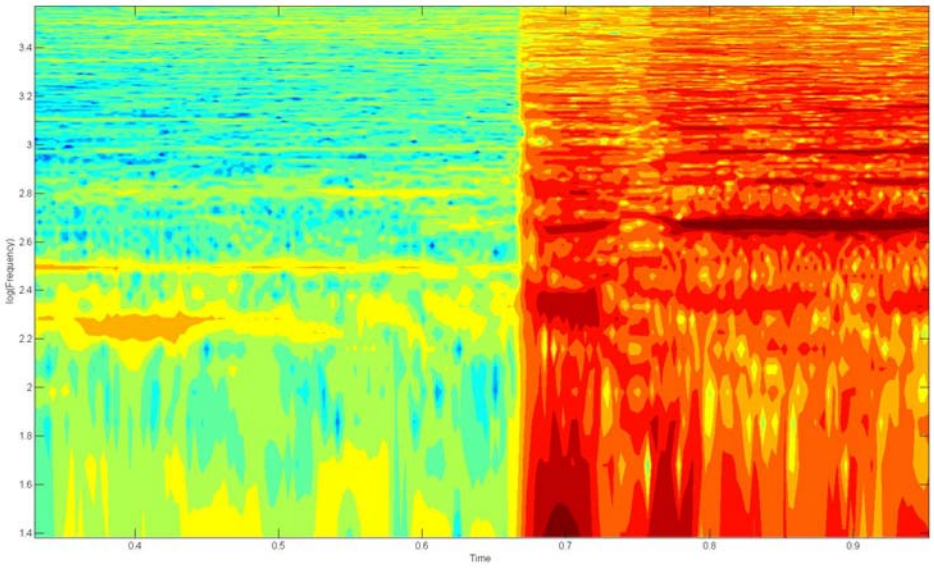


Raw signal:

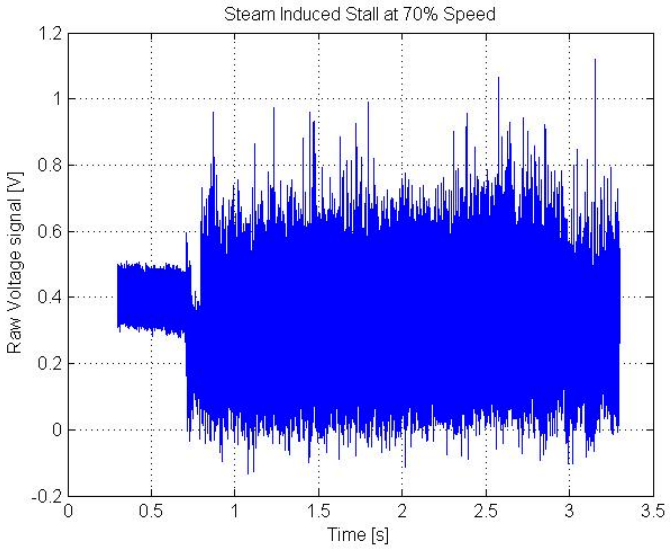

RPM trace:

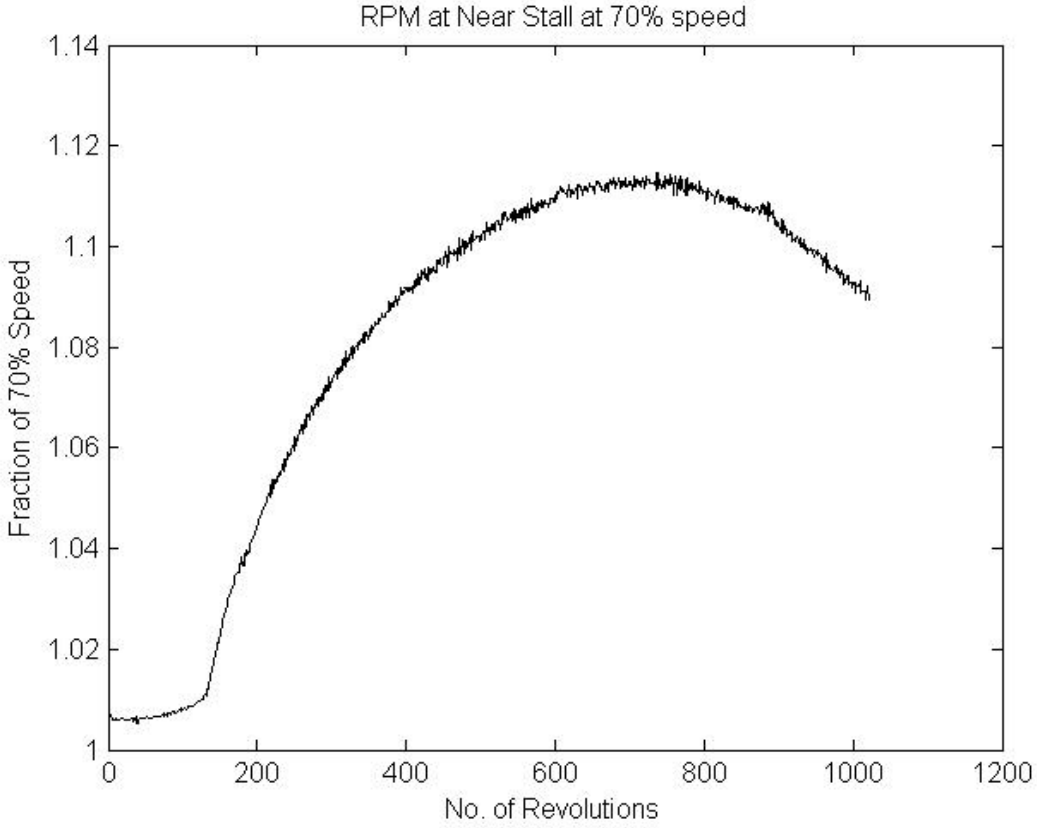
RPM at Near Stall at 70% speed
Fraction of 70% Speed
No. of Revolutions
1.14
1.12
1.1
1.08
1.06
1.04
1.02
1
0
200
400
600
800
1000
1200

Kulite 2:

Contour plot:

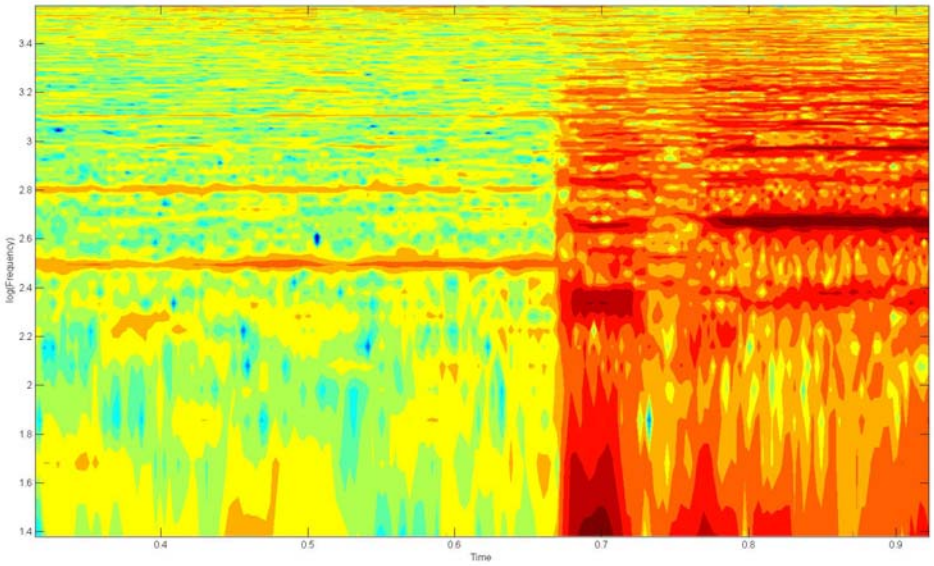


Raw signal:

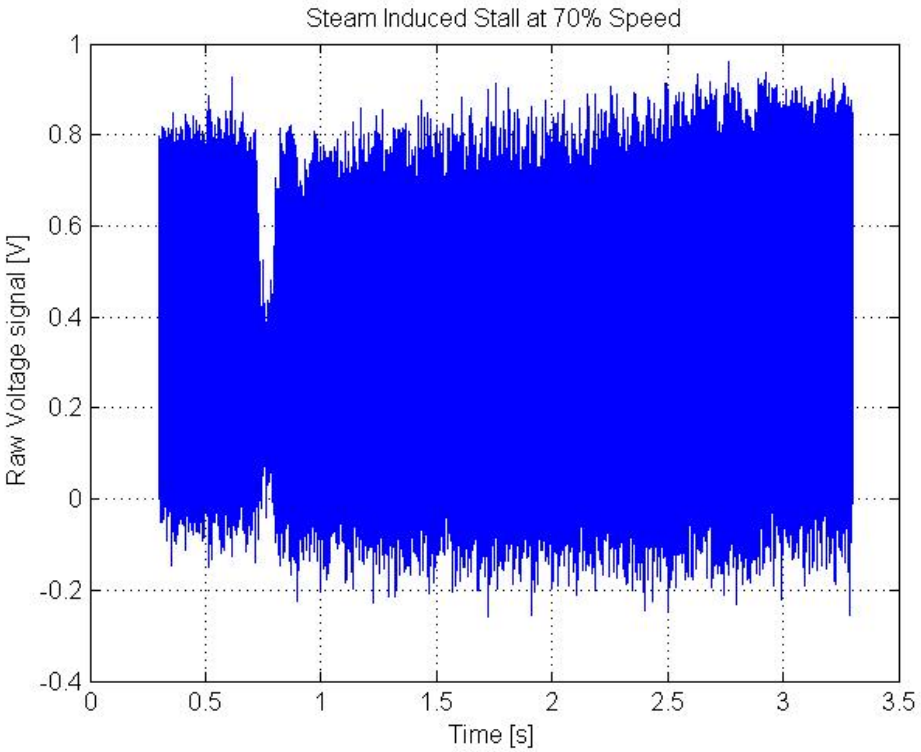

Kulite 7:

Contour plot:

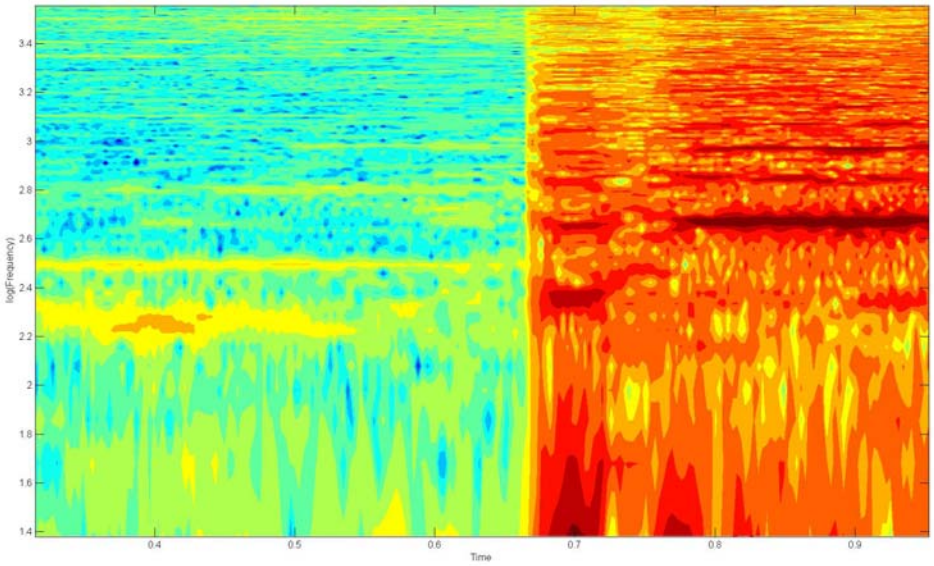


Raw signal:

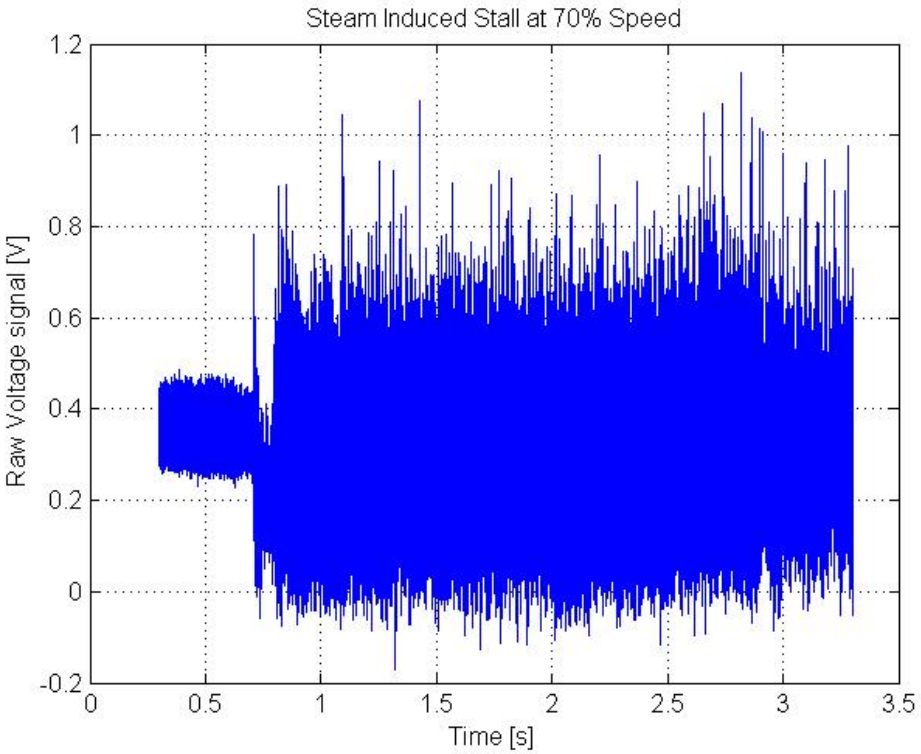

Kulite 8:

Contour plot:

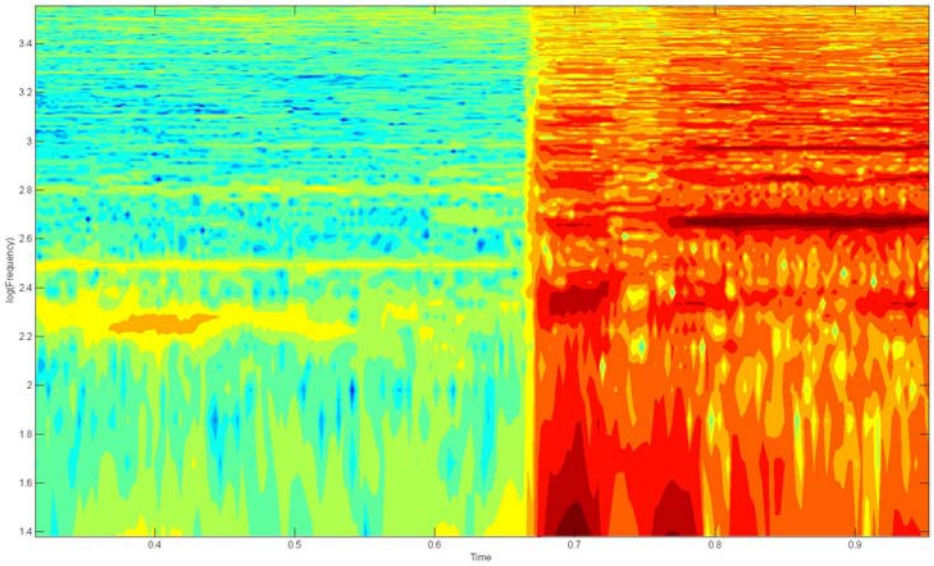


Raw signal:

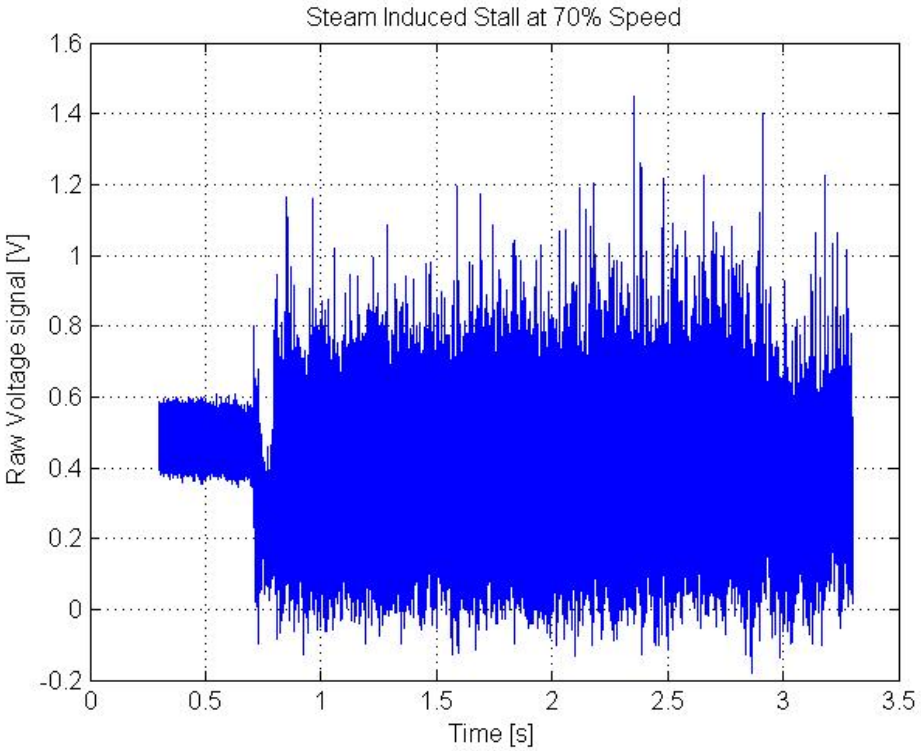

Kulite 9:

Contour plot:

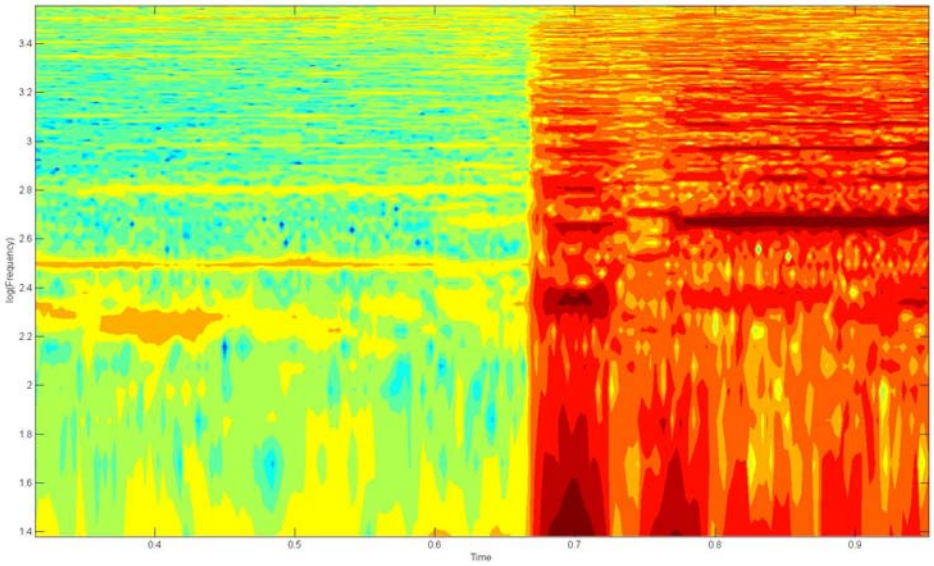


Raw signal:

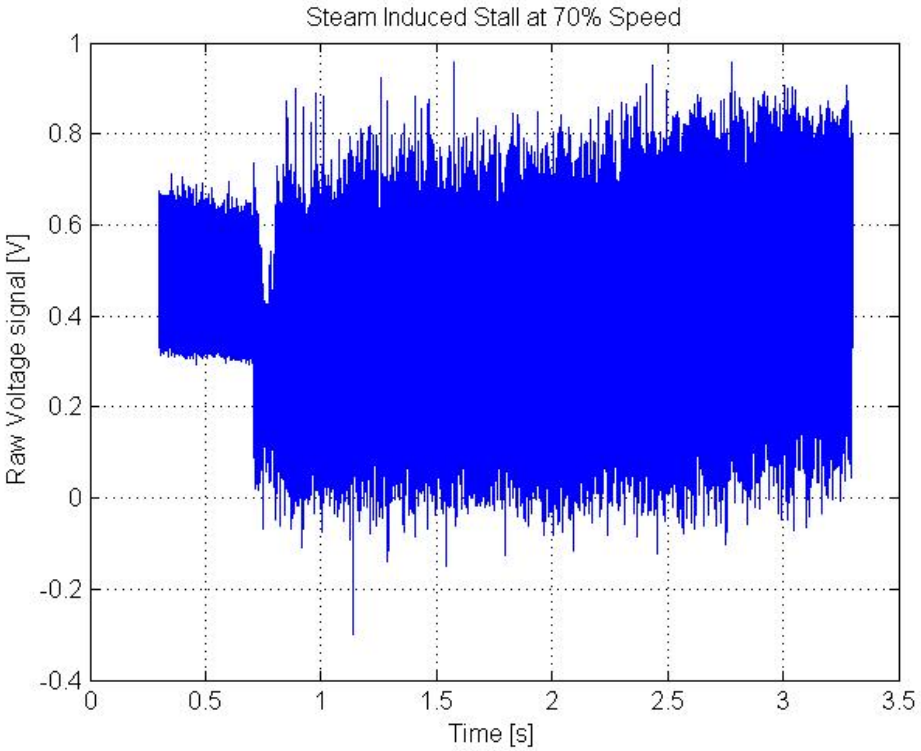

90% Speed, steam stall:

Kulite 1:

Contour plot:

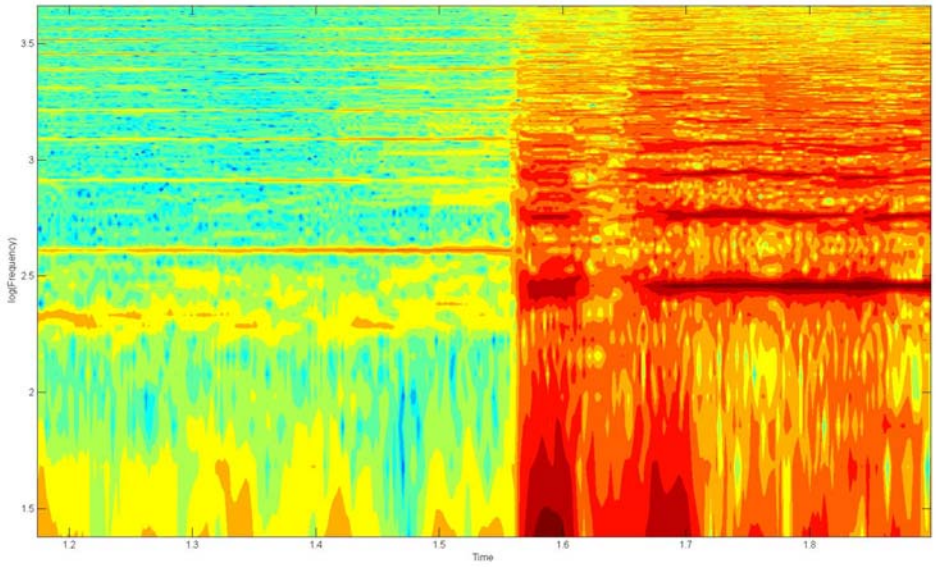


Raw signal:

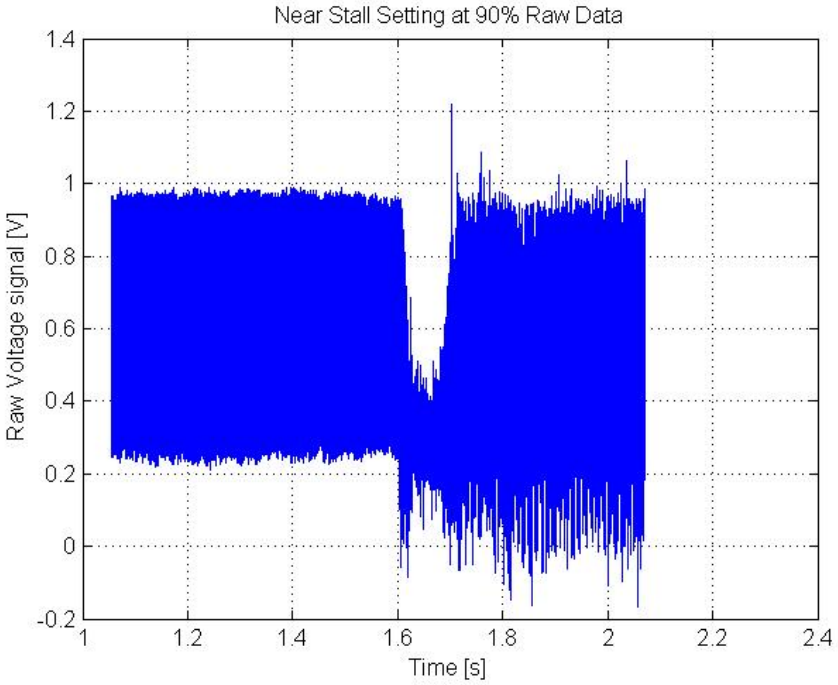

RPM trace:

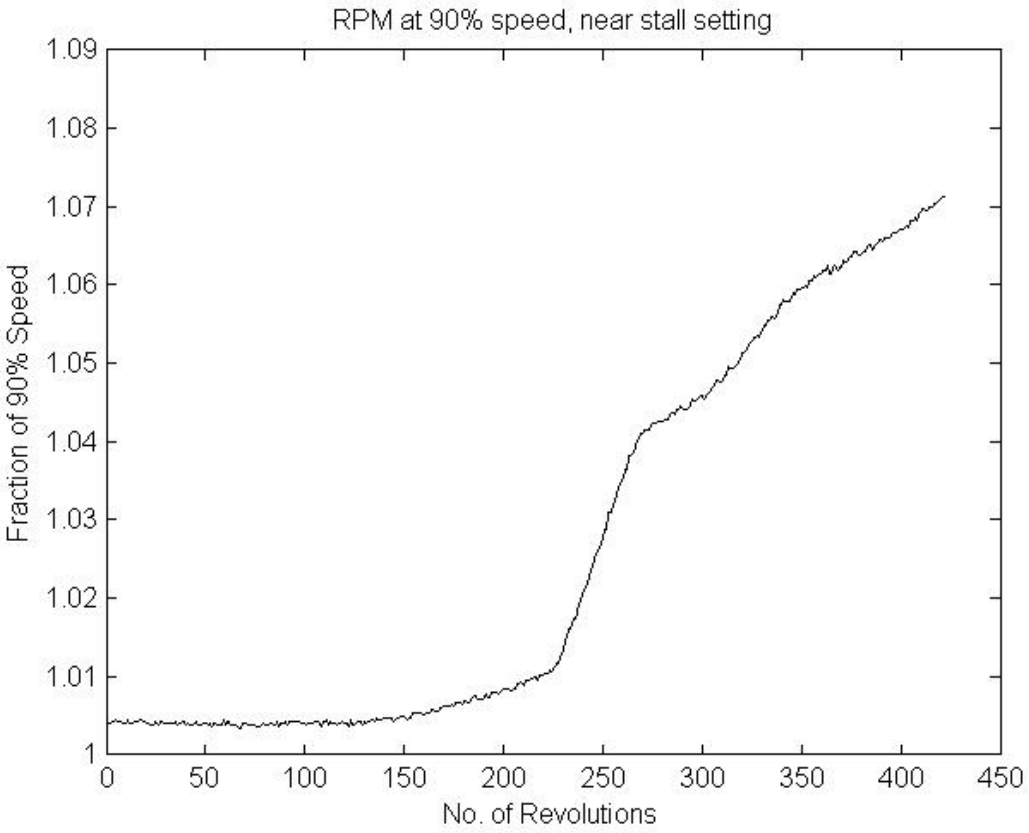
RPM at 90% speed, near stall setting
Fraction of 90% Speed
No. of Revolutions
1.09
1.08
1.07
1.06
1.05
1.04
1.03
1.02
1.01
1
0
50
100
150
200
250
300
350
400
450

Kulite 2:

Contour plot:

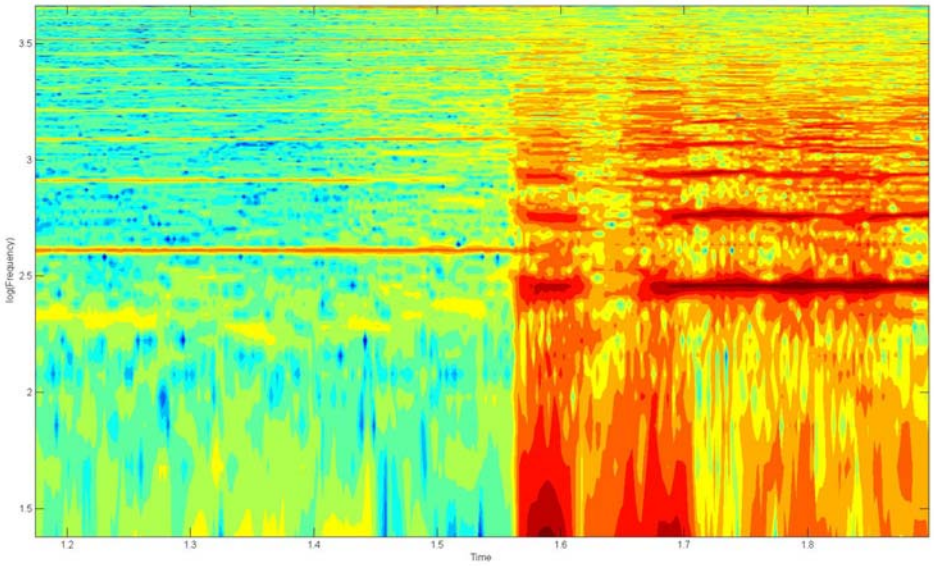


Raw signal:

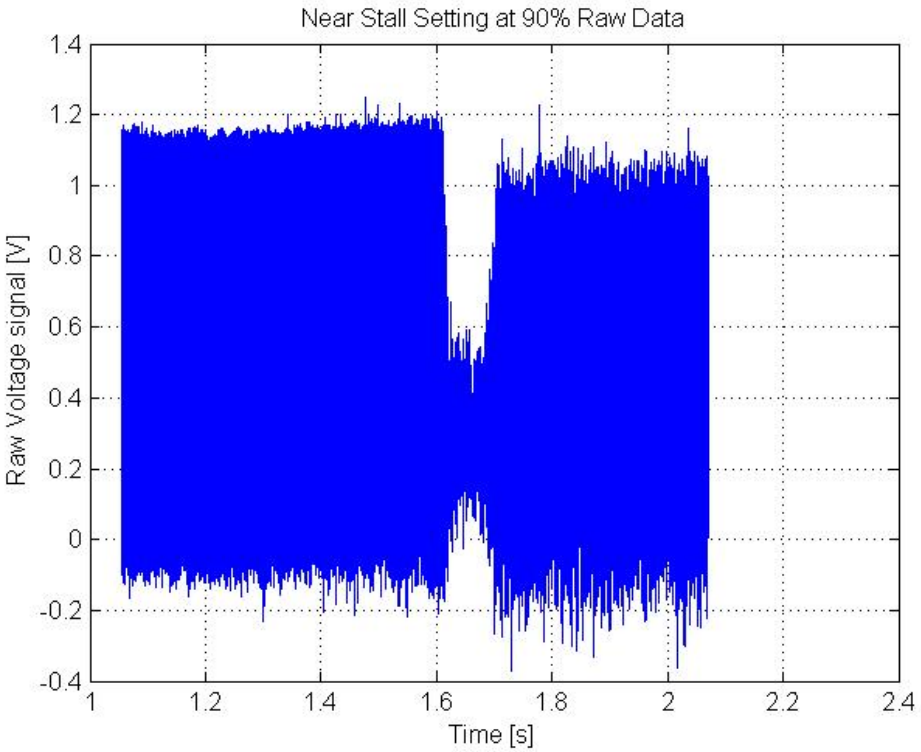

Kulite 7:

Contour plot:

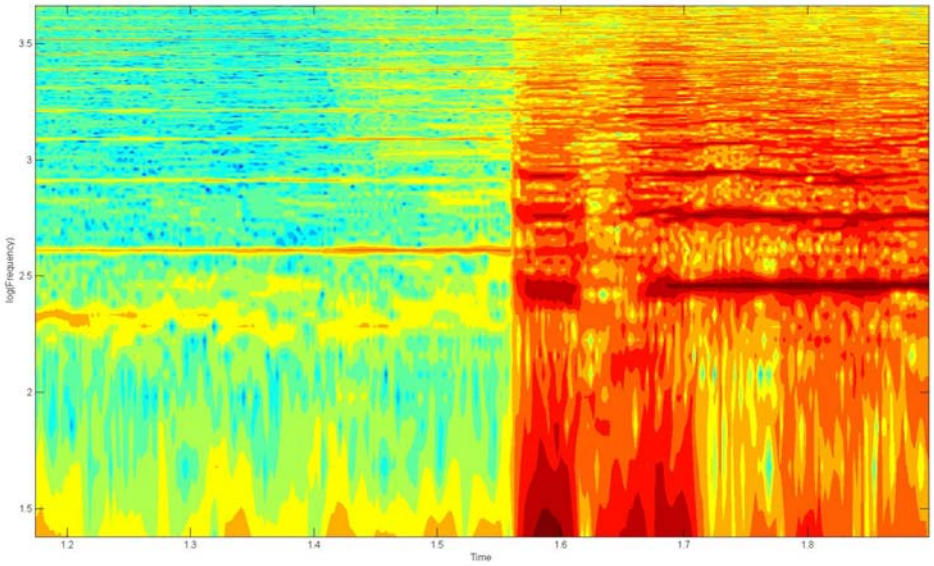


Raw signal:

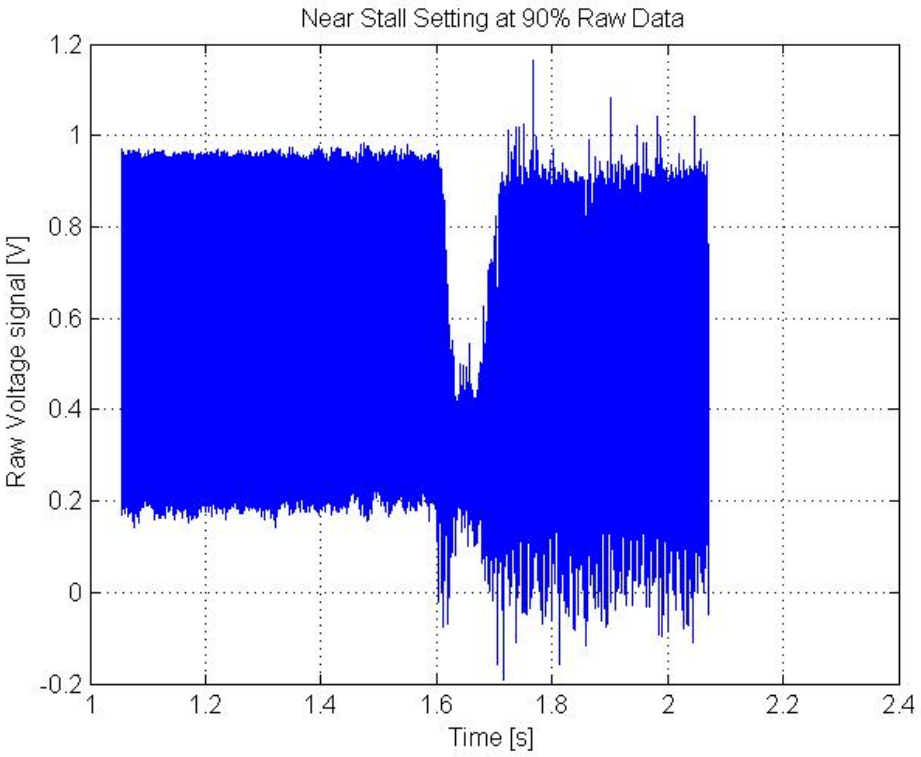

Kulite 8:

Contour plot:

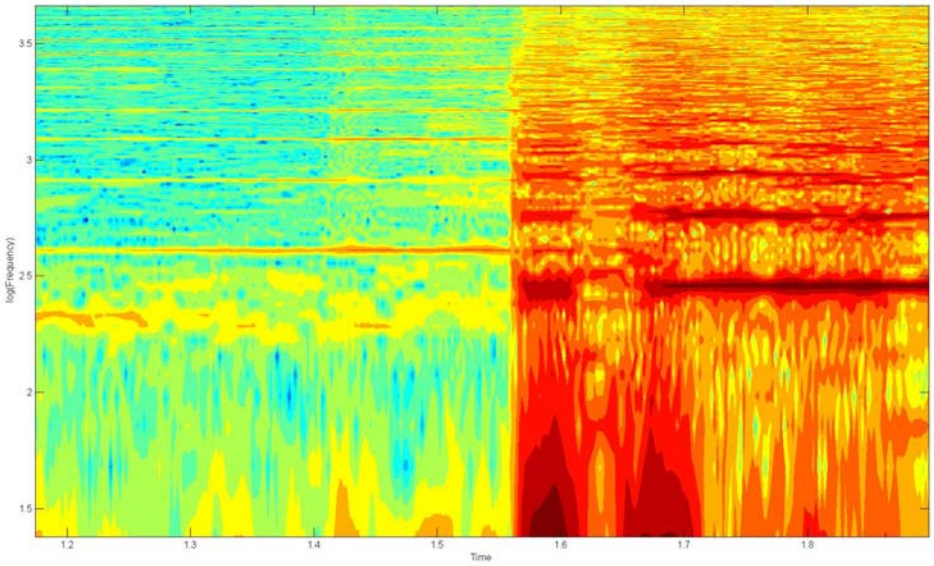


Raw signal:

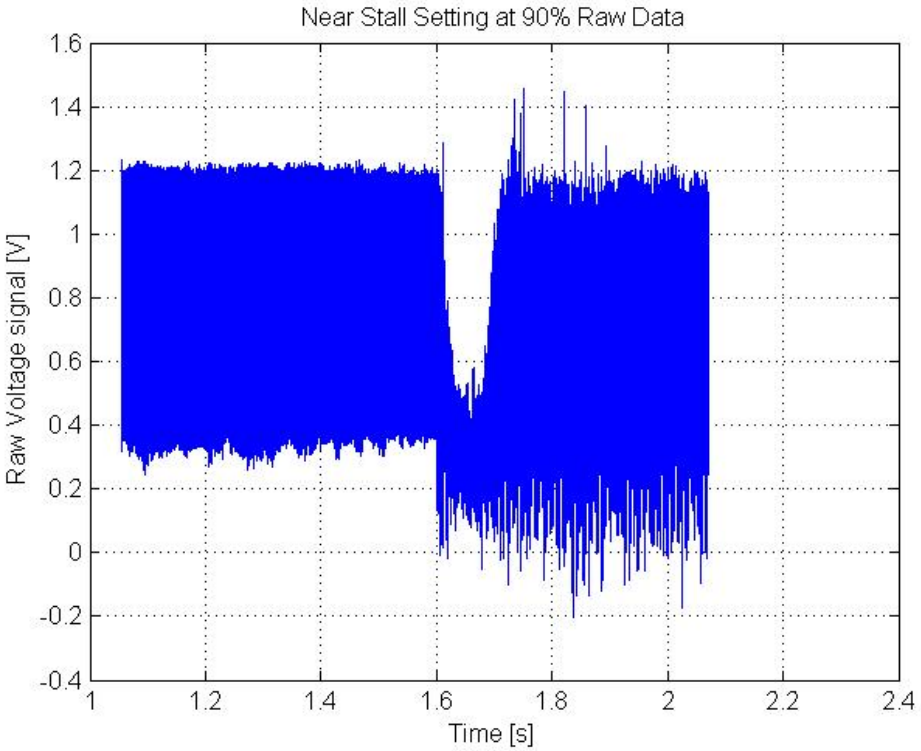

Kulite 9:

Contour plot:

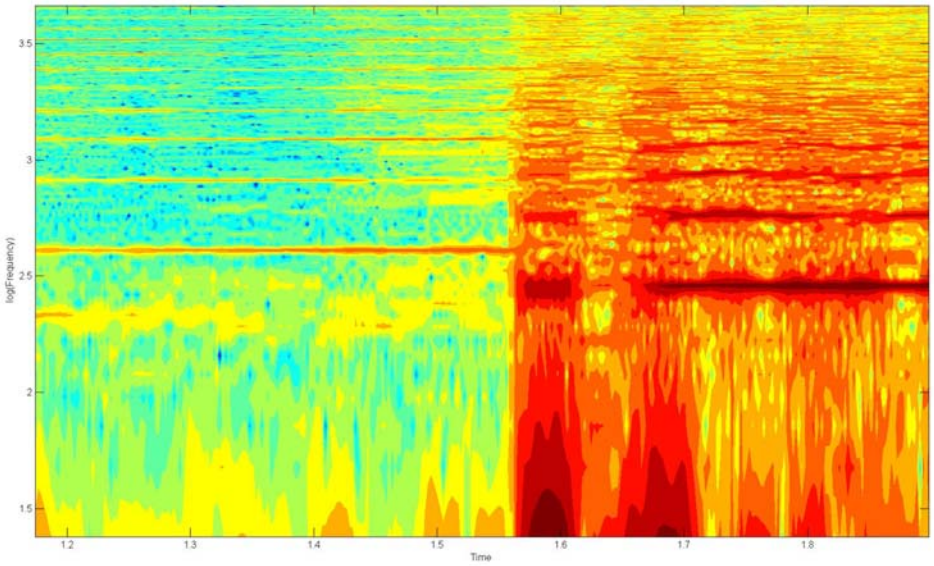


Raw signal:

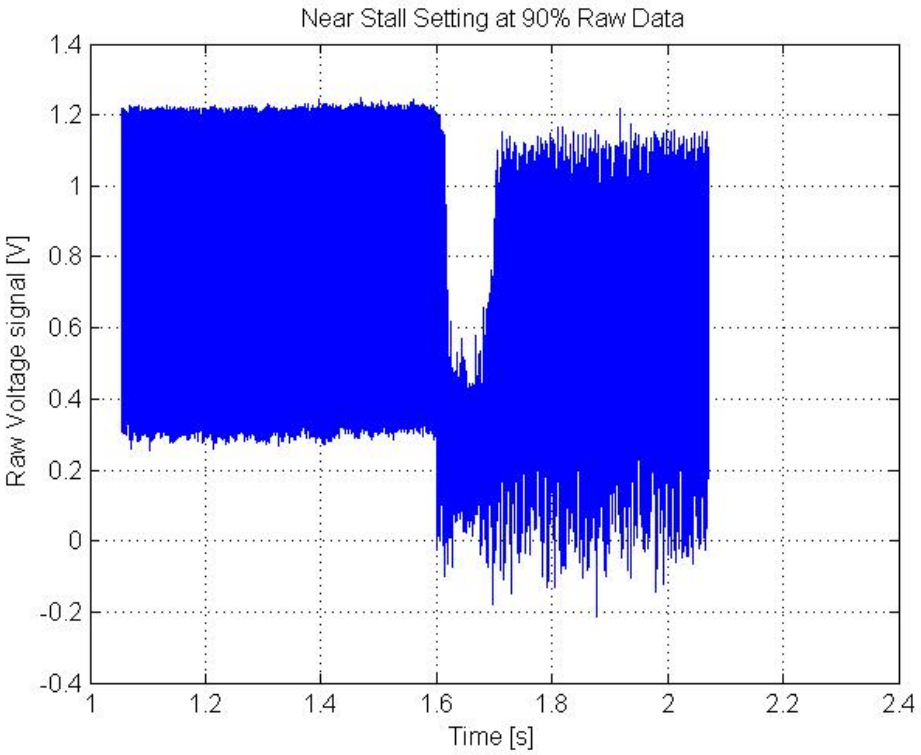

95% Speed, steam stall:

Kulite 1:

Contour plot:

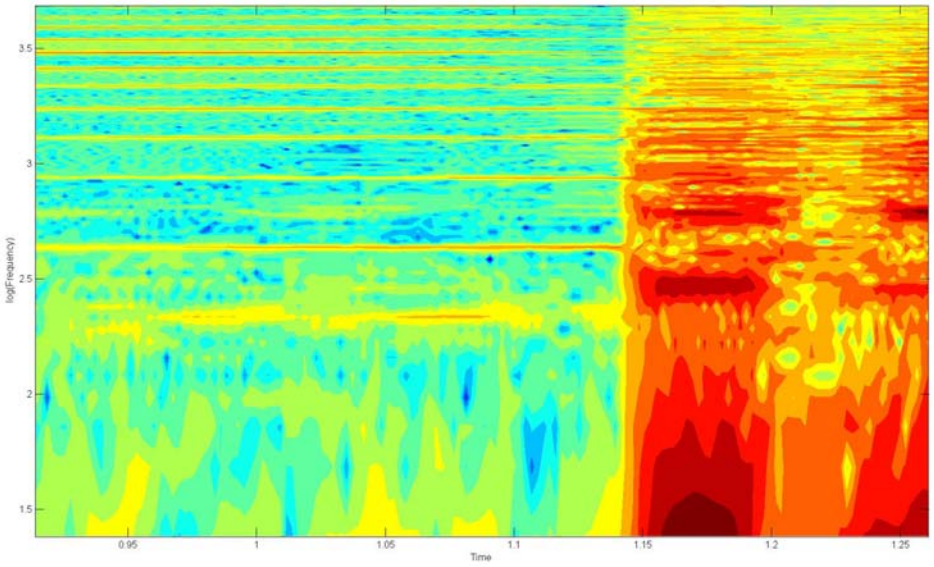


Raw signal:

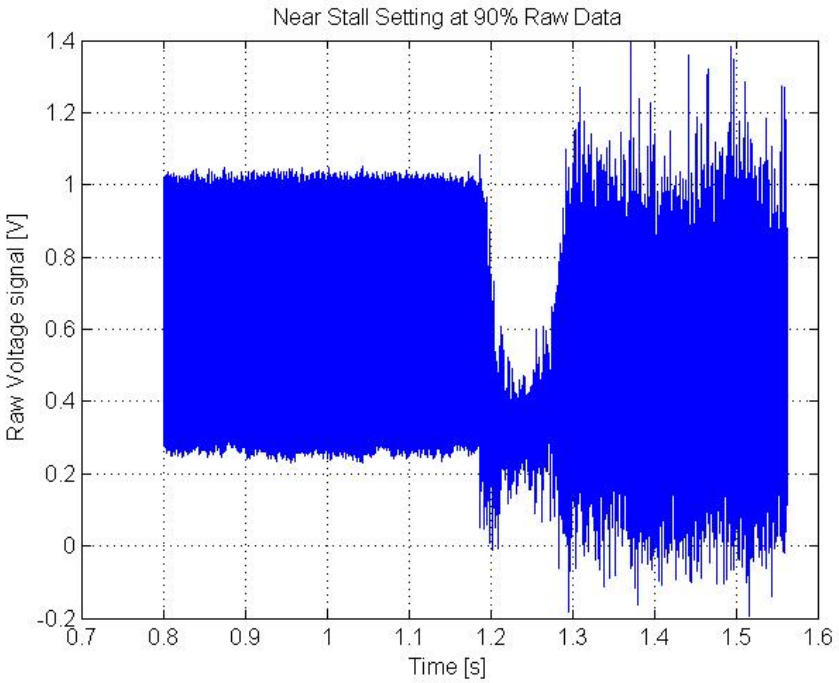

RPM trace:

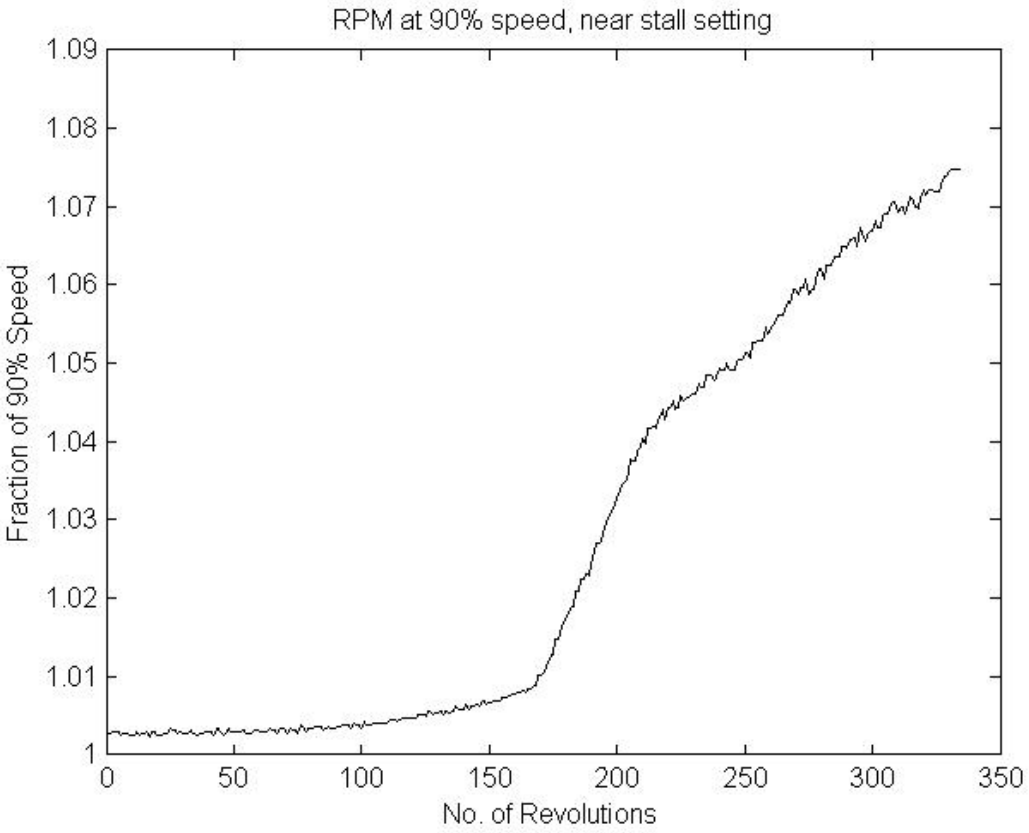
RPM at 90% speed, near stall setting
Fraction of 90% Speed
No. of Revolutions
1.09
1.08
1.07
1.06
1.05
1.04
1.03
1.02
1.01
1
0
50
100
150
200
250
300
350

Kulite 2:

Contour plot:

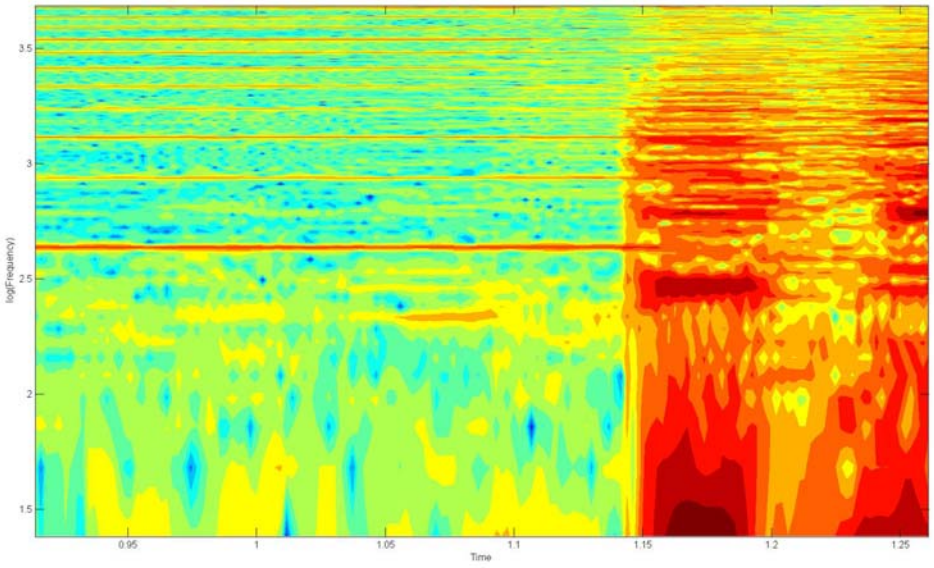


Raw signal:

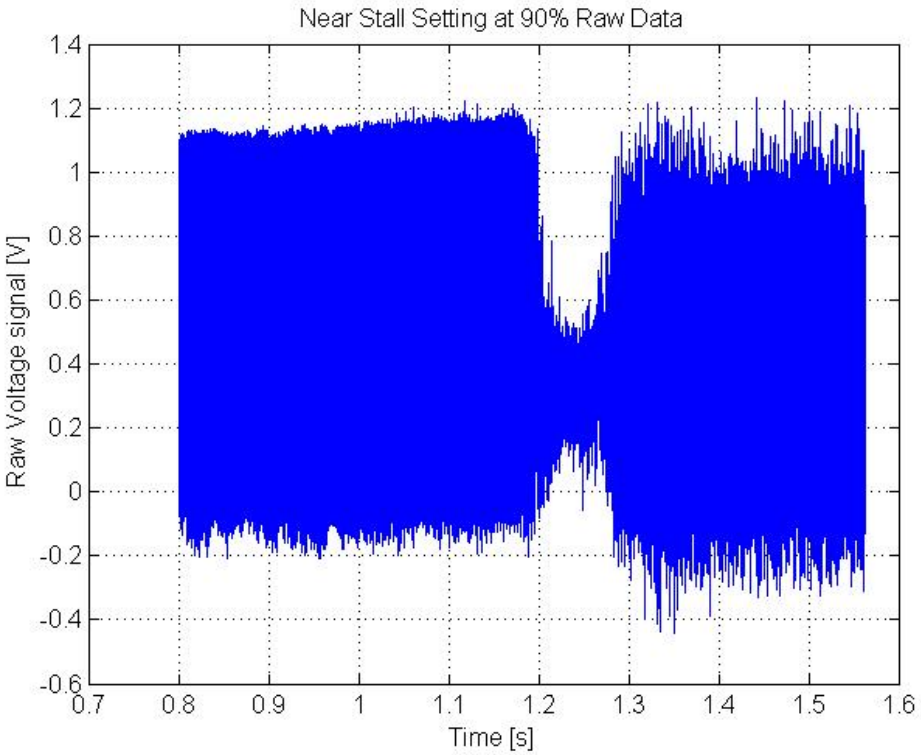

Kulite 7:

Contour plot:

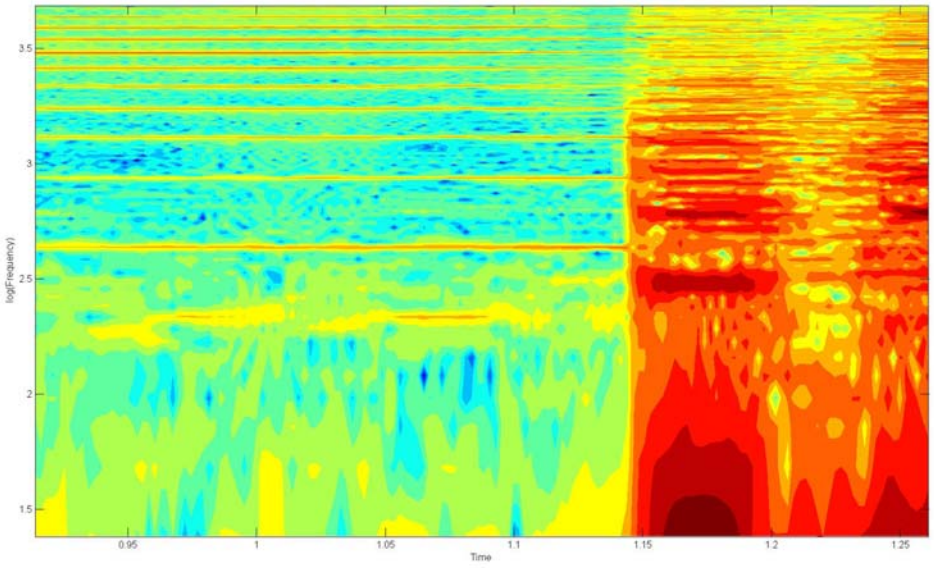


Raw signal:

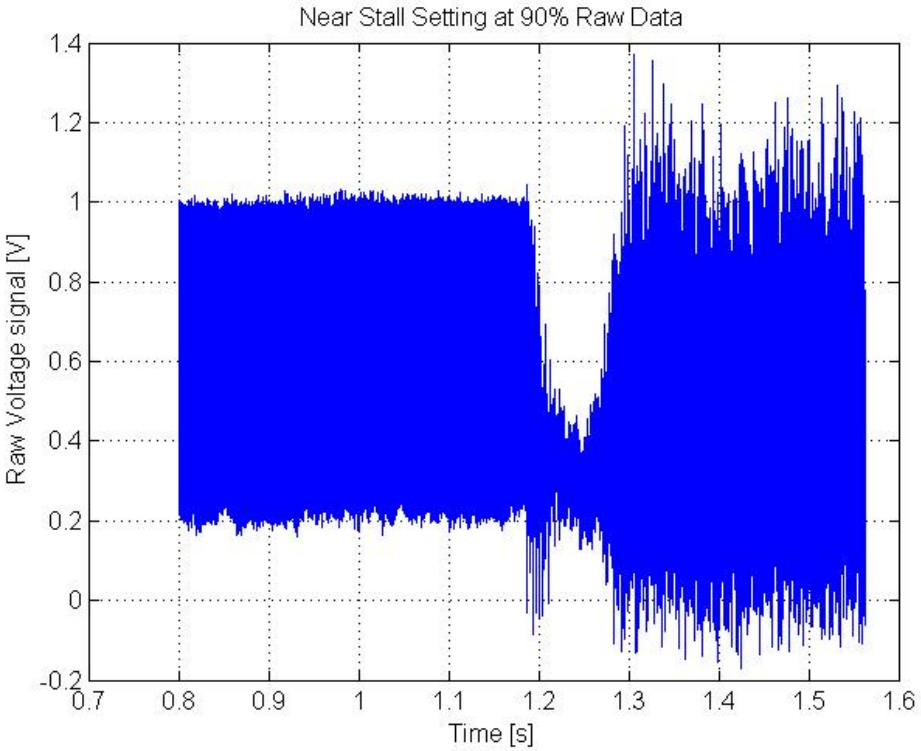

Kulite 8:

Contour plot:

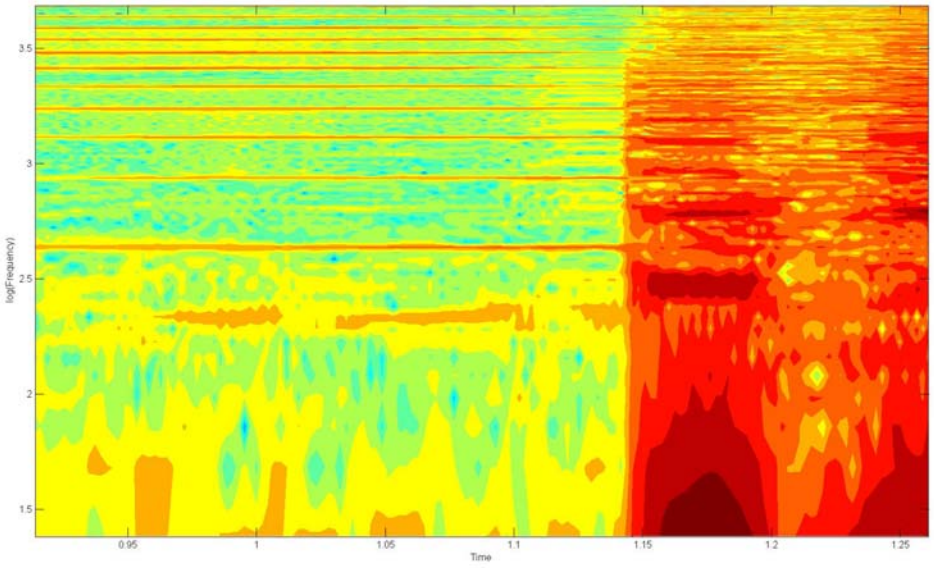


Raw signal:

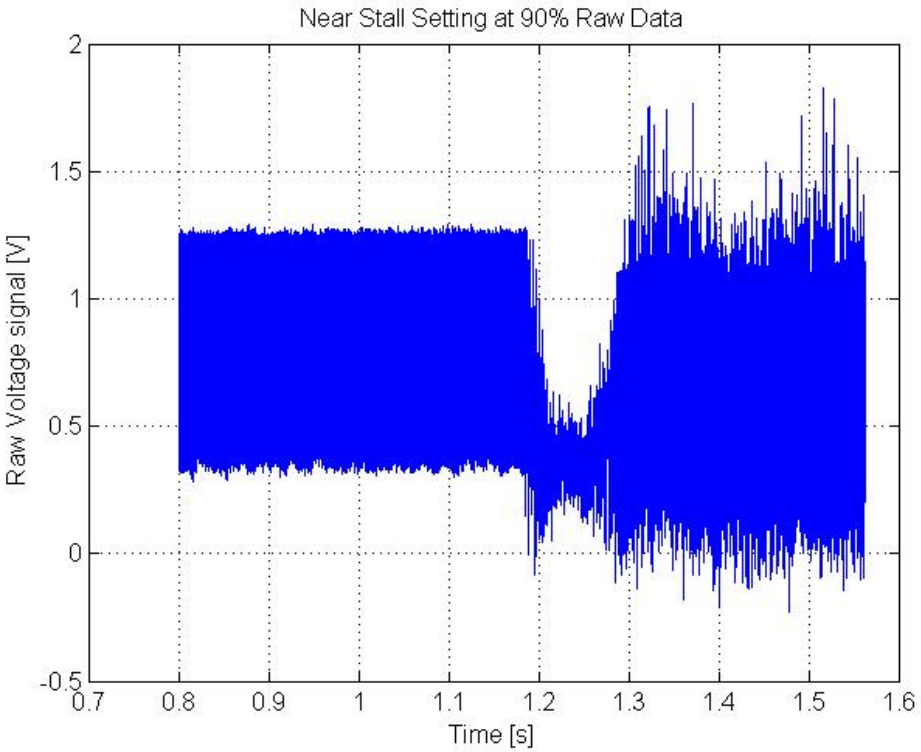

Kulite 9:

Contour plot:

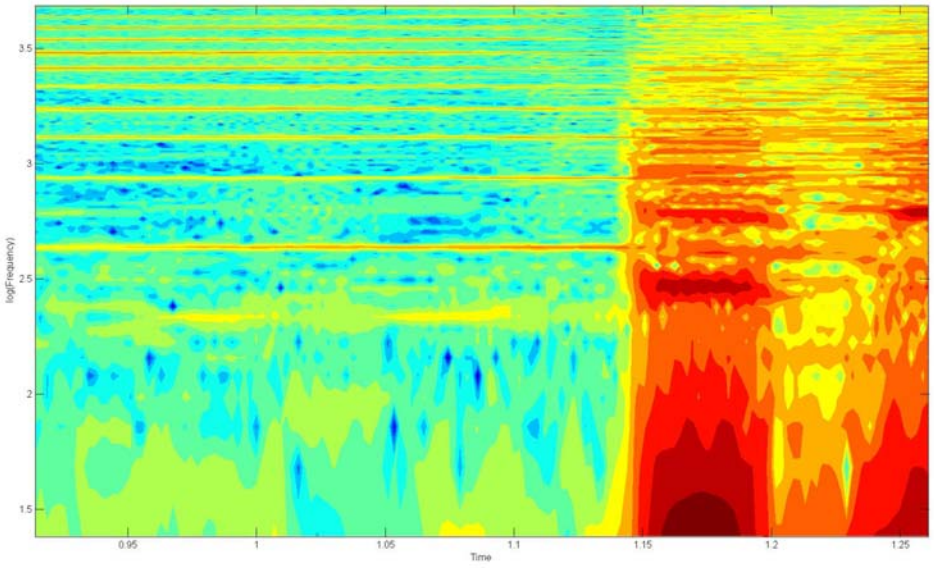


Raw signal:

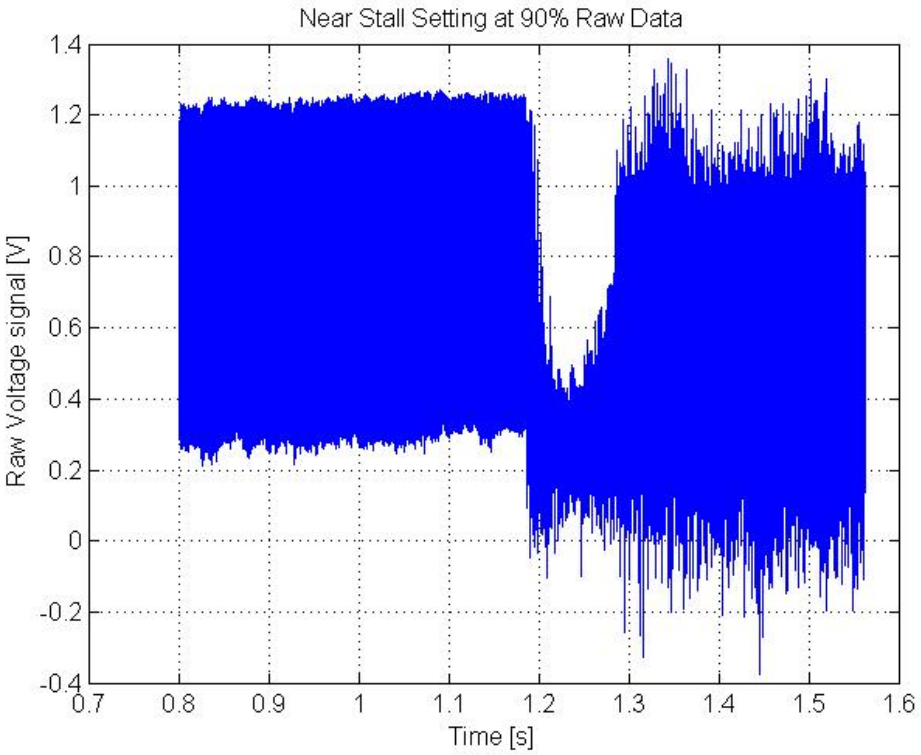

# APPENDIX F: HOT-FILM AUTOCORRELATIONS

70% Speed:

Steam run, no stall:

Autocorrelation:

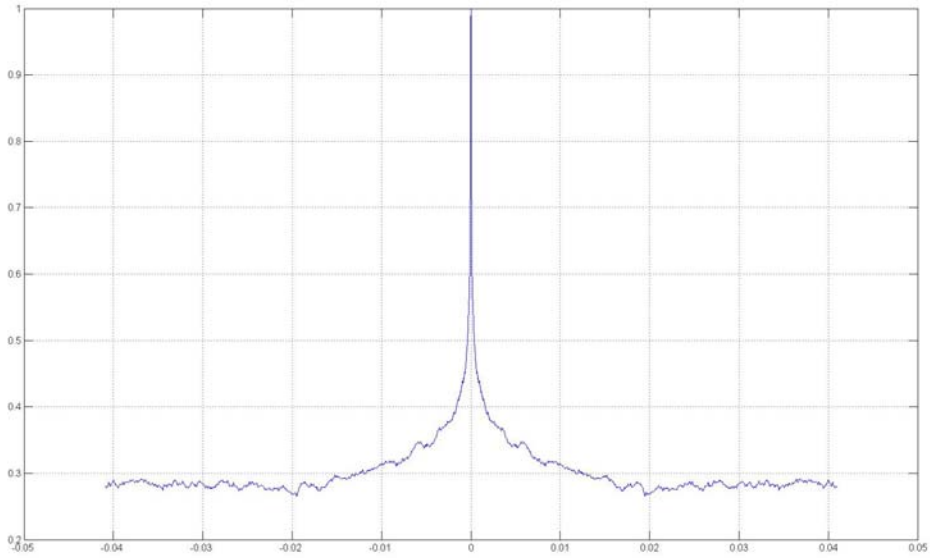


Periodogram:

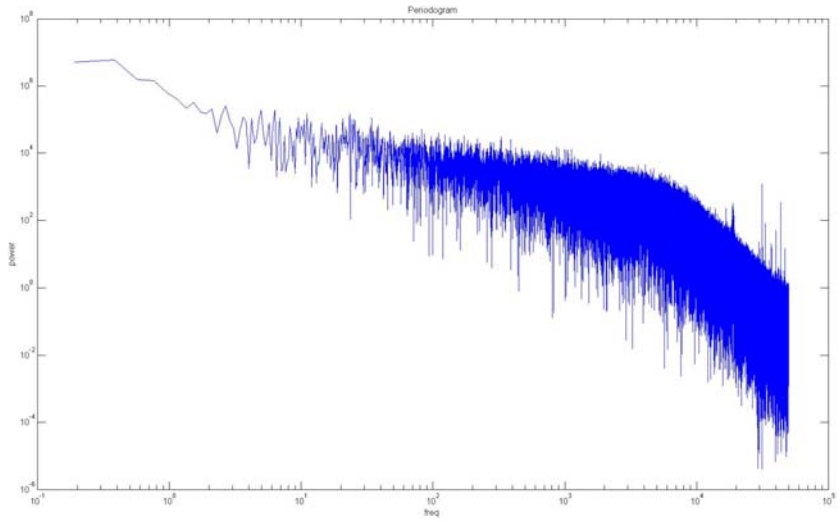

Steam stall:

Autocorrelation:

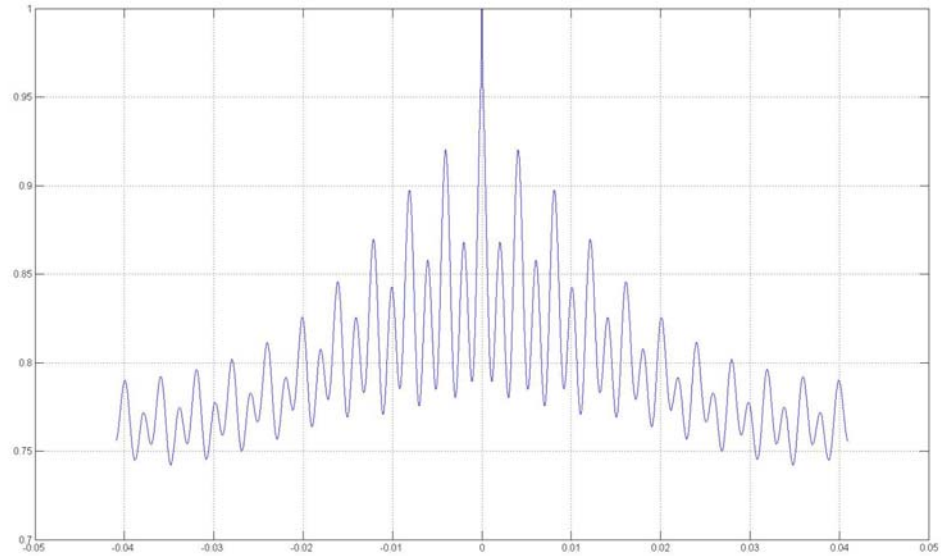


Periodogram:

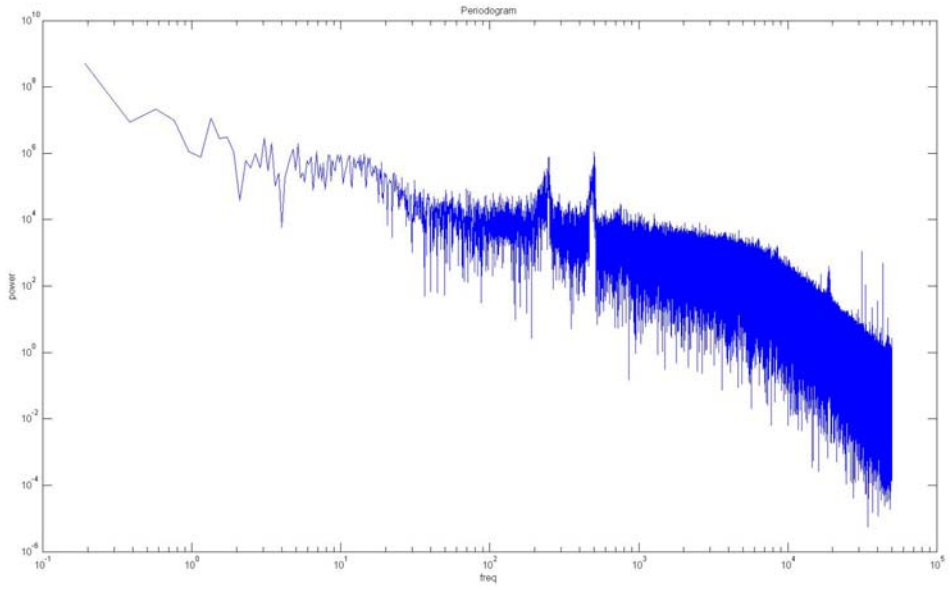

90% Speed:

Steam run, no stall:

Autocorrelation:

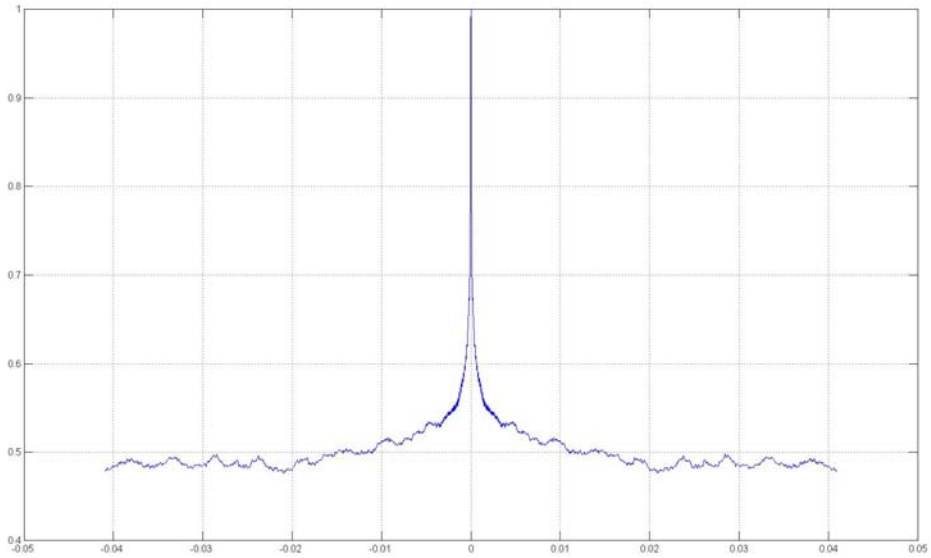

Periodogram:

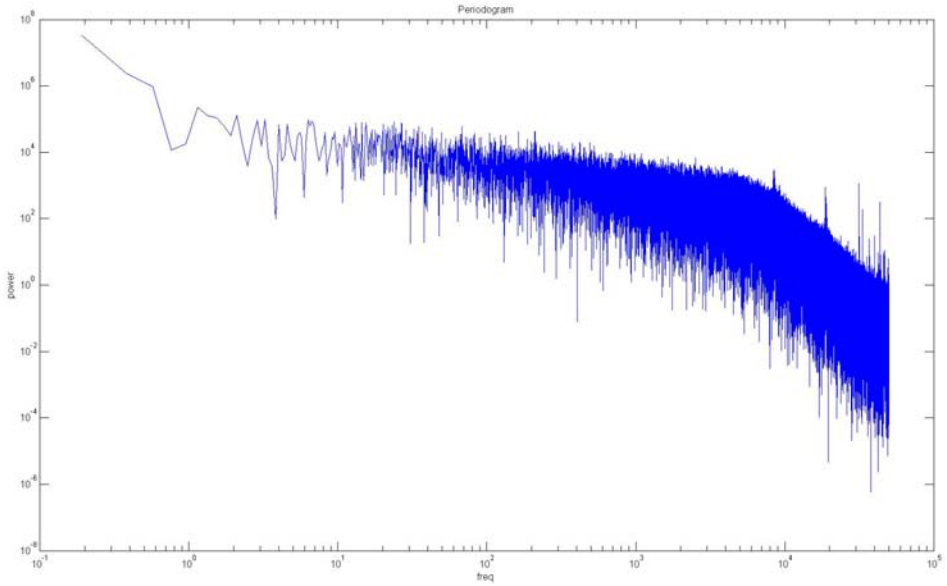

Steam stall:

Autocorrelation:

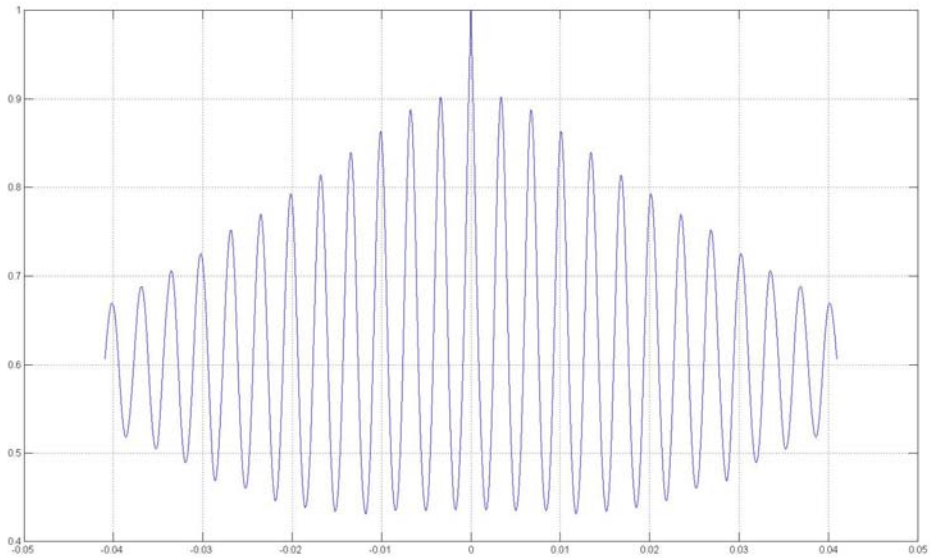

Periodogram:

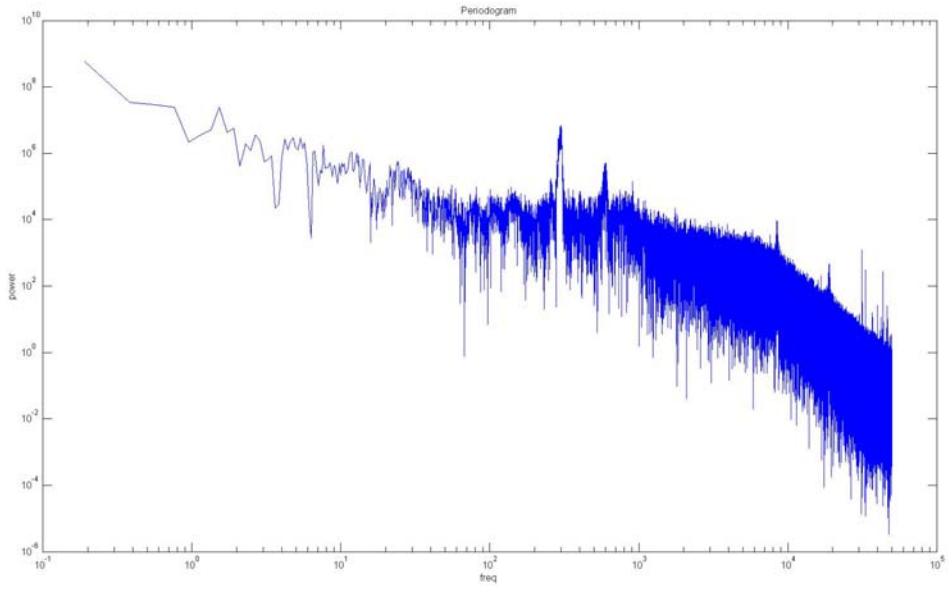

95% Speed:

Steam run, no stall:

Autocorrelation:

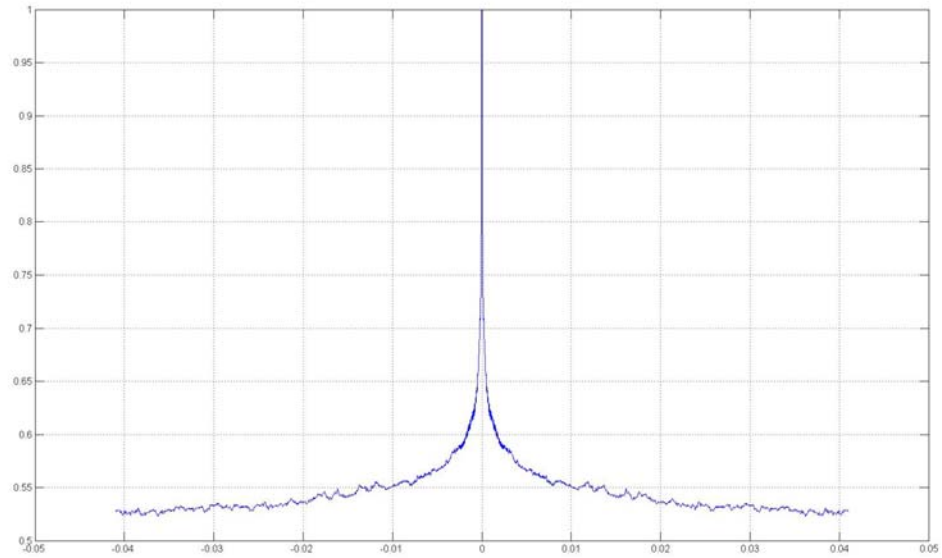

Periodogram:

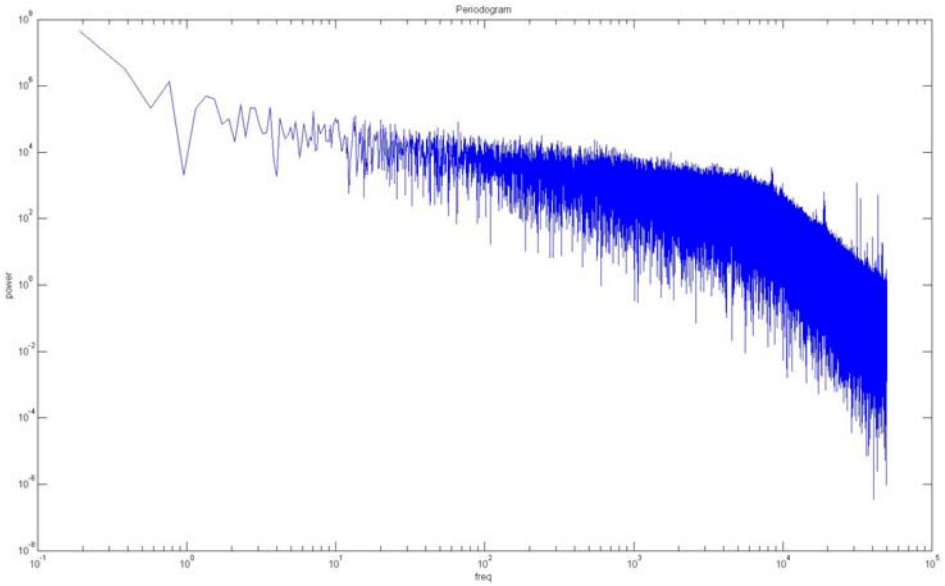

Steam stall:

Autocorrelation:

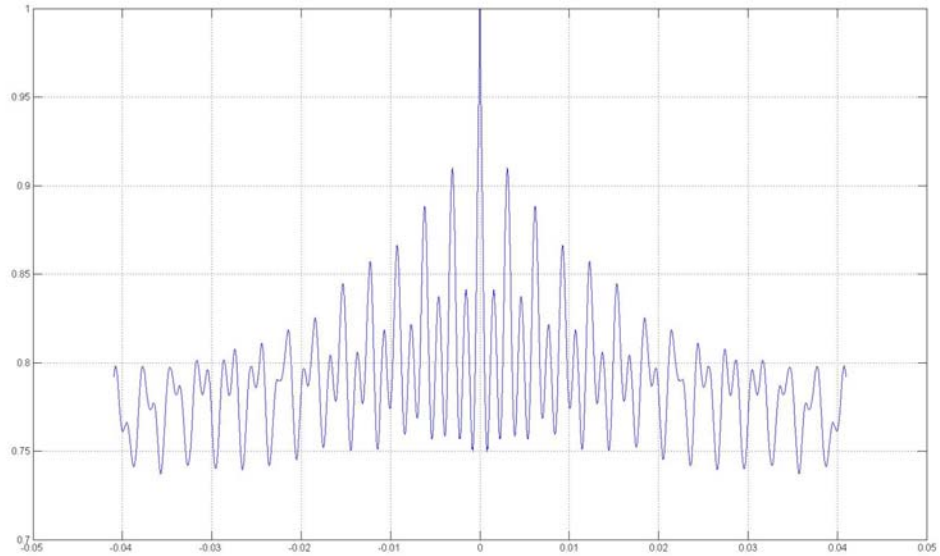


Periodogram:

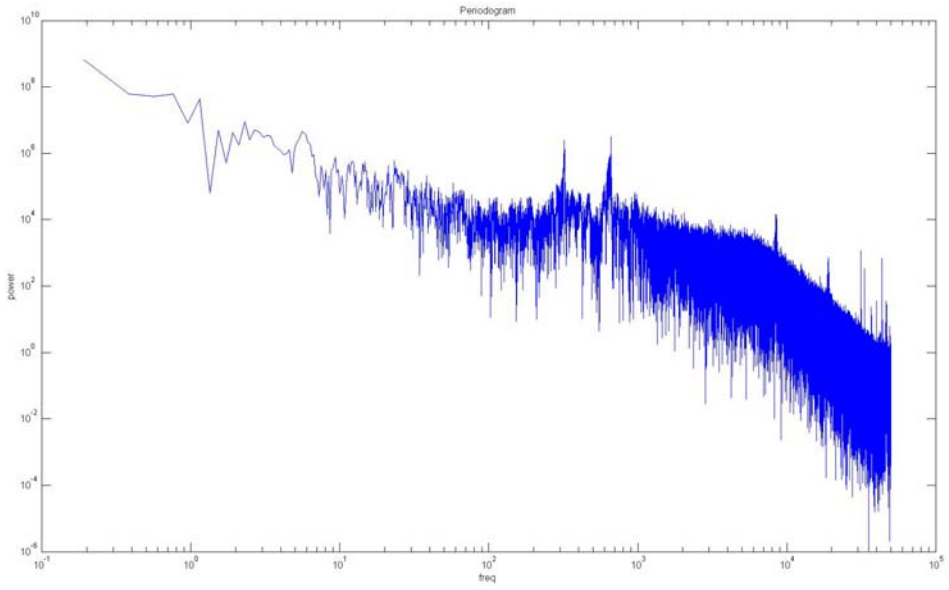

# APPENDIX G: STEAM STRIP CHARTS

70% Speed, steam run, no stall:

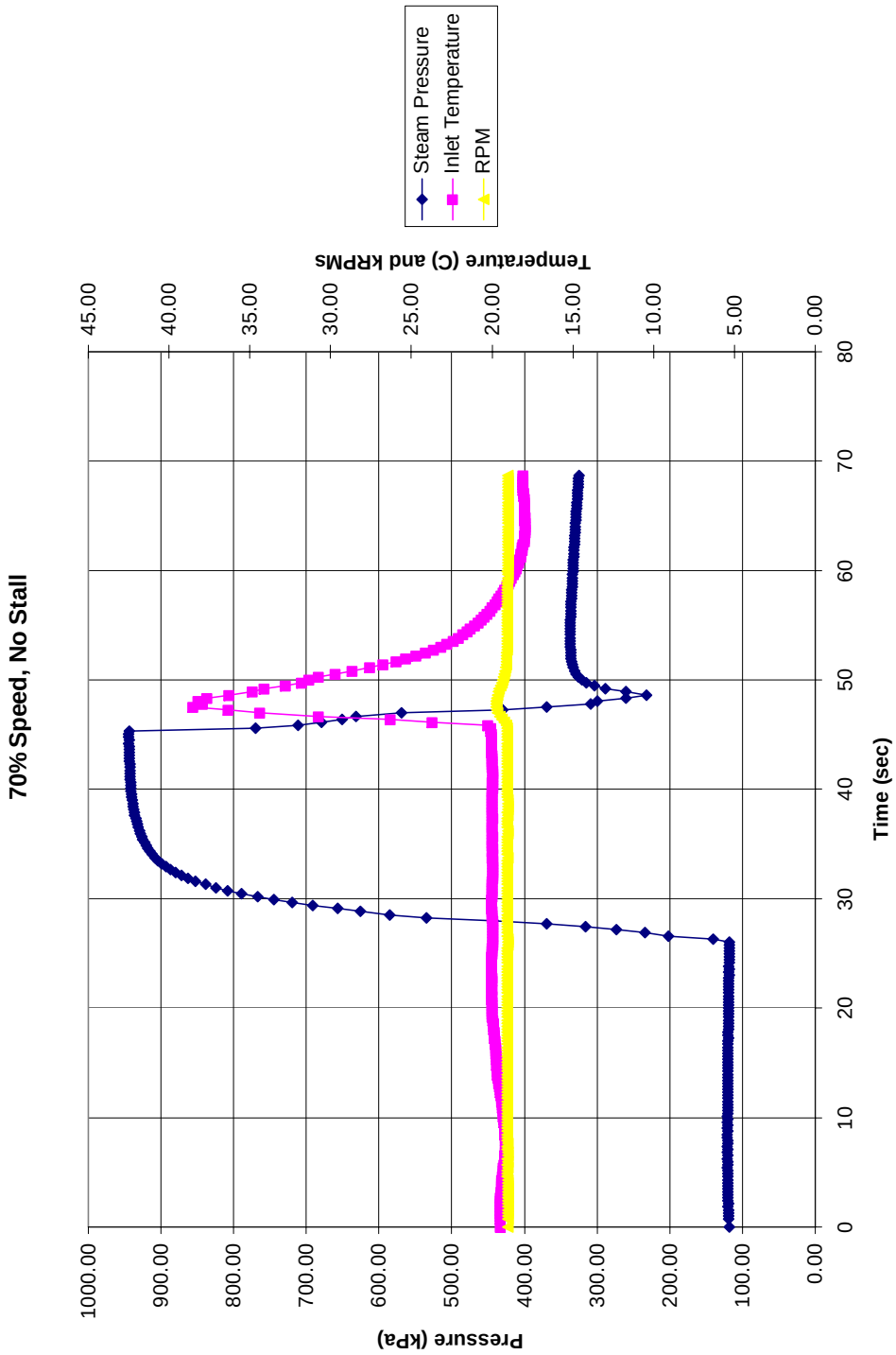

70% Speed, steam stall:

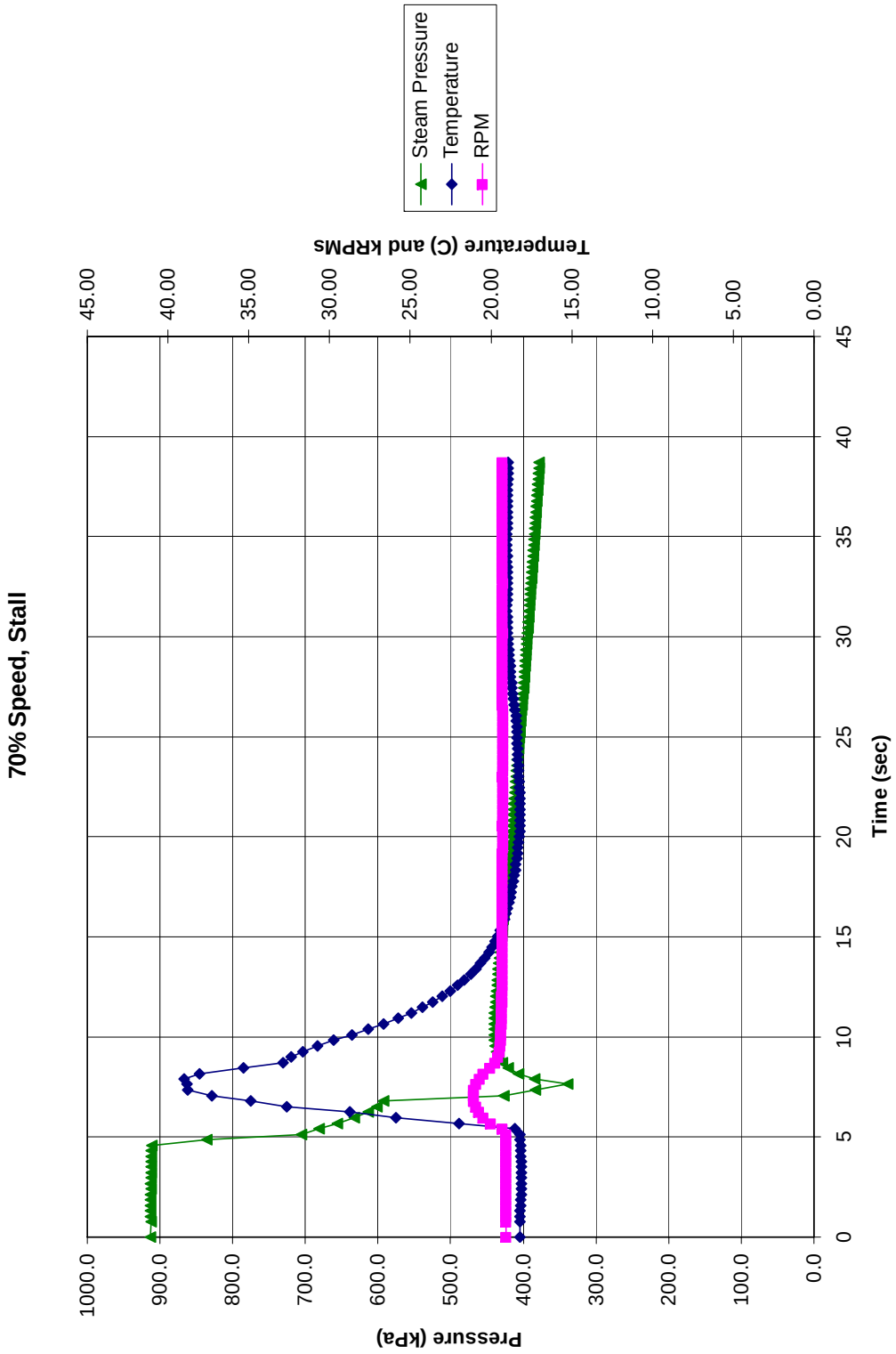

90% Speed, steam run, no stall:

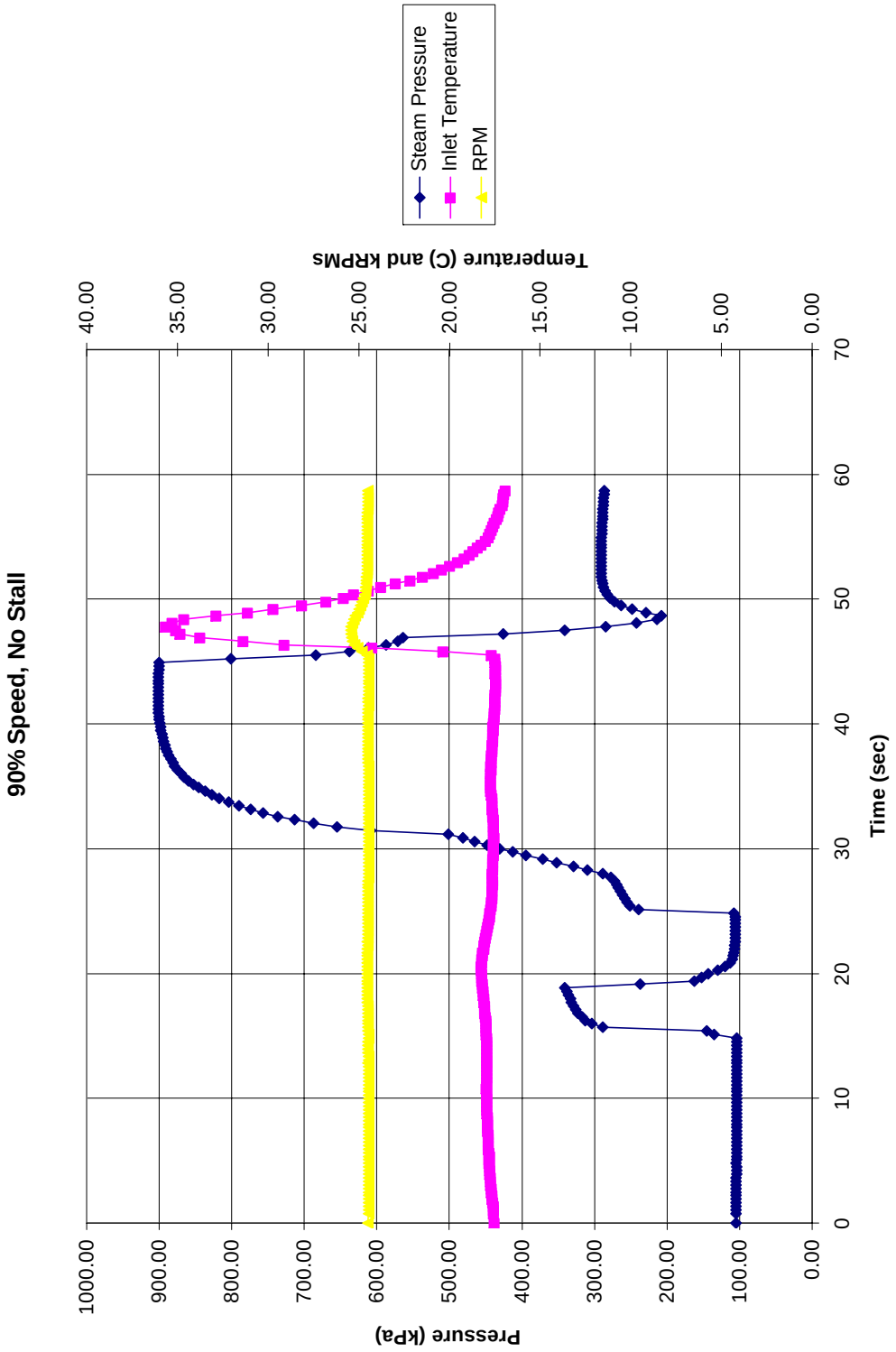

90% Speed, steam stall:

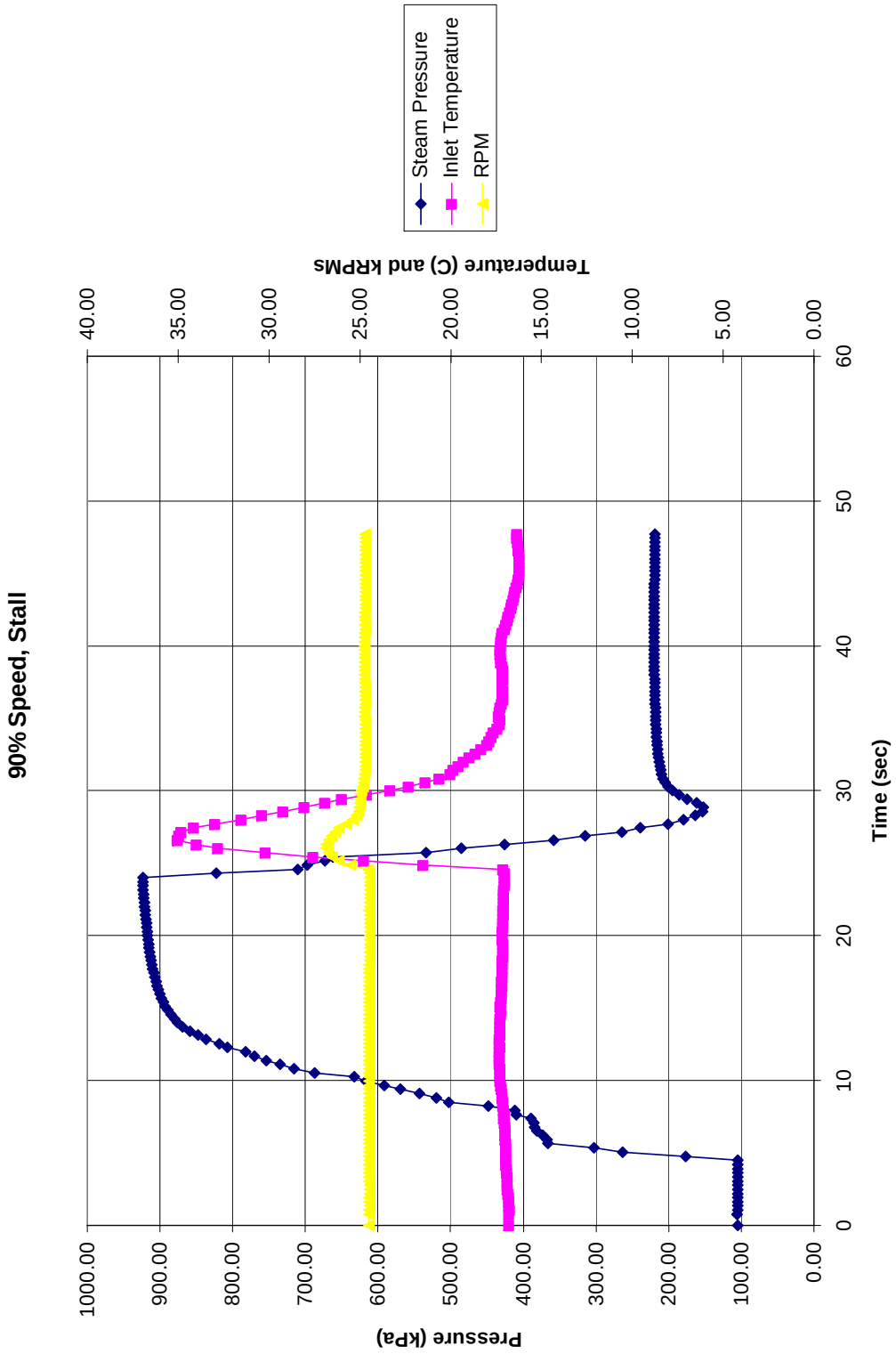

95% Speed, steam run, no stall:

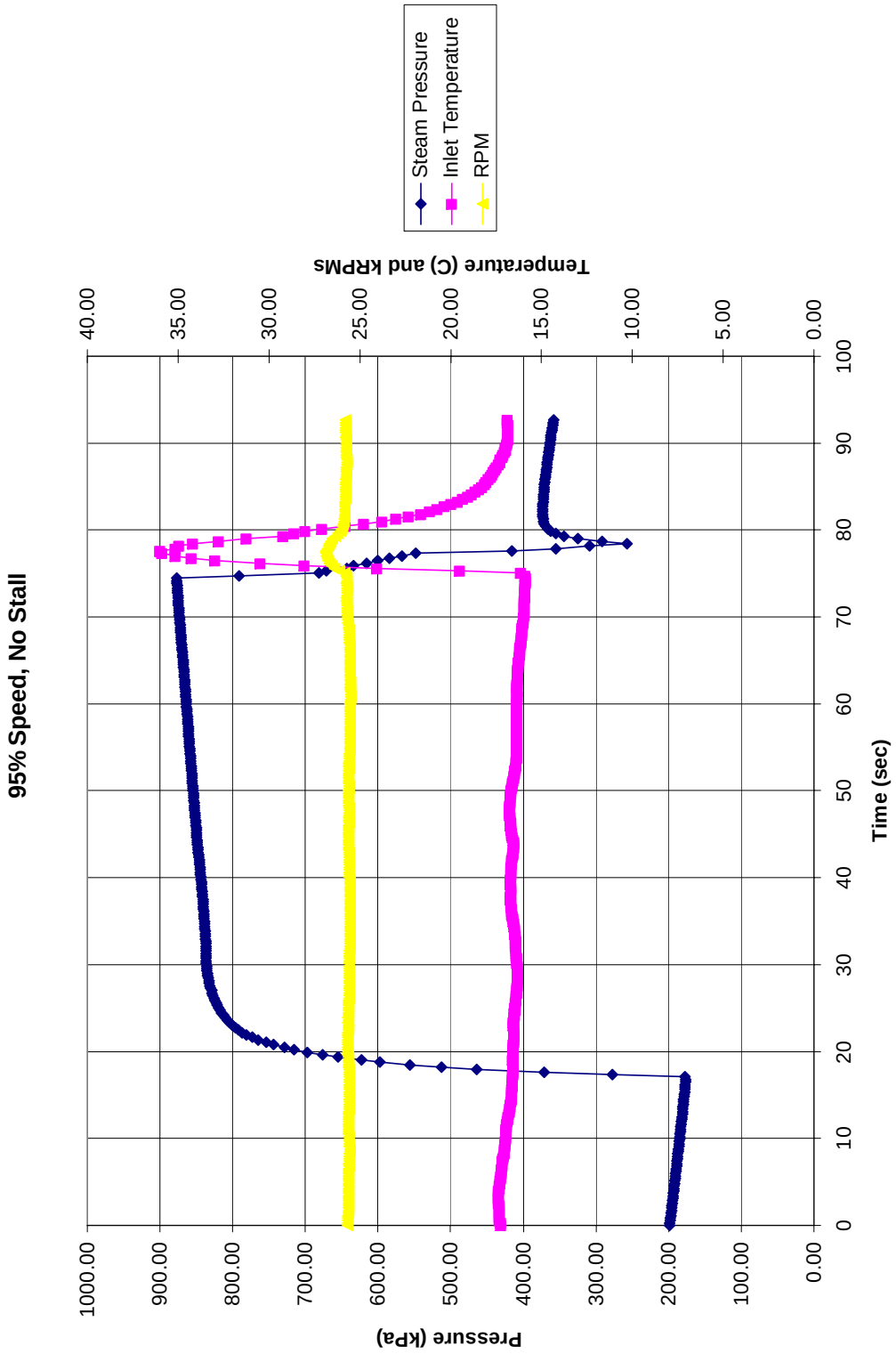

95% Speed, steam stall:

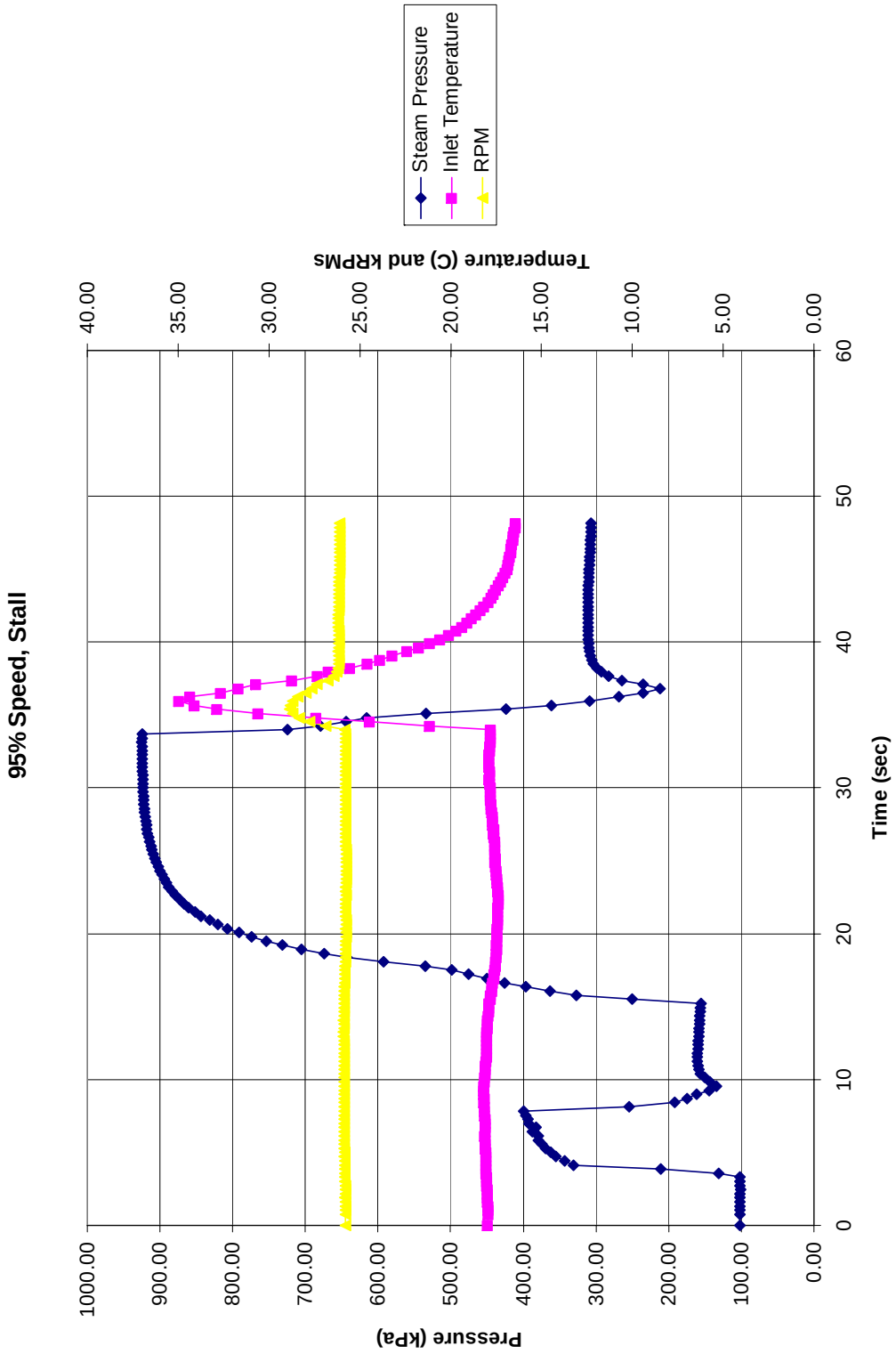

# INITIAL DISTRIBUTION LIST

1. Defense Technical Information Center
   Ft. Belvoir, Virginia

2. Dudley Knox Library
   Naval Postgraduate School
   Monterey, California

3. Distinguished Professor and Chairman Anthony Healey
   Department of Mechanical and Aeronautical Engineering
   Naval Postgraduate School
   Monterey, California

4. Professor Garth Hobson
   Department of Mechanical and Aeronautical Engineering
   Naval Postgraduate School
   Monterey, California

5. Assistant Professor Anthony Gannon
   Department of Mechanical and Aeronautical Engineering
   Naval Postgraduate School
   Monterey, California

6. Professor Raymond Shreeve
   Department of Mechanical and Aeronautical Engineering
   Naval Postgraduate School
   Monterey, California

7. Ensign Joe Koessler
   Naval Postgraduate School
   Monterey, California